FORWARD MODEL CALCULATIONS FOR DETERMINING ISOTOPIC COMPOSITIONS OF MATERIAL USED IN A RADIOLOGICAL DISPERSAL DEVICE

A Thesis

by

DAVID EDWARD BURK

Submitted to the Office of Graduate Studies of
Texas A&M University
in partial fulfillment of the requirements for the degree of

MASTER OF SCIENCE

May 2005

Major Subject: Nuclear Engineering

FORWARD MODEL CALCULATIONS FOR DETERMINING ISOTOPIC COMPOSITIONS OF MATERIAL USED IN A RADIOLOGICAL DISPERSAL DEVICE

A Thesis

by

DAVID EDWARD BURK

Submitted to Texas A&M University
in partial fulfillment of the requirements
for the degree of

MASTER OF SCIENCE

Approved as to style and content by:

William S. Charlton (Chair of Committee)	Yassin A. Hassan (Member)
James Olson (Member)	William E. Burchill (Head of Department)

May 2005

Major Subject: Nuclear Engineering

ABSTRACT

Forward Model Calculations for Determining Isotopic Compositions of Material Used in a Radiological Dispersal Device.

(May 2005)

David Edward Burk, B.S., Arkansas Tech University

Chair of Advisory Committee: Dr. William S. Charlton

In the event that a radiological dispersal device (RDD) is detonated in the U.S. or near U.S. interests overseas, it will be crucial that the actors involved in the event can be identified quickly. If irradiated nuclear fuel is used as the dispersion material for the RDD, it will be beneficial for law enforcement officials to quickly identify where the irradiated nuclear fuel originated. One signature which may lead to the identification of the spent fuel origin is the isotopic composition of the RDD debris.

The objective of this research was to benchmark a forward model methodology for predicting isotopic composition of spent nuclear fuel used in an RDD while at the same time optimizing the fidelity of the model to reduce computational time. The code used in this study was Monteburns-2.0. Monteburns is a Monte Carlo based neutronic code utilizing both MCNP and ORIGEN. The size of the burnup step used in Monteburns was tested and found to converge at a value of 3,000 MWd/MTU per step. To ensure a conservative answer, 2,500 MWd/MTU per step was used for the benchmarking process. The model fidelity ranged from the following: 2-dimensional pin cell, multiple radial-region pin cell, modified pin cell, 2D assembly, and 3D assembly.

The results showed that while the multi-region pin cell gave the highest level of accuracy, the difference in uncertainty between it and the 2D pin cell (0.07% for ^{235}U) did not warrant the additional computational time required. The computational time for the multiple radial-region pin cell was 7 times that of the 2D pin cell. For this reason, the 2D pin cell was used to benchmark the isotopics with data from other reactors.

The reactors from which the methodology was benchmarked were Calvert Cliffs Unit #1, Takahama Unit #3, and Trino Vercelles. Calvert Cliffs is a pressurized water reactor (PWR) using Combustion Engineering 14×14 assemblies. Takahama is a PWR using Mitsubishi Heavy Industries 17×17 assemblies. Trino Vercelles is a PWR using non-standard lattice assemblies. The measured isotopic concentrations from all three of the reactors showed good agreement with the calculated values.

ACKNOWLEDGMENTS

I would like to offer my sincere thanks to my advisor Dr. William Charlton, and committee members Dr. Yassin Hassan and Mr. James Olson, without whom this thesis would not have been possible. My wife, Heather, parents, Marie and Tinker, sister, Jennifer, and brother, Matthew deserve a great deal of appreciation for their loving support during the past two years. I would like to thank my mentors Dr. Robert Olive and Mr. Kenneth Baim who have been great role models and have taught me the value of a goal oriented life. I would also like to acknowledge peers of my graduate study including Alex Pasciak, Kaydee Kohlhepp, Taraknath Woddi, Mark Scott, and John Boydston, whose help and friendship have been invaluable. Last but not least I would like to offer my thanks to God for allowing me this wonderful opportunity.

TABLE OF CONTENTS

Page

CHAPTER Page

LIST OF FIGURES

Page

LIST OF TABLES

Page

Page

CHAPTER I

INTRODUCTION AND LITERATURE REVIEW

I.A. Objective

In the event that a Radiological Dispersal Device (RDD) is detonated in the U.S. or near U.S. interests overseas, it will be crucial that the actors involved in the event can be identified quickly. If spent nuclear fuel is used as the material for the RDD, law enforcement officials will need information on the origin of the spent fuel. One signature which may lead to the identification of the spent fuel origin is the isotopic composition of the RDD debris. In order to use this signature, it is necessary to have a well developed understanding of the uncertainties in predicting the isotopic composition of spent nuclear fuel from fundamental reactor physics calculations.

The objective of this research was to benchmark a forward model methodology for predicting the isotopic composition of spent nuclear fuel used in an RDD while at the same time optimizing the fidelity of the model to reduce computational time. There are two major differences between this research and previous research in this area [1, 2]. The first difference is that the methodology developed here must be purposefully generic since the material recovered from the RDD will not contain important reactor modeling information such as axial location, boron concentration, location in the core, and a detailed irradiation history. The second difference is that the optimization and benchmarking performed in this study will focus on isotopic signatures of specific interest to attributing RDD material.

This thesis follows the style of *Nuclear Technology*.

Once complete, this forward model can then be used in conjunction with the SENTRY database at Los Alamos National Laboratory (LANL) to determine the specific reactor facility of origin, date when the fuel was removed from the reactor, and the fuel manufacturer. The SENTRY database at Los Alamos National Laboratory contains reactor data from around the world. Using the forward model methodology developed in this research, detailed time-dependent data for the isotopic composition of fuel irradiated in any reactor listed in the SENTRY database can be determined. If an RDD event occurs, material can be collected and compared to the data from the forward model calculations to identify the specific origin of the spent fuel. Operationally, this determination must be completed within approximately five (5) days of the event. This would allow for a timely response by law enforcement officials.

I.B. Radiological Dispersal Device

An RDD is "any device, other than a nuclear explosive device, specifically designed to employ radioactive material by disseminating it to cause destruction, damage, or injury by means of the radiation produced by the decay of such material" [3]. While it is unlikely that the detonation of an RDD would inflict a large number of casualties, the psychological terror resulting in the use of such a device would be immense. In addition, an RDD can also be used as an effective method of restricting or denying human occupation of a particular area.

The idea of using radiation as a weapon is, in fact, not a new idea. The British National Academy of Sciences first proposed the idea of using radiological warfare as a battlefield weapon in 1941. Their plan was to drop bombs filled with violent radioactive materials over enemy territories. However, the development of the atomic bomb halted

further development of the plan. The idea, though, would be revisited in 1947 by the United States. Over the next several years, the U.S. conducted an active test program into the viability of RDDs. It would later be decided that although it might have profound psychological effects, it was not an effective battlefield weapon and the program was abandoned. Only in the wake of recent terrorist events has the idea gained prowess as an effective weapon of terror.

The most common type of RDD combines a conventional explosive, such as dynamite, with radioactive material. In most cases, the conventional explosive itself would be more immediately lethal than the radioactive material being dispersed. There will most likely not be enough radiation present in a dirty bomb to kill people or cause severe illness. However, certain radioactive materials, if dispersed in the air, could contaminate up to several city blocks, creating fear and panic and requiring a potentially costly cleanup [4].

The extent of local contamination would depend on a number of factors. These factors include the size of the explosion, the amount and type of radioactive material used, and weather conditions. Prompt identification of the radioactive material used would greatly assist local authorities in advising the community on protective measures. Subsequent decontamination of the affected area could involve considerable time and expense [4].

I.B.1. Large Radioactive Source

In the event that a terrorist does detonate an RDD, the type of material most likely used would be a large radioactive source. These sources are used in a variety of commercial and industrial applications and can be obtained much easier than special nuclear material or spent nuclear fuel. These applications include medical treatment/diagnostics, well-logging sources, and food irradiation to name a few. Most of these materials are, in fact, self-securing in that they are radioactive enough to seriously injure or kill anyone who is not properly shielded from them. While there are security measures in place, they are not very effective at stopping a terrorist or other military group that might be willing to use deadly force. Another obstacle is the scientist or engineer who works at the site and who is aware of the security and knows how to shield themselves from the radiation. This has become the major obstacle in places such as the former Soviet Union whose scientists are looking at this option as a way to help support their starving families.

Once the terrorist obtains the material, it is not very difficult to conceal it. Most of these sources are very small in size (less than a couple inches in diameter) and can be shielded by little more than a small drum of lead or polyurethane (depending on the type of radiation being emitted). Because of this, a terrorist could potentially store one of these sources in the basement of their house or in any number of obscure locations that would make it almost impossible for law enforcement officials to find it. Assuming that the source is properly shielded, a terrorist could also transport the source in something as simple as the back of a truck or car.

A large radioactive source, once dispersed (blown up), would not possess enough radioactivity per area of land to be deadly to the people in that area. Most of the damage would in fact be due to the conventional explosion. As the amount of radioactivity at the detonation site would not be severe, this type of RDD would not deny use of an area for a long period of time. Although the damage from one of these devices would not be severe, the psychological impact would none-the-less be tremendous. It would take a long time for people to again feel safe in the area of the detonation as the thought of radiation, no matter how minuscule, is terrifying to most of the population.

I.B.2. Spent Nuclear Fuel

Spent nuclear fuel is a by-product of every nuclear reactor in the world. When ^{235}U fissions it forms products known as fission fragments. These fission fragments are highly radioactive and can have long half lives. Obtaining spent nuclear fuel is extremely difficult. The fuel is bound in assemblies which contain hundreds of fuel rods. The fuel rods are surrounded in a dense cladding and welded into the assembly. Fuel assemblies can weigh in excess of one ton and are generally about 12 feet long. Because of the high levels of radioactivity in spent nuclear fuel, they are kept in large pools of water for several years after being removed from the reactor. This cool-down time allows for some of the radioactivity to decay off and allows for safer transfer of the fuel. Once the cool down time is complete, most fuel is then sent to dry cast storage to remain until it is either disposed of or reprocessed.

In order to obtain fuel from the spent fuel pool or dry cast storage, a terrorist must first penetrate the reactor facility. This in itself would be an extreme undertaking as these facilities have enormous security defenses. Once the facility has been penetrated, a

terrorist would need to gain access to a crane in order to move the fuel. As the fuel is quite large in both size and weight, a large vehicle would be required. Unless a special vehicle incorporating a tremendous amount of shielding was used, the occupants would die from the radiation in a short time. Assuming that the terrorist was able to get this far, they would then have to contend with state military forces who would soon be on the scene. Because of the tremendous difficulty of this scenario, it is not likely to ever occur.

The most likely scenario for a terrorist to obtain spent nuclear fuel would be if the terrorist had state sponsorship. If this were the case, the government could allow or even assist the terrorist in obtaining the fuel from the reactor facility. The government would most likely also assist in concealing the fuel from outsiders so that the terrorist could properly mount their attack. This type of proliferation is difficult to detect without outside sources monitoring the facility to ensure such sponsorship does not occur.

If a spent nuclear fuel assembly were used as an RDD and detonated, the results would be disastrous. Both the large amount of material and the radiation associated with it would kill anyone in the direct path of the post-detonation material. The amount of area affected would definitely be larger than that of the large radioactive source RDD, but would not nearly as large as a nuclear weapon. Due to the long half-lives of some of the isotopes in the fuel, the affected area would remain uninhabitable for years and possibly even decades to come. If the psychological effects of large radioactive source RDD were terrifying, then the psychological effects of the spent nuclear fuel RDD would be horrifying.

I.C. Previous Research

Computerized reactor modeling and simulation has gained much ground since the development of MCNP [5] in the 1970's. Since that time, modeling techniques have been used to examine various aspects of nuclear reactors such as flux profiles, isotopic concentrations, fuel burnup, reactivity margins, and criticality.

Monte Carlo codes have been widely accepted for their use in flux calculations, but have not yet gained acceptance in isotopic calculations due to their large computational requirements. For this reason, many isotopic calculations rely on deterministic codes such as CASMO [6, 7], HELIOS [8], SCALE [9, 10], or ORIGEN [11, 12, 13].

MCNP (Monte Carlo N-Particle Transport) is a widespread Monte Carlo transport code used for stochastic simulation and the coupled transport of neutrons, photons, and electrons. Neutrons and photons are tracked on an interaction-by-interaction basis using random numbers fit to both theoretical and experimental probability distribution functions to describe the differential behavior of a particular interaction type. The transport of electrons in MCNP is performed using a condensed history approximation, which is effective in predicting the average behavior of an energetic electron after undergoing many interactions. MCNP can be used for a variety of applications including, but not limited to, dosimetry, radiation shielding, radiography, accelerator target design, and fission and fusion reactor design. The popularity of this code is largely due to its versatility, comprehensive geometry features, and its overall physics capabilities, including continuous energy treatment [5].

CASMO [6, 7] is a multi-group, two-dimensional transport theory code which can also perform burnup calculations on boiling water reactor (BWR) and pressurized water reactor (PWR) assemblies. CASMO uses the method of characteristics [14] to solve the integral form of the neutron transport equation:

$$\psi_g(\vec{r},\vec{\Omega}) = \psi_g(\vec{r} - R\vec{\Omega},\vec{\Omega}) \exp\left[-\int_0^R \Sigma_{t,g}(\vec{r} - R'\vec{\Omega}) dR' \right] + \int_0^R q_g(\vec{r} - R\vec{\Omega},\vec{\Omega}) \exp\left[-\int_0^{R'} \Sigma_{t,g}(\vec{r} - R''\vec{\Omega}) dR'' \right] dR' \quad (1)$$

where ψ_g is the angular flux for energy group *g*, $\vec{r}$ is the position of the neutron moving in the direction $\vec{\Omega}$ and subtended by the distance R, $\Sigma_{t,g}$ is the total cross section for group *g*, and q_g is the neutron source for group *g*. CASMO then uses fluxes from this solution to determine isotopic material compositions via a numerical solution to the Bateman equation:

$$\frac{dN_A(t)}{dt} = -(\sigma_A^g \phi + \lambda_A) N_A(t) + \sigma_C^\gamma \phi N_C(t) + \lambda_B N_B(t) \quad (2)$$

where N_X is the amount of isotope *X*, *t* is time, ϕ is the scalar flux, σ_X^g is the microscopic absoption cross section of isotope *X* for group *g*, and λ_X is the decay constant for isotope *X*. CASMO's nuclear data set covers an energy range from 0 to 10 MeV and its two-dimensional calculations are performed in true heterogeneous geometry. The code can accommodate non-symmetric fuel bundles, while half, quadrant, or octant symmetry can be utilized. Additionally, a predictor-corrector approach is used in the depletion calculation, which greatly reduces the number of burn-up steps necessary for a given accuracy. The output is flexible and gives few group cross-sections and reaction

rates for any region of the assembly for use in overall reactor calculation. However, since this code can only model BWR and PWR reactor types, its use for this research is very limited and was thus not chosen for this work.

SCALE [9, 10] is a well established code system that includes deterministic neutron transport solvers and that has been widely used in characterization of light water reactor (LWR) spent fuel. SCALE combines the multicode sequences SAS2H and ORIGEN-S to determine the isotopic composition of spent fuel. This combination of codes solves depletion and decay calculations as well as a 1D neutronics model in order to obtain burnup-dependent cross sections. This information is then used to obtain spent fuel isotopics. SCALE is still very limited in the fact that it has only been validated for use with light water reactors (LWR).

ORIGEN (Oak Ridge Isotope GENeration code), which performs the burnup and decay calculations, is a deterministic code that predicts solutions to the burnup equations using a matrix exponential method to solve a large system of coupled, linear, first-order ordinary differential equations with constant coefficients of the following form:

$$\frac{dN_i}{dt} = P_i - L_i \tag{3}$$

$$P_i = \sum_{x \to i} \Sigma_x^j \varphi + \sum_{j \to i} \lambda_j N_j \tag{4}$$

$$L_i = \Sigma_a^i \varphi + \lambda_i N_i \tag{5}$$

where P_i is the amount of isotope *i* produced, L_i is the amount of isotope *i* lost, φ is the one-group scalar flux, N_x is the amount of isotope *X*, and Σ_x^y is the macroscopic cross section for isotope *Y*. ORIGEN requires a predetermined reactor specific library in order to acquire one-group cross sections, fission yields, and flux spectra. ORIGEN has gained

popularity largely due to its relative ease of use and minimal computational time (generally less than a few seconds on most PCs).

Recently, benchmarking has been performed [1, 2] on a LANL developed code known as Monteburns [15]. Monteburns is a Monte Carlo based neutronic code utilizing both MCNP and ORIGEN. MCNP serves as the transport solver and ORIGEN serves as the burnup module. Monteburns transfers one-group cross sections and flux values from MCNP to ORIGEN. The following equations demonstrate how the one-group fluxes and cross sections are generated with these codes. MCNP calculates one-group fluxes ($\bar{\phi}_i$) for any volume *i* by using the track length estimator of particle fluxes. One-group cross sections are calculated using track length estimators for reaction rates which essentially uses:

$$\bar{\sigma}_x^i = \frac{\int_0^\infty \int_{4\pi} N_i \sigma_x^i(E) \psi(\vec{\Omega}, E)\, d\Omega\, dE}{N_i \bar{\phi}} \tag{6}$$

Once the burnup and decay calculations have been performed by ORIGEN, Monteburns then transfers the isotopic compositions of the materials back to MCNP. Through the use of MCNP, Monteburns allows for the calculations of complex geometries and material compositions. This implies that Monteburns can simulate a vast array of different reactor types and is thus the code of choice for this project (where the type of material used in an RDD could be from nearly any type of reactor including thermal reactors, fast reactors, naval reactors, and research reactors). Fig. 1 demonstrates how Monteburns utilizes both MCNP and ORIGEN to obtain material compositions [15].

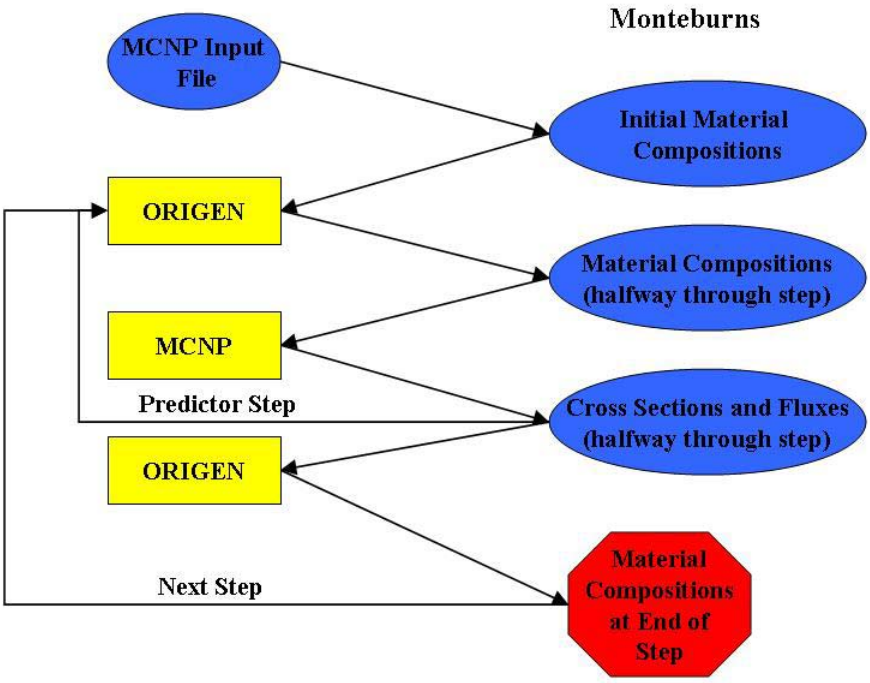

Fig. 1. Interaction of Monteburns with MCNP and ORIGEN.

I.D. Description of RDD Forensics Problem

The events of September 11, 2001 clearly show the willingness of terrorists to use unconventional means for inflicting great casualties. Nuclear terrorism is also one of those possible means. While it is unlikely that terrorist groups would have the capability to fabricate a nuclear weapon, these groups would likely have the capability to produce an RDD (or the so-called "dirty bomb"). The threat of a terrorist using an RDD inside the U.S. or against U.S. interests overseas is greater than ever. This is due both to the increased sophistication of terrorist organizations and to the large amount of nuclear and radiological material at use or in storage throughout the world. The materials listed in

Table I are possible sources of material for use in an RDD. It is possible that terrorist organizations already have radiological materials in their possession. Nuclear smuggling events since the early 1990's have suggested that large amounts of nuclear and radiological material have been pilfered from former Soviet Union nations [16]. Figure 2 shows the confirmed illicit trafficking incidents from 1993-2003 as recorded in the International Atomic Energy Agency (IAEA) illicit trafficking database [16].

TABLE I

Radioactive Sources and Isotopes

Radioactive Sources	**Isotopes**
Industrial Radiography	^{192}Ir, ^{60}Co
Neutron Sources	PuBe, AmBe, AmLi, ^{252}Cf
Food Irradiation	^{137}Cs, ^{60}Co
Medical Isotopes	^{60}Co, ^{153}Sm, ^{99}Tc
Radioisotope Thermoelectric Generators	^{90}Sr, ^{238}Pu
Well-Logging Sources	AmBe, PuBe, ^{137}Cs
Reprocessing Facility Waste Products	Np, Am, Cu
Spent Nuclear Fuel	U, Pu, Np, Am, Cu, Nd

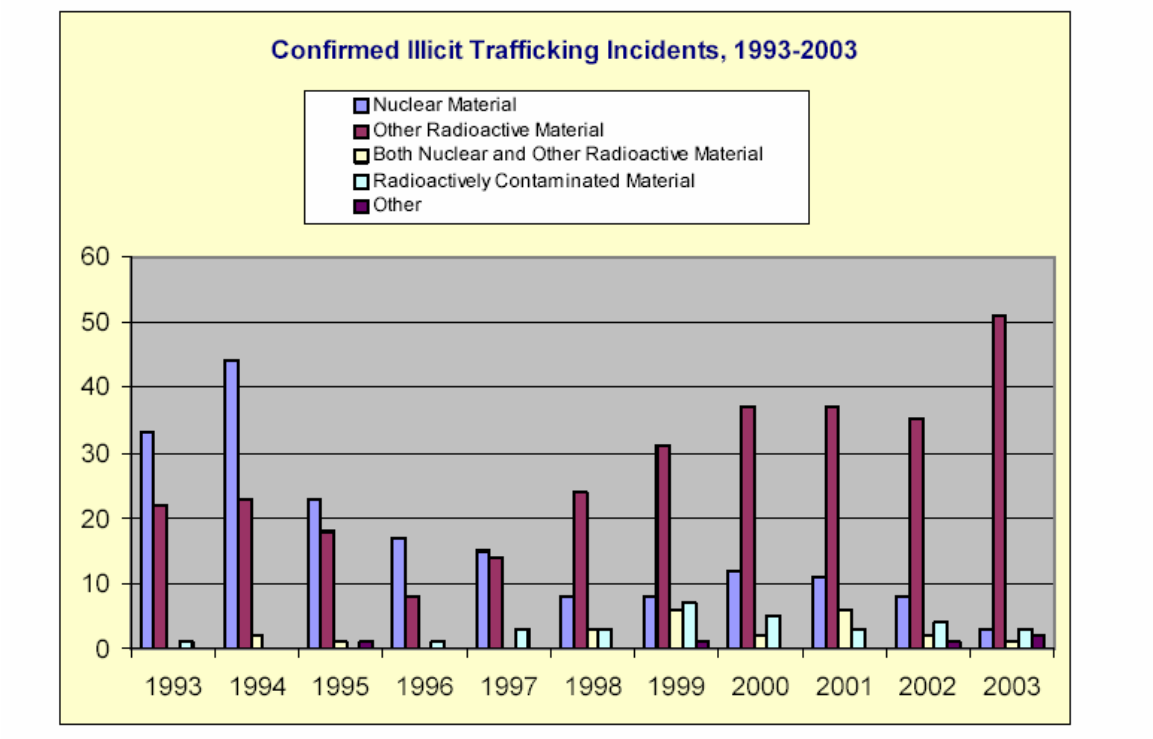

Fig. 2. Confirmed illicit trafficking incidents, 1993-2003.

Generally these materials can be divided into two categories: (a) *large radioactive sources* and (b) *spent fuel sources*. All of the sources from Table I, with the exception of spent nuclear fuel and reprocessing facility waste products, are considered large radioactive sources. These materials are fairly well characterized and generally consist of only one major radioisotope and potentially several impurities or trace isotopes. These sources vary from highly radioactive to low levels of radioactivity. The security involved in guarding these sources typically ranges from low-to-medium level.

Spent fuel sources consist of spent nuclear fuel and reprocessing facility waste products. These sources are poorly characterized in their current state though they were well characterized prior to irradiation in a nuclear reactor. These sources are highly-radioactive and even a single fuel assembly could kill anyone exposed directly to its

radiation. The level of security in place for these sources is generally high except for a few instances (submerged Russian naval reactor cores, research reactor cores, etc).

If someone acquired one of these materials, fabricated an RDD, and detonated it; then it would be crucial that the perpetrator of this act be determined. To identify the actors involved in this event, forensic evidence will be used to build a case against an individual or group. One principal piece of forensic evidence is the origin of the material used in the device (i.e., the name and location of the facility from which the material was acquired as well as the date of that acquisition). If scientists can determine the attributes of the detonated material such as isotopic composition, then this information can be compared against expected attributes of materials stored worldwide or known to have been diverted/stolen to determine the origin. While various residue characteristics can be used, we will limit our discussion here to using isotopic compositions of the residue.

In the case of *large radioactive sources*, establishing the material origin involves determining the isotopic composition of the radioactive material used and any trace or impurity isotopes in the material. The type of material used (e.g., ^{60}Co) will allow for determination of a number of possible suspect origins. Then the trace isotopes will be used to determine the most likely specific origin of the material. While the data necessary to identify the origin of the material is immense, the mathematical means for finding a most likely origin is well developed.

For *spent fuel sources*, the isotopic composition of the material at detonation is generally unknown. Thus a measurement of the isotopic composition of the debris can not be directly compared to a database of isotopic materials to identify the source of the RDD. Instead these isotopic compositions will be used to determine the characteristics of

the reactor that was used to produce the material. Specifically the reactor type, fuel burnup, fuel age, initial fuel enrichment, and operational history will be determined. The reactor characteristics will then be matched to known reactor systems to determine the most likely system that could have produced this material. It should also be noted that distinguishing between separated (i.e., reprocessed material) and unseparated material is simply a function of identifying the lack of expected isotopes (e.g., the lack of any fission product nuclides).

I.E. Nuclear Forensics Project Overview

The determination of the attributes of the spent fuel material involves three fundamental components:

1. Forward Model for calculating present day isotopic composition of material given initial material input to a reactor and known reactor operational parameters.
2. Database of Nuclear Materials and Nuclear Reactors.
3. Inverse Model for determining initial material input to a reactor and reactor operational parameters from present day isotopic composition measurements.

The forward model is used for the determination of spent fuel isotopic composition given the design characteristics and operating history of a known reactor facility. This model performs isotopic inventory calculations forward in time given the initial fuel dimensions, initial fuel material compositions, the fuel power history, and the fuel decay time (i.e., the time since permanent discharge from the reactor). The forward

model is based on well-developed reactor physics techniques for calculating spent fuel compositions and is commonly used in present day reactor physics calculations.

The database contains known reactor facilities that include numerous facility characteristics including fuel designs, operational history, and refueling schedules. This database (named SENTRY) is maintained by LANL and contains an enormous amount of information concerning nuclear facilities worldwide. This database also contains details on any known material diversions. A schematic for the forward model and database showing the steps of forward model calculations is given in Fig. 3.

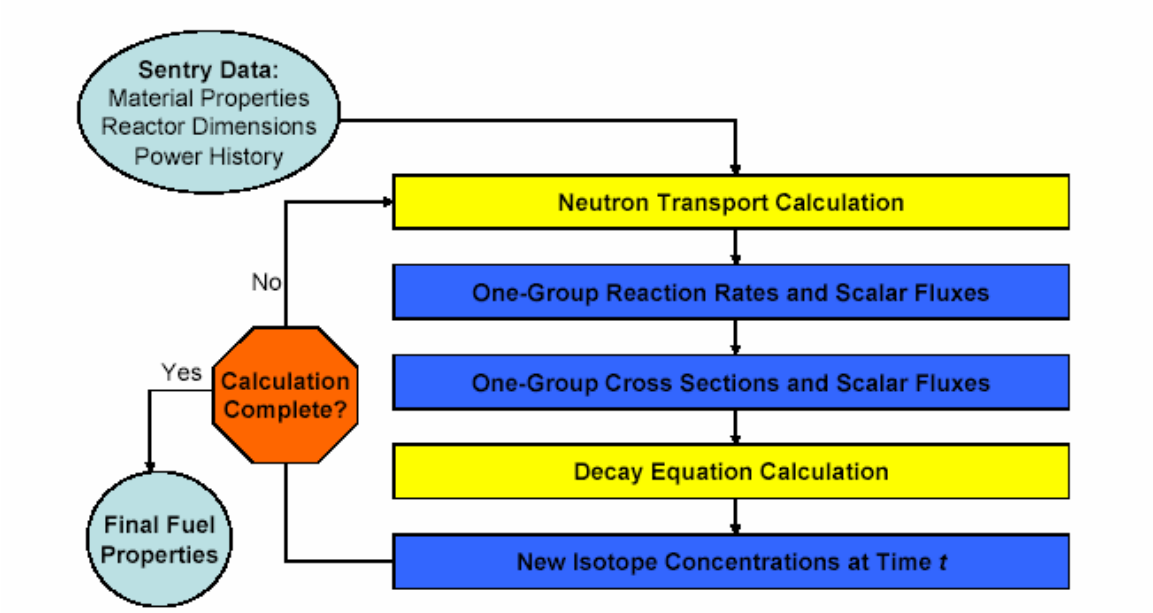

Fig. 3. Forward Model dataflow.

The inverse model uses measured isotopic signatures from RDD residue to predict the most likely characteristics of the facility used to produce those signatures. The inverse model used in this project is based on analytical inversions of the burnup equations. Specific monitors are used for each attribute of interest and are as follows:

1. *Burnup monitors*. These are stable or long-lived isotopes that are invariantly produced under most conditions (i.e., a certain percentage of this monitor is produced per fission that occurs in the fuel). ^{148}Nd has been widely used in previous efforts [10, 17] as an accurate burnup monitor.

2. *Reactor type monitors*. This type of monitor varies significantly based on the neutron spectrum in the fuel and the fission isotopes in the fuel.

3. *Fuel age*. This type of monitor is produced directly from fission and has a short enough half-life that some portion of it decays between discharge from the core and use as an RDD.

4. *Enrichment*. This type of monitor varies directly as a function of the fuel enrichment.

Each of these monitors is used in a hierarchical fashion as shown in Fig. 4. This implies that information from one attribute monitor is fed to the subsequent attribute monitor. The uncertainties associated with each calculation are propagated and the most likely set of attributes are predicted.

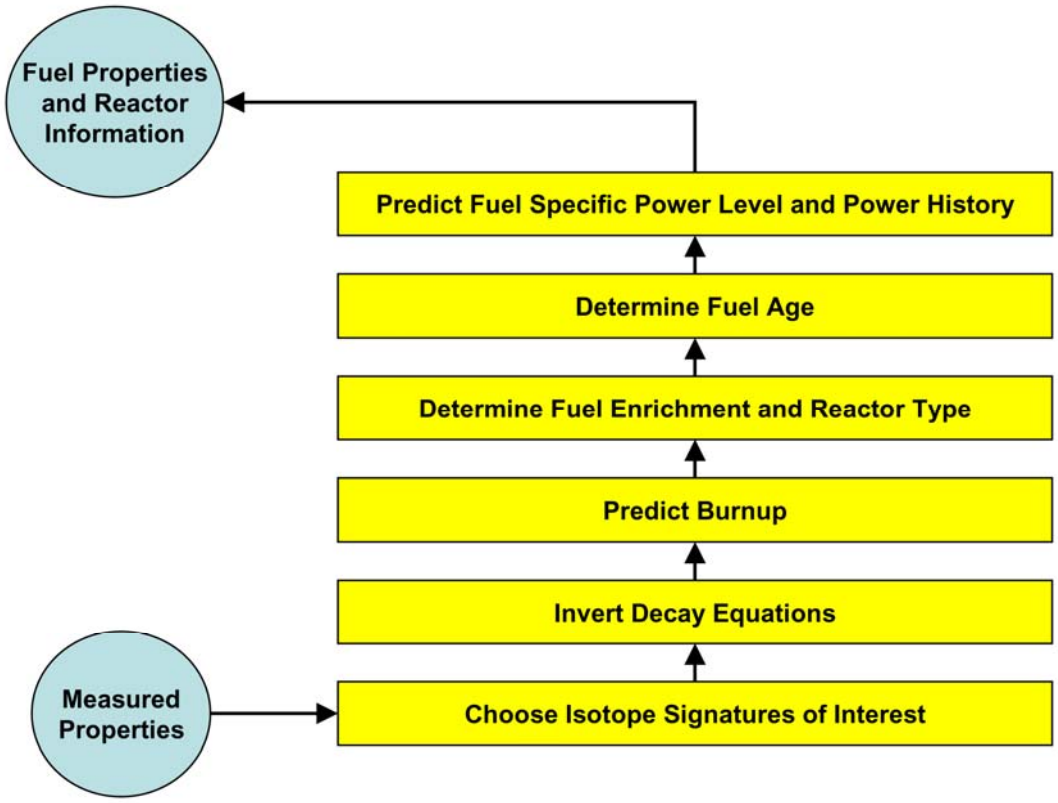

Fig. 4. Inverse Model dataflow.

A general overview of the entire forensics methodology is shown in Fig. 5. The green dotted line indicates a path that is performed prior to the event occurring. This path is the Forward Model being first used to generate a set of one-group cross sections for all possible reactor types (BWR, PWR, CANDU, VVER, etc.). This data is then stored in the SENTRY database.

The solid black lines indicate the major flow of the forensics problem from start to finish. The solid blue lines indicate secondary information transfer from various pieces of the system. As can be seen in Fig. 5, immediately following an RDD event, samples will be collected and analyzed via mass spectroscopy. The result of this analysis will yield concentrations of isotopes as well as uncertainties in the measurements. At this point, if the material is determined to be something other than spent nuclear fuel (i.e. a large radioactive source), then it does not take the path of the Forward/Inverse Model analysis. It instead goes through an inverse decay model analysis for determination of age and trace isotopes. This information can then be fed into the search tool (developed by LANL). The search tool then compares the data with known information in the SENTRY database for possible matches.

If the collected material is determined to be spent nuclear fuel, the measurements and uncertainties are sent to the Inverse Model. The analysis of the Inverse Model will determine factors such as burnup, age, enrichment, and reactor type. This information is then sent to a search tool. The search tool takes the output from the Inverse Model and compares it with data stored in the SENTRY database. The search tool then establishes a list of possible reactors of origin along with the probabilities of each.

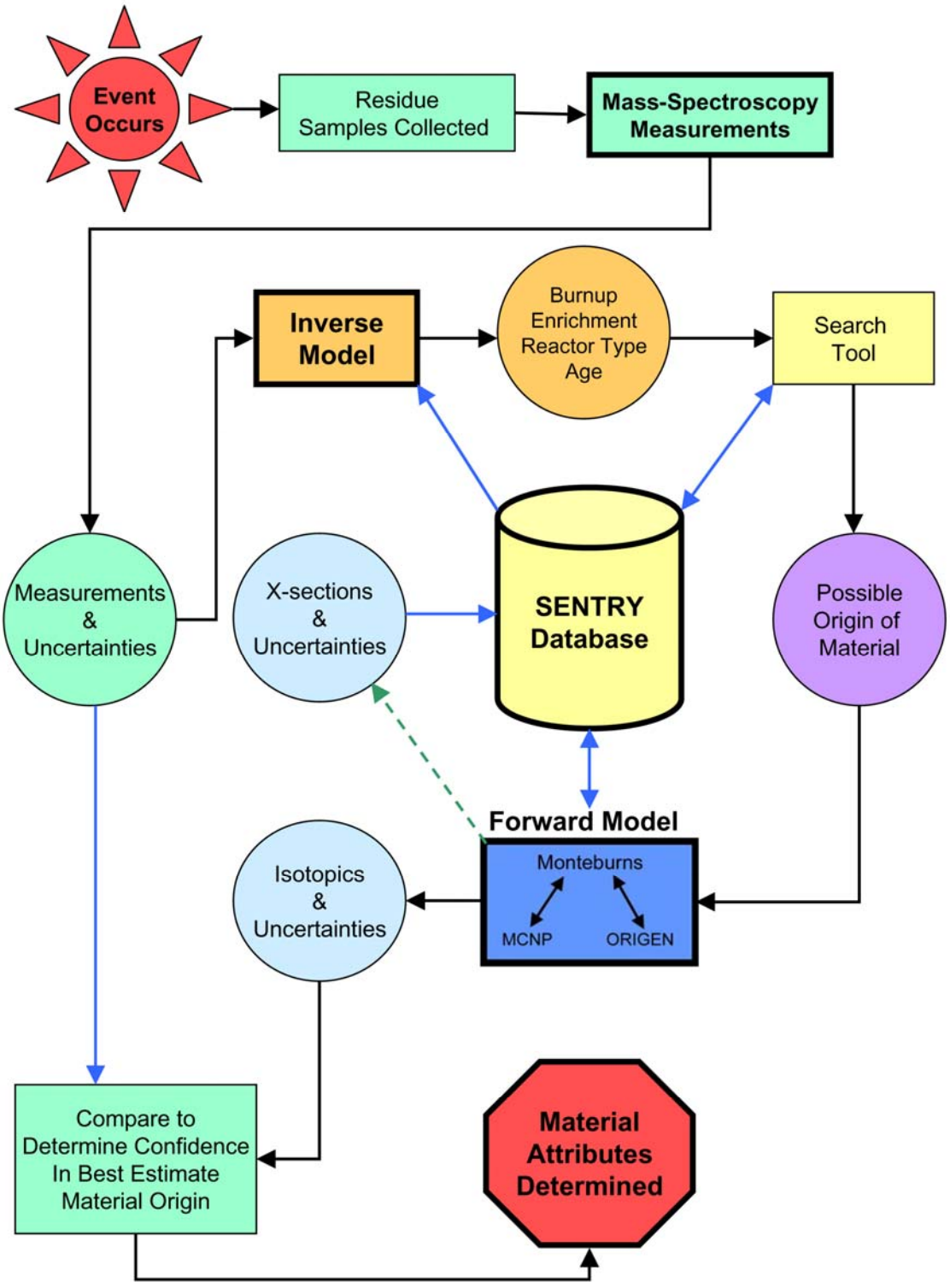

Fig. 5. Nuclear forensics attribution methodology.

For verification purposes, the possible reactors of origin are then fed back into the Forward Model. This step is important because the Inverse Model can't produce results as accurate as the Forward Model. Thus, the Inverse Model is used to produce a likely set of candidate source reactors. We then need the Forward Model to get to a unique identification. The Forward Model then produces a set of isotopics (and uncertainties) that is expected to match the measured data from the event. A comparison is done between the two to determine the confidence in the best estimate result. This research deals with both the pre-and post-event development of the Forward Model.

I.F. Isotopes of Interest

A literature review was performed in order to find spent fuel isotopic measurement data from several different reactors. The measured data used was from the following reactors: Takahama Unit #3 [17], Calvert Cliffs Unit #1 [18], and Trino Vercellese Unit #2 [19, 20]. The analyzed spent fuel from each of these reactors was taken from fuel assemblies believed to be an average of the fuel in the reactor. Each of the fuel assemblies was disassembled and individual pellets from selected fuel rods were analyzed.

The Inverse Model study produced a list of isotopes which could be used to determine each of the attributes of interest previously mentioned. The isotopes measured in the literature review were compared to the list produced by the Inverse Model. The isotopes benchmarked in the Forward Model were those found to be in both lists. Table II shows the complete list of isotopes of interest and their respective attribute. Table III contains the list of isotopes used in the Forward Model benchmarking along with the attribute associated with it.

TABLE II

Isotopes of Interest

Attribute of Interest	**Isotope**
Burnup monitors	^{140}Ce ^{100}Mo ^{148}Nd ^{101}Ru ^{99}Tc
Reactor type monitors	^{240}Pu ^{109}Ag ^{153}Eu ^{156}Gd
Fuel age	^{109}Cd ^{137}Cs ^{154}Eu ^{155}Eu ^{147}Pm ^{241}Pu ^{106}Ru ^{90}Sr
Enrichment	^{235}U ^{238}U ^{237}Np ^{238}Pu ^{239}Pu ^{240}Pu ^{241}Pu

TABLE III

Evaluated Isotopes in Forward Model

Attribute of Interest	**Isotope**
Burnup monitors	^{148}Nd
Reactor type monitors	^{240}Pu
Fuel age	^{241}Pu, ^{154}Eu, ^{137}Cs
Enrichment	^{235}U, ^{238}U, ^{239}Pu, ^{240}Pu, ^{241}Pu

CHAPTER II

FORWARD MODEL DEVELOPMENT

II.A. Introduction

This chapter describes the development of the Forward Model methodology. The first sections describe the reactor and measured data used to develop the models. The latter sections describe, in detail, the various levels of model fidelity developed and their results. This chapter concludes with a determination as to the required level of model fidelity for the nuclear forensics problem.

II.B. Event Scenario

We will assume that the terrorist will make use of a single complete fuel assembly in the manufacturing of their RDD. This assembly may be intact or crushed/ground into pieces of fine powder. This implies that the terrorist will not use only the top portion of an assembly or mix assemblies from different reactors. Any of these actions would decrease the quantity of radioactive material available for dispersion. This assumption is built on the fact that fuel assemblies are heavy and difficult to disassemble (with many parts being welded together). Also anyone handling a spent fuel assembly may receive a lethal dose of radiation.

While the physical data collected at the detonation site will yield important information, there is even more information which will remain unknown. This information includes boron concentrations in the moderator, accurate irradiation history, axial location in the assembly, radial location in the core, and proximity to control rods

and burnable poisons. While much of this information is considered essential in modern reactor model development, it must be neglected to facilitate the scenario at hand.

II.C. Takahama Unit #3 Test Case

The reactor from which the Forward Model methodology was developed was the Takahama Unit #3 reactor. This reactor was chosen because the measured data [17] is fairly recent (2001) and it boasts a wide array of isotopes.

II.C.1. Takahama Unit #3 Reactor Design Information

The Takahama Unit #3 [17] reactor is operated by Kansai Electric Power Company (KEPCO). Takahama Unit #3 is a 3-loop pressurized water reactor (PWR) with an electric output of 870 MW. The reactor core contains 157 assemblies arranged in a cylindrical geometry. Each assembly is 4.1 m in height and contains a 17×17 square fuel matrix of which there are 264 fuel rods and 25 water holes. Of the 264 fuel rods, 14 of them contain 6.0 wt% gadolinium which is used as a burnable poison. Table IV shows the basic characteristics of the reactor fuel. Table V shows the initial (pre-irradiation) isotopics of the uranium in the Takahama Unit #3 rods of interest.

TABLE IV

Nominal Reactor Parameters for Takahama Unit #3

Vendor	Mitsubishi
Type	17×17 (square)
Pin-to-pin pitch	1.26 cm
Fuel pellet diameter	0.805 cm
Clad outer diameter	0.95 cm
Fuel density	10.42 g/cm^3
Fuel enrichment	4.11 wt% ^{235}U
Active fuel length	366 cm
Clad material	Zircaloy-4
Clad density	6.53 g/cm^3
Coolant material	Light water
Coolant density	0.714 g/cm^3
Specific power	37.39 W/g

TABLE V

Initial Isotopic Compositions of SF95and SF97 Fuel Rods

Isotope	**Weight Percent of Isotope**
^{234}U	0.04
^{235}U	4.11
^{238}U	95.85

II.C.2 Measured Data

The specific fuel rods that were analyzed from the Takahama Unit #3 reactor were SF95 and SF97 [17]. SF95 came from the NT3G23 assembly which underwent two irradiation cycles and SF97 from the NT3G24 assembly which underwent three irradiation cycles. Both of these rods were located in similar positions in their respective assemblies and contained the same initial fuel characteristics (shown in Table V). Five samples (~1g U) were taken at various heights from each of the fuel rods and measured by isotope dilution mass spectrometry.

TABLE VI

Uncertainties in Measured Isotopic Concentrations (g/TIHM) for Takahama Unit #3

Isotope	**1σ Standard Deviation (%)**
^{235}U	0.1
^{238}U	0.1
^{237}Np	10.0
^{238}Pu	0.5
^{239}Pu	0.3
^{240}Pu	0.3
^{241}Pu	0.3
^{154}Eu	3.0
^{137}Cs	3.0
^{148}Nd	3.0

A gamma-ray spectrum measurement was also performed using a high-resolution germanium detector. The isotope concentrations were then decay corrected to account for the cool-down time since being discharged from the reactor. Isotopes belonging to decay chains were corrected using Bateman's formula, while others were corrected using only their half-lives. The resulting isotopic composition was given in terms of grams per ton initial heavy metal (g/TIHM). The estimated uncertainties for each of these measurements were recorded and are listed in Table VI.

The burnup of the fuel was evaluated using the ^{148}Nd method [21] in Fissions per Initial Metal Atom (%FIMA). This method uses the following equations:

$$Burnup = \frac{NF \times 100}{1 + \frac{Pu}{U} + \frac{Np}{U} + \frac{Am}{U} + \frac{Cm}{U} + NF} \tag{7}$$

and

$$NF = \frac{^{148}Nd}{U} \times \frac{1}{Y_{148}} \tag{8}$$

where Y_{148} denotes the fission yield of ^{148}Nd, NF is the number of fissions, and $\frac{Pu}{U}$, $\frac{Np}{U}$, $\frac{Am}{U}$, $\frac{Cm}{U}$ are the measured isotopic ratios of that isotope verses uranium. The 1σ standard deviation of the burnup evaluation was estimated to be within 3% [21].

II.D. Model Fidelity

To find the appropriate level of model fidelity for a given reactor, a series of tests were conducted on a reactor model possessing differing levels of fidelity. Models of the Takahama Unit #3 reactor were analyzed for both computational time requirements and accuracy of isotopic concentrations utilizing levels of fidelity ranging from 2D pin cells to 3D assemblies. The level of fidelity possessing the best combination of these two parameters was then used in the benchmarking process.

II.D.1. 2D Pin Cell

The first model analyzed was a 2D pin cell. This model consisted of a single fuel rod (fuel and cladding) surrounded by moderator. The fuel region consisted of a single radial region of fuel surrounded by cladding. The gap between fuel and cladding was ignored. The width of the pin cell was equal to the pin-to-pin spacing for the assembly (see Table IV). The pin cell was surrounded by reflecting boundaries on all sides. All of the materials in this model were inputted at room temperature (300 K). The density of the fuel was 10.42 g/cc. The water density was 1 g/cc. The clad density was 6.531 g/cc. A detailed set of isotopics, densities, and dimensions is given in Fig. 6.

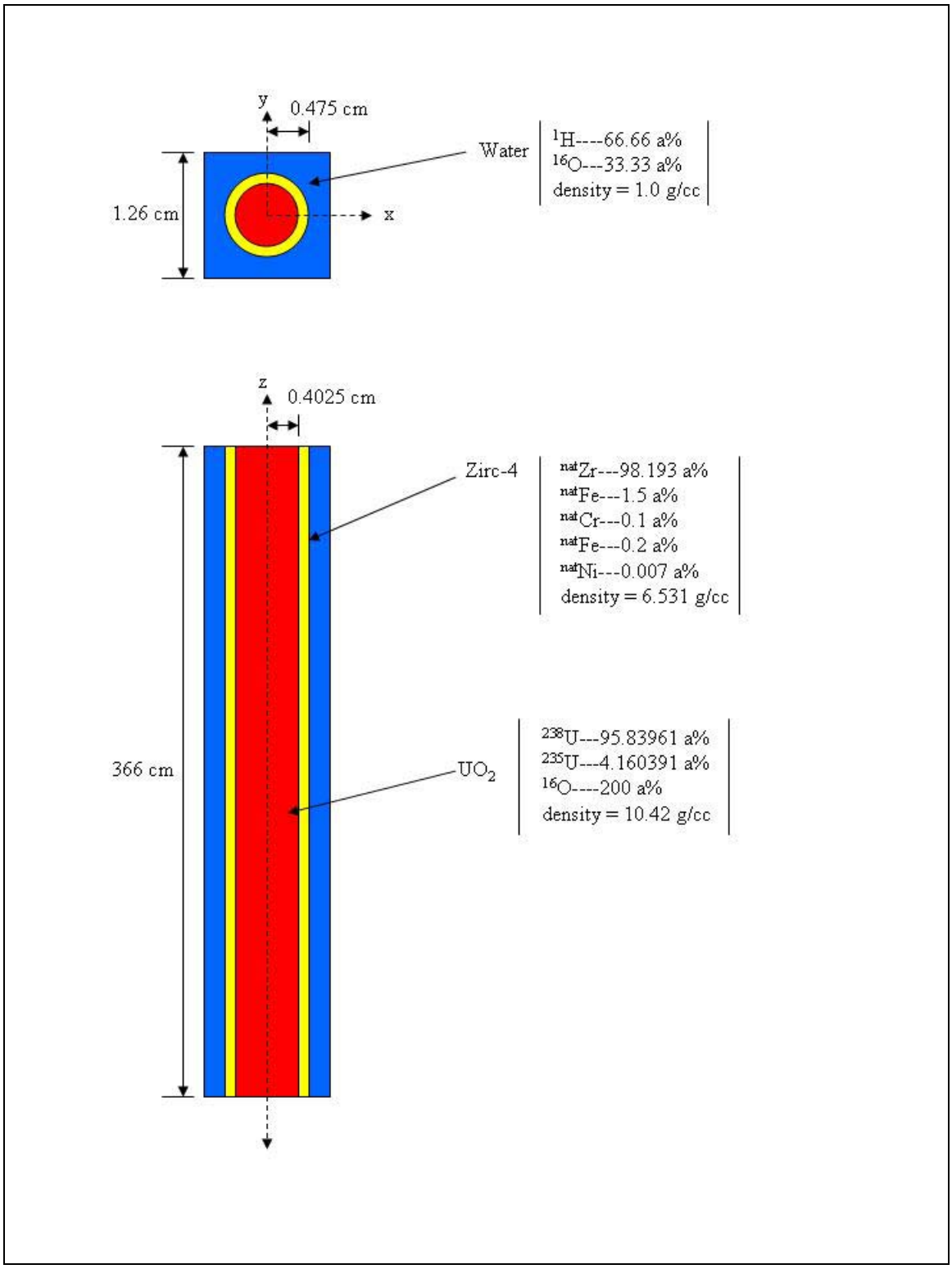

Fig. 6. Graphical representation of the 2D pin cell.

II.D.1.A. MCNP Statistical Accuracy

Since MCNP is a Monte Carlo simulation code, the number of particles to be simulated was first determined. The accuracy of two parameters were considered: the critical eigenvalue (from Kcode calculation) and the scalar flux in the fuel (from an F4 track length estimator for the flux). A criticality simulation in MCNP consists of a specific number of particles per cycle, a total number of cycles, and a number of cycles to skip before recording results. The optimal level of each of these parameters was determined by iteration until the estimated uncertainty in the criticality and flux were both less than 0.1% with the smallest required computational time. An additional consideration in this effort is that these simulations were performed using a parallelized version of MCNP. This significantly decreases the required computational time but also adds some additional considerations due to the manner in which a parallelized criticality simulation is performed. The manner by which the computer system processes the code is as follows:

1. Code is received by the master node.
2. The master node breaks the code into 20 pieces and sends each piece to a separate node.
3. Each node sends the results back to the master node at the end of one cycle.
4. This process is repeated for each MCNP cycle until the code is complete.

Due to this configuration, the greatest lag in the system is during the time when the nodes are communicating with the master. In order to facilitate the need for decreased computational time, it was more beneficial to increase the number of particles per cycles and decrease the total number of cycles to obtain the desired level of statistical

accuracy. In the end, it was found that the optimal combination of these parameters was 1000 particles per cycle and 325 total cycles for this particular model. This combination was used for all variations of the 2D pin cell, but was re-determined for the multi-region and assembly models.

II.D.1.B. Monteburns Convergence

The Monteburns code utilizes three different input files: MCNP deck, Monteburns input deck, and irradiation history feed file. At this point, the MCNP input deck (containing geometry and material composition) has already been created. The Monteburns input deck contains information on the individual isotopes to be tallied, power (MW) of the model, and the number of the burnup steps in the feed file. Most of this information is taken directly from the reactor data given in the literature [17].

As previously mentioned, ORIGEN requires a predetermined reactor specific library in order to acquire one group cross sections, fission yields, and flux spectra. This library is one of the inputs in the Monteburns input file. Although Monteburns will modify this library using the MCNP output, it is still required for initial conditions. For this methodology, the PWRU library was chosen.

The isotopes to be tallied in Monteburns consisted of the previously mentioned isotopes of interest and a standard set of actinides. A list of these actinides can be found in Table VII. Tallying these additional actinides improves the overall accuracy of the code by allowing Monteburns to update the one-group cross section sets for various reactions. It should be noted that while tallying all of the isotopes for which there are libraries would significantly increase the accuracy of the code, the tremendous increase in

computational time would far outweigh the benefits. For this reason, extra isotope tallies must be chosen very carefully.

The feed file contains the irradiation history of the fuel. The feed file allows the user to specify as few or many burnup steps as the situation requires. While more burnup steps (resulting in lower burnup per step) are desirable for purposes of accuracy, each step requires additional computational time.

TABLE VII

Monteburns Tally Isotopes

Isotopes				
^{233}U	^{239}U	^{240}Pu	^{99}Mo	^{147}Pm
^{234}U	^{237}Np	^{241}Pu	^{99}Tc	^{147}Sm
^{235}U	^{238}Np	^{242}Pu	^{101}Ru	^{153}Eu
^{236}U	^{239}Np	^{240}Am	^{109}Ag	^{154}Eu
^{237}U	^{238}Pu	^{241}Am	^{137}Cs	^{156}Gd
^{238}U	^{239}Pu	^{242}Am	^{148}Nd	^{157}Gd

A convergence test was performed to determine the optimal allowed burnup per step. The convergence test consisted of 12 different Monteburns input decks and feed files. Each of these feed files contained a total burnup of 47,500 MWd/MTU but varied in the total number of steps used from 3 to 25. This corresponds to a range from 15,833 to 1,900 MWD/MTU per step. Using ^{235}U and ^{87}Rb, the grams of material at the end of the irradiation cycle were graphed. While ^{235}U was chosen for obvious reasons as a fissile isotope, ^{87}Rb was chosen because it is a typical fission product and is located at the

peak of the fission product yield curve. Convergence points were found with both isotopes to be around 15 steps. This corresponds to a burnup step of 3,160 MWd/MTU. To ensure that the outputs remained conservative, the burnup step to be used for the remainder of this research was chosen to be 2,500 MWd/MTU. Figures 7 and 8 show the graphical convergence of ^{235}U and ^{87}Rb. 2,500 MWd/MTU per step would correspond to 19 burnup steps on this graph.

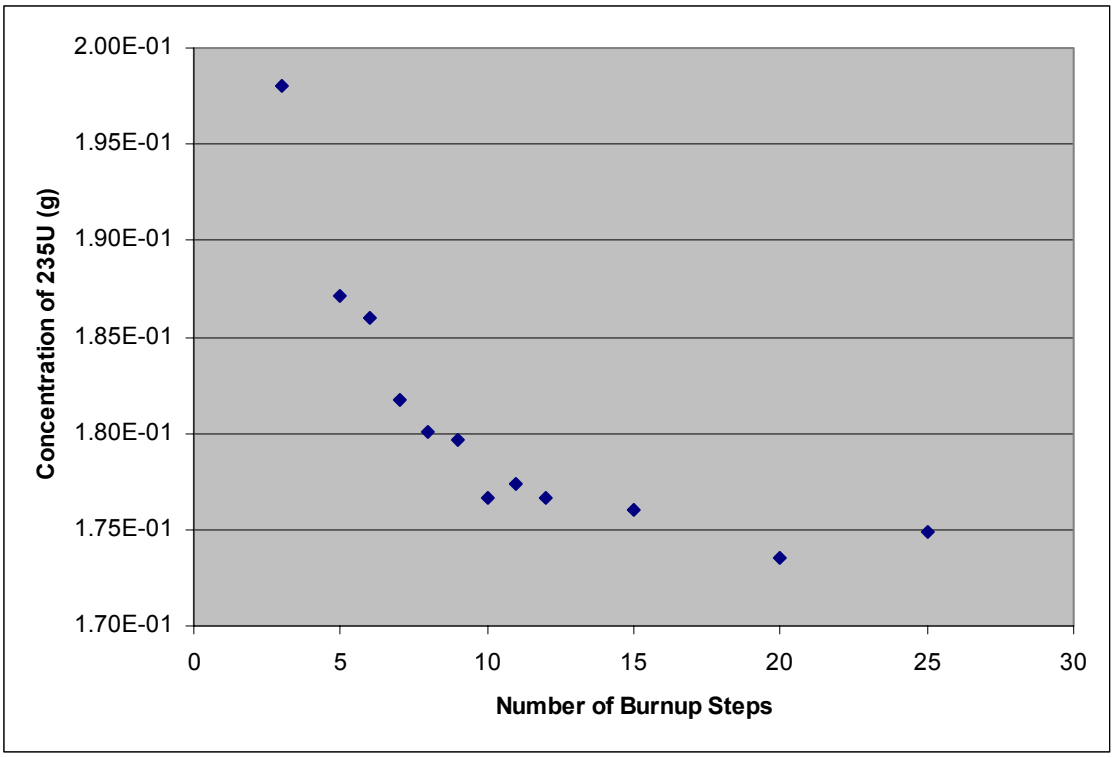

Fig. 7. Monteburns convergence of ^{235}U with burnup step.

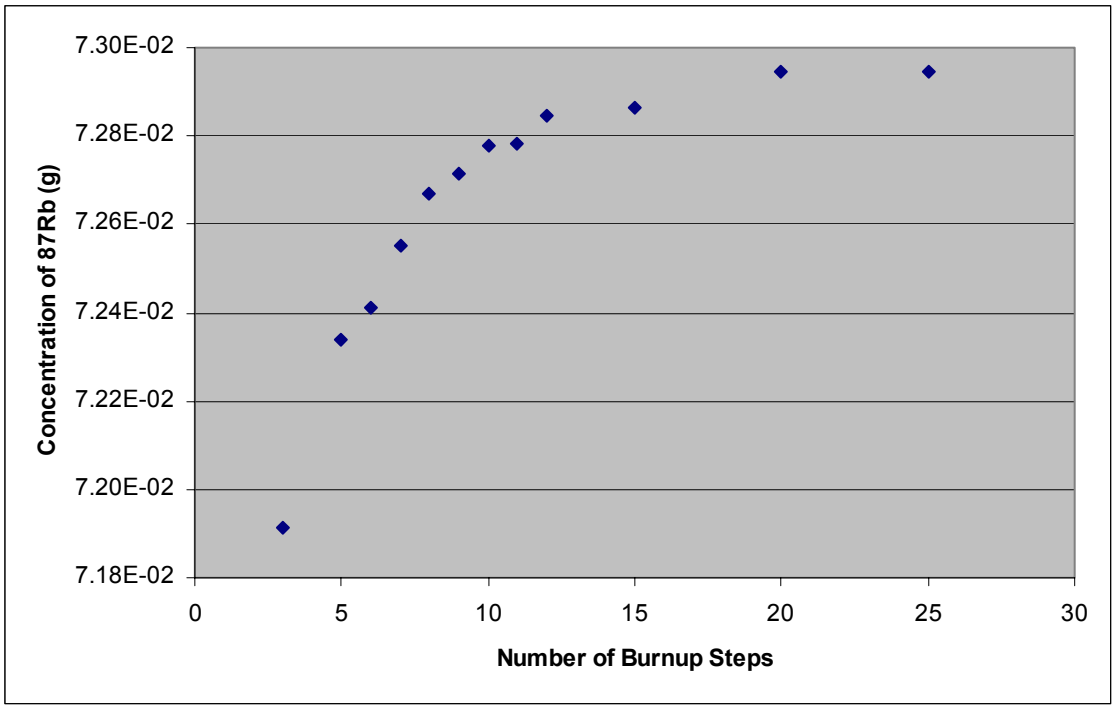

Fig. 8. Monteburns convergence of ^{87}Rb with burnup step.

It should be noted that none of the cases considered in this research contained Gd burnable absorber isotopes in the pins measured. It is expected that the inclusion of burnable absorbers would increase the required number of burnup steps to allow for convergence due to the large absorption cross sections of gadolinium. This effect however was not studied here and is left as future work.

II.D.1.C. Results From 2D Pin Cell

The isotopic concentration (g/TIHM) of ^{235}U for the 2D pin cell was analyzed using the Root Mean Square (RMS) method as shown in the following equation:

$$RMS = \frac{\sqrt{\sum_{i=1}^{I}(x_i - m)^2}}{I} \tag{9}$$

where x_i is the calculated value, m is the measured value, and I is the total number of measured values. The percent 1σ standard deviation of ^{235}U was found to be 18.81% for this model. As the concentration of ^{235}U is a direct relation to the burnup of the fuel, this large of an error showed some serious deficiencies in this level of model fidelity.

II.D.2. Advanced 2D Pin Cell

The advanced 2D pin cell model contained the same geometrical properties as the previously mentioned 2D pin cell. The difference was in the operating properties of the materials used. In the previous model, all of the materials were at room temperature (300 K). It is well known that neutron cross sections vary with changes in temperature. Some of these effects include doppler broadening of the cross section resonances, change in density of the moderator, and the thermal neutron scattering effects. The thermal neutron scattering effects are included through the use of an S(α,β) treatment in MCNP. This generates neutron cross sections (particularly for nuclides such as hydrogen) for neutron energies less than 4 eV. A detailed set of isotopics, densities, and dimensions for the advanced 2D pin cell with all the correction factors is given in Fig. 9.

The first correction factor implemented was the density of the moderator. As axial locations are not known in these models, the average moderator temperature in the core was used to determine the density. Using steam tables [22], the average density of the moderator in the core was determined. The 2D pin cell was then re-run utilizing the moderator density correction factor.

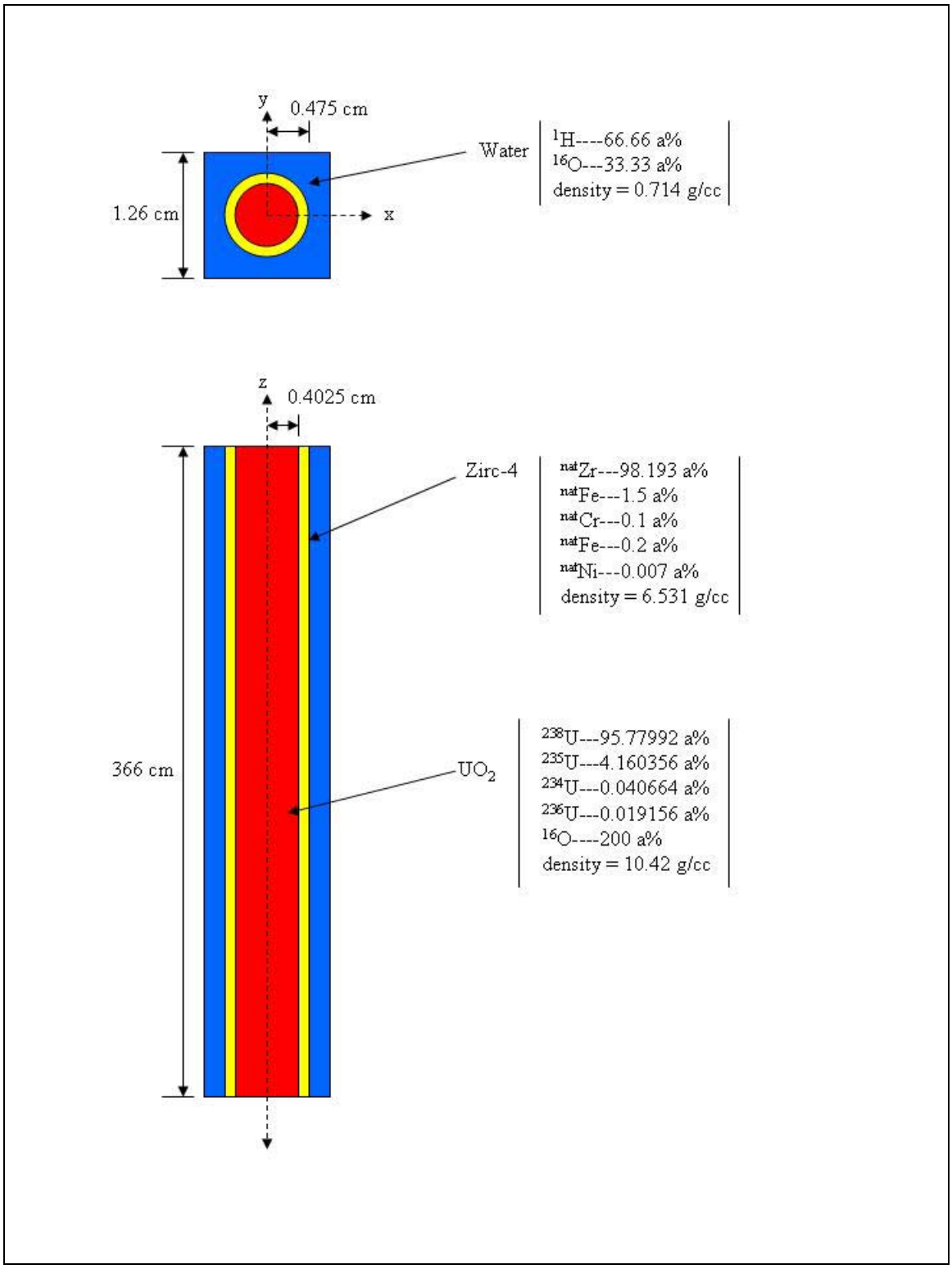

Fig. 9. Graphical representation of advanced 2D pin cell with all correction factors.

The next correction factor applied was the S(α,β) tally. This tally consisted of an "mt" card in the MCNP input file. The "mt" card chosen was the lwtr.62t. This cross section was created from the ENDF/B-VI Rev 3 and the sab2002 library and is for use specifically with hydrogen in light water at a temperature of 600K. This correction factor, along with the fuel temperature and moderator density correction factors, were used to re-run the 2D pin cell.

The next correction factor was the fuel temperature. A review of the available cross sections in the MCNP library found a cross section that better fit the environment of the model. The cross sections chosen were 92235.15c, 92238.15c, and 94239.15c. These three cross sections were created from the endf62mt library with a temperature of 800K. The 2D pin cell model was then re-run with this correction factor in place.

The last correction factor to be used was the addition of U^{234} and U^{236} to the initial fuel isotopics. While this information may not be known for the Forensics problem, there are a set of equations that can be used to accurately predict the concentrations of these isotopes based on the enrichment of the fuel. These equations are as follows:

$$^{234}U\ \ wt\% = 0.0089 \times {}^{235}U\ \ wt\% \tag{10}$$

$$^{236}U\ \ wt\% = 0.0046 \times {}^{235}U\ \ wt\% \tag{11}$$

where ^{X}U is an isotopic designation and *wt%* is the weight percent of that isotope with respect to the rest of the fuel.

While ^{236}U does not exist in nature, it should be noted that the inclusion of ^{236}U isotopes in fresh fuel is only for U.S. born fresh fuel. This occurs because U.S. enrichment plants are contaminated with ^{236}U due to a previous processing of naval reactor spent fuel through the plants.

TABLE VIII

RMS Percent Error of ^{235}U in Advanced 2D Pin Cell

Correction factor	**1σ Standard Deviation (%)**
No Correction	18.81
Moderator Density	7.86
S(αβ) card	3.65
Fuel Temperature	2.31
^{234}U & ^{236}U	1.56

TABLE IX

RMS Percent Error of 2D Pin Cell Utilizing All of the Correction Factors

Isotope	**1σ Standard Deviation (%)**
^{235}U	1.56
^{238}U	0.04
^{238}Pu	8.25
^{239}Pu	4.41
^{240}Pu	2.58
^{241}Pu	6.81
^{237}Np	6.14
^{137}Cs	1.65
^{148}Nd	0.64
^{154}Eu	16.42

The results showed a significant increase in accuracy with each additional correction factor being used. It should also be noted that the addition of these correction factors did not significantly change the computational time required to run the code. For this reason, all four correction factors were used in all the models that followed. Table VIII shows the RMS percent error of ^{235}U of the various correction factors tested in the advanced 2D pin cell. Table IX shows RMS percent error of all of the isotopes of interest for the advanced 2D pin cell utilizing all of the correction factors.

II.D.3. Multi-Radial Region Pin Cell

The multi-radial region pin cell was comprised of the same physical geometry as the 2D pin cell as well as all of the correction factors from the advanced 2D pin cell model; however, in this model the fuel region is broken into several different radial regions. This adjustment allows for a more accurate simulation of the burnup effects due to pin self-shielding. To account for this, the fuel region was broken into several radial regions using the following exponential equation [1]:

$$r(i) = R_{fo}\left[\frac{1-\exp(-\Sigma_a i)}{1-\exp(-\Sigma_a N_r)}\right] \tag{12}$$

where $r(i)$ is the outer radius of fuel region i, R_{fo} is the fuel outer radius, N_r is the total number of radial fuel regions, and Σ_a is the one-group macroscopic absorption cross section. A detailed set of isotopics, densities, and dimensions for the multi-radial region pin cell is given in Fig. 10.

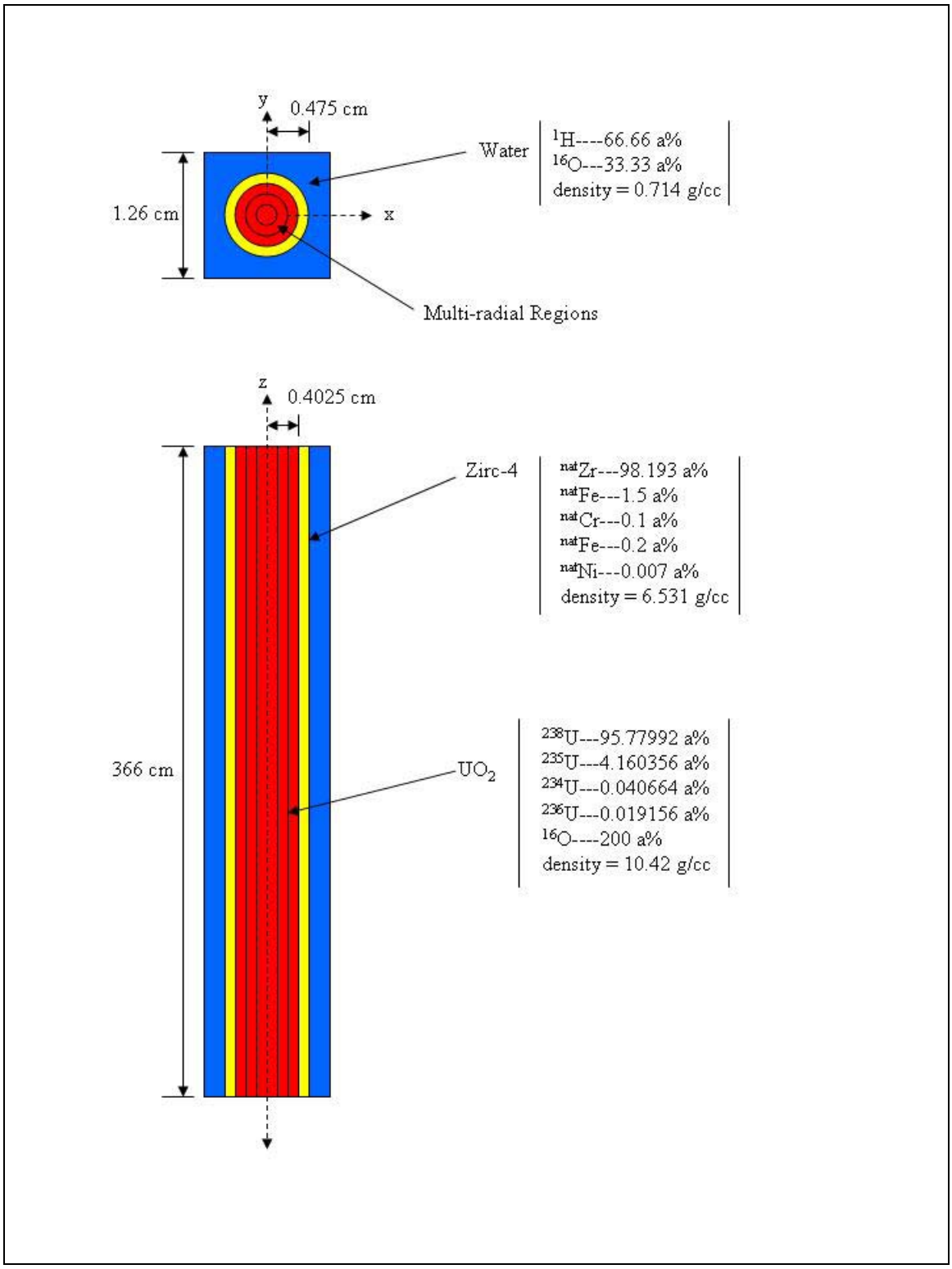

Fig. 10. Graphical representation of the multi-radial region pin cell.

The number of radial regions in the model was varied from 1 to 7. The results showed that seven radial regions is the optimum converging point. The addition of radial regions added significant computational time to the model. The computational time required for the seven-region model was approximately seven times greater than that of the single region model. When compared to that of the advanced 2D pin cell, the seven-region model had an increase in accuracy of only 0.07% for ^{235}U. As the accuracy for most of the isotopes being examined was around the 2-5% range, this increase was inconsequential. For this reason, it was decided that the Forward Model would contain only one radial fuel region. The results of this model can be seen in Table X.

TABLE X

RMS Percent Error of the Multi-Radial Region Pin Cell

Isotope	**1σ Standard Deviation (%)**
^{235}U	1.49
^{238}U	0.05
^{238}Pu	10.76
^{239}Pu	4.63
^{240}Pu	2.34
^{241}Pu	6.70
^{237}Np	7.57
^{137}Cs	1.63
^{148}Nd	0.66
^{154}Eu	16.45

II.D.4. Modified Pin Cell

The modified pin cell contained the correction factors of the advanced 2D pin cell as well as a single radial region in the fuel. The geometry however was modified to increase the amount of moderator surrounding the fuel pin. This accounts for the increased moderator in the assembly due to water holes and the interassembly regions. The formula which determined the amount of moderator in the model was as follows [1]:

$$P_{FM} = \frac{P_{asb}}{\sqrt{N_{pins}}} \tag{13}$$

where P_{FM} is the adjusted pin-to-pin pitch, P_{asb} is the assembly pitch, and N_{pins} is the number of fuel pins per assembly. A detailed set of isotopics, densities, and dimensions for the modified pin cell is given in Fig. 11.

The results of this model did not compare with previous research [1] in that the accuracy of the modified pin cell was worse than that of the advanced 2D pin cell. In particular, the amount of ^{235}U was well below the level it should have been. This indicated that the additional moderator had over-thermalized the system and caused too much fission to occur. This outcome, peculiar at first, was further investigated to verify the validity of the results. The results were verified by building both an advanced 2D pin cell model and a modified pin cell model in which the appropriate amount of boron was in the system. The results of this model can be seen in Table XI.

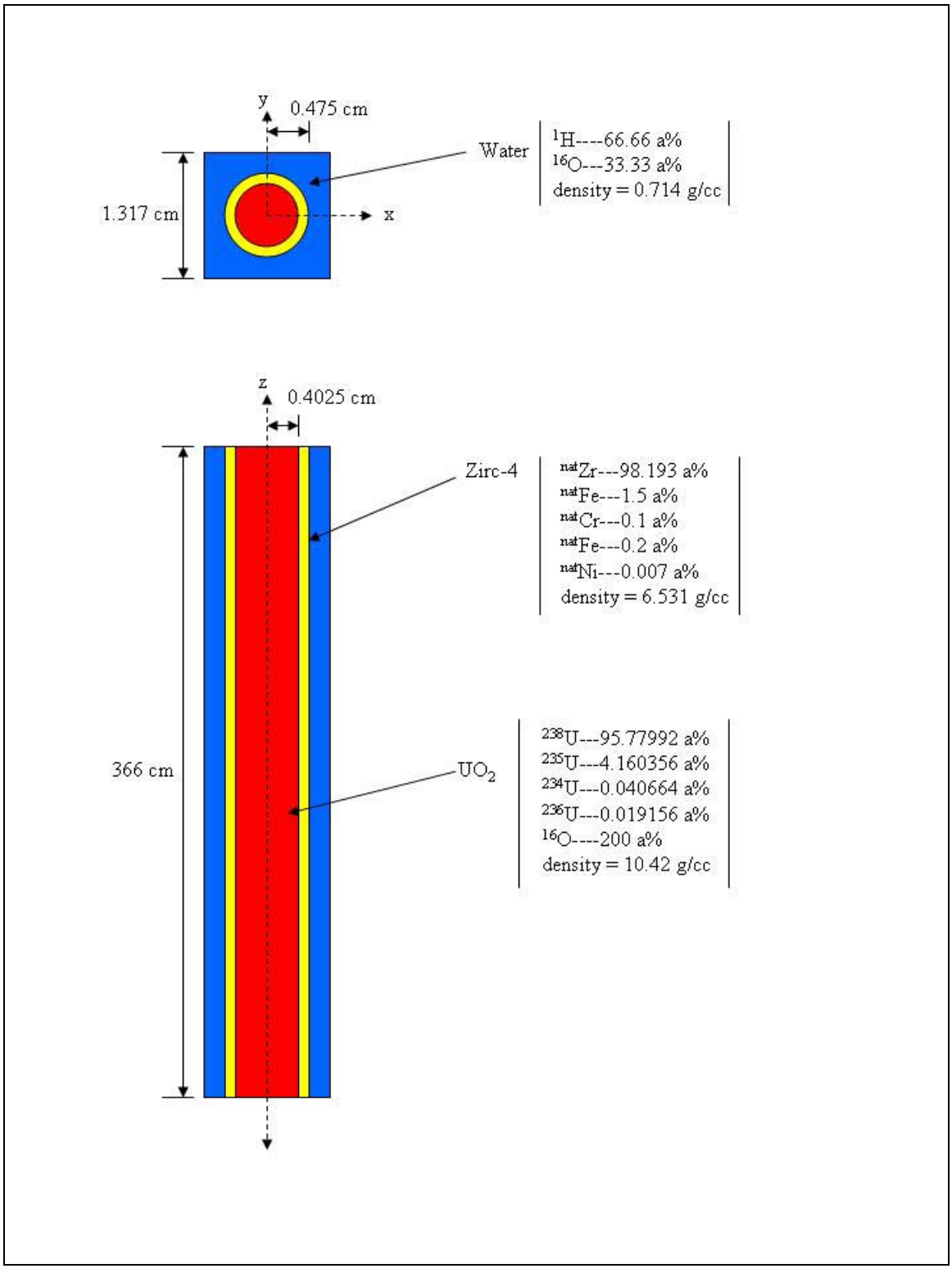

Fig. 11. Graphical representation of the modified pin cell.

TABLE XI

RMS Percent Error of the Modified Pin Cell

Isotope	1σ Standard Deviation (%)
^{235}U	5.03
^{238}U	0.13
^{238}Pu	19.59
^{239}Pu	11.63
^{240}Pu	1.96
^{241}Pu	13.47
^{237}Np	12.22
^{137}Cs	1.64
^{148}Nd	0.59
^{154}Eu	13.29

The results of the advanced 2D pin cell with boron showed that the amount of ^{235}U was far greater than it should have been. However, the results from the modified pin cell (with boron) showed staggering accuracy. It was determined that although the addition of boron in a non-modified pin cell will over-moderate the system, the modified pin cell appropriately compensates for this by increasing the thermalization of the system. This test concluded that the first results from the modified pin cell had in fact been correct and that this model would not yield the desired accuracy that had been hoped. It was thus concluded that the advanced 2D pin cell was still the most accurate model for

this scenario. Fig. 12 shows a graphic representation of the ^{235}U content as a result of advanced 2D pin cell, modified pin cell, and advanced 2D pin cell with boron.

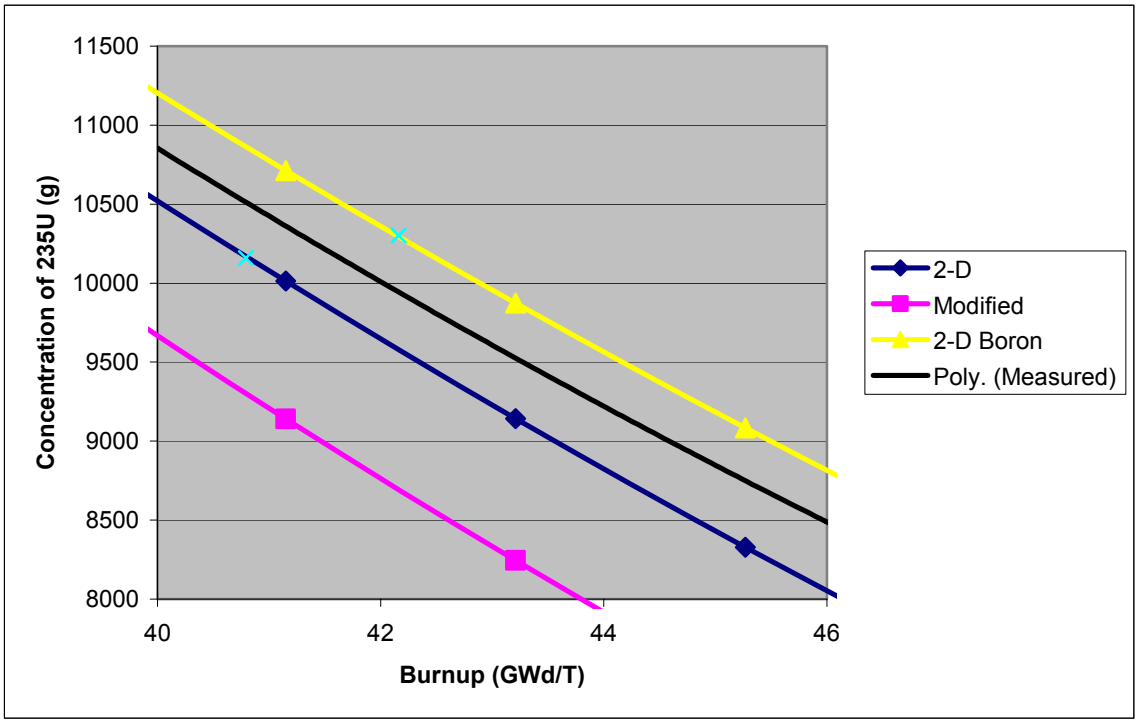

Fig. 12. ^{235}U concentrations from various model tests.

II.D.5. 2D Assembly

This model consisted of a full assembly of fuel rods, water holes, and Gd-bearing fuel rods. Each of the fuel rods consisted of only one radial region and included the correction factors of the advanced 2D pin cell. The inter-assembly area was not accounted for. The outer surfaces of the assembly again consisted of reflecting boundaries.

This was a 2D model. This model contained reflecting boundaries on the axial top and bottom of the fuel region assembly. As with the previous models (section

II.D.1.B.), MCNP tests were run to determine the required number of cycles and particles per cycle. As the size of the assembly model was almost 300 times the size of the pin cell models, a larger number of particles (60,000 particles per cycle with 200 cycles) and was required to retain the desired accuracies of MCNP. A detailed set of isotopics, densities, and dimensions for the 2D assembly is given in Fig. 13. The results of this model can be found in Table XII.

TABLE XII

RMS Percent Error of the 2D Assembly

Isotope	**1σ Standard Deviation (%)**
^{235}**U**	2.22
^{238}**U**	0.08
^{238}**Pu**	12.79
^{239}**Pu**	6.32
^{240}**Pu**	1.81
^{241}**Pu**	7.71
^{237}**Np**	7.74
^{137}**Cs**	1.58
^{148}**Nd**	0.69
^{154}**Eu**	15.73

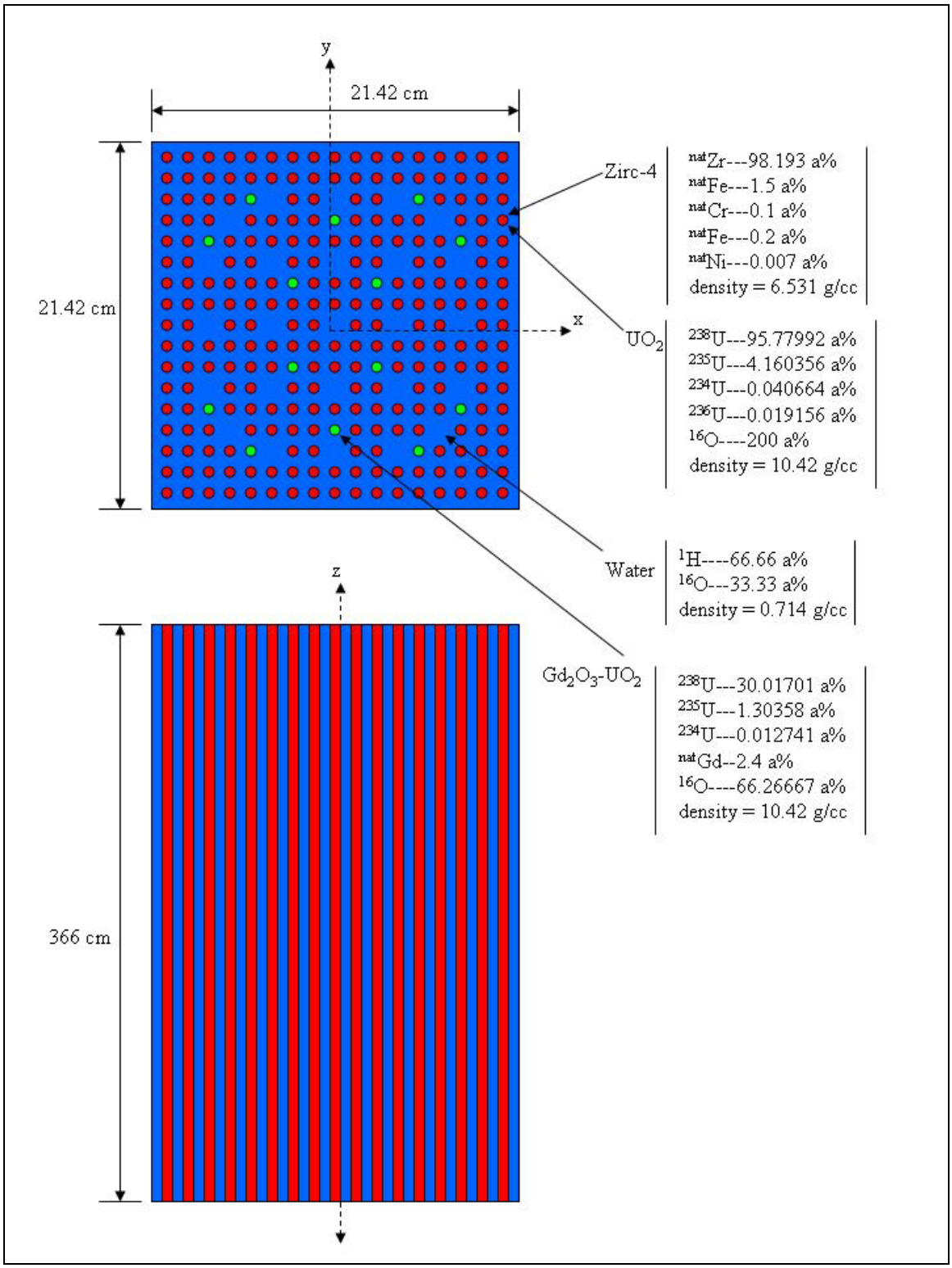

Fig. 13. Graphical representation of the 2D assembly model.

II.D.6. 3D Assembly

This model was a 3D model. This model retained the same geometrical characteristics as the 2D assembly except that the reflecting axial boundaries were removed and replaced with an appropriate stainless steel cap and moderator region. This effectively changed the axial neutron flux profile in the fuel rod. With the neutron flux in the upper and lower quadrants being reduced, the number of fissions occurring in those regions will also be reduced. This will in turn change the axial isotopic concentrations of the fuel rod. A detailed set of isotopics, densities, and dimensions for the 3D assembly is given in Fig. 14. Table XIII shows the results from the 3D assembly model.

TABLE XIII

RMS Percent Error of the 3D Assembly

Isotope	**1 σ Standard Deviation (%)**
^{235}U	2.26
^{238}U	0.07
^{238}Pu	12.63
^{239}Pu	6.26
^{240}Pu	1.85
^{241}Pu	7.69
^{237}Np	7.98
^{137}Cs	1.56
^{148}Nd	0.69
^{154}Eu	15.66

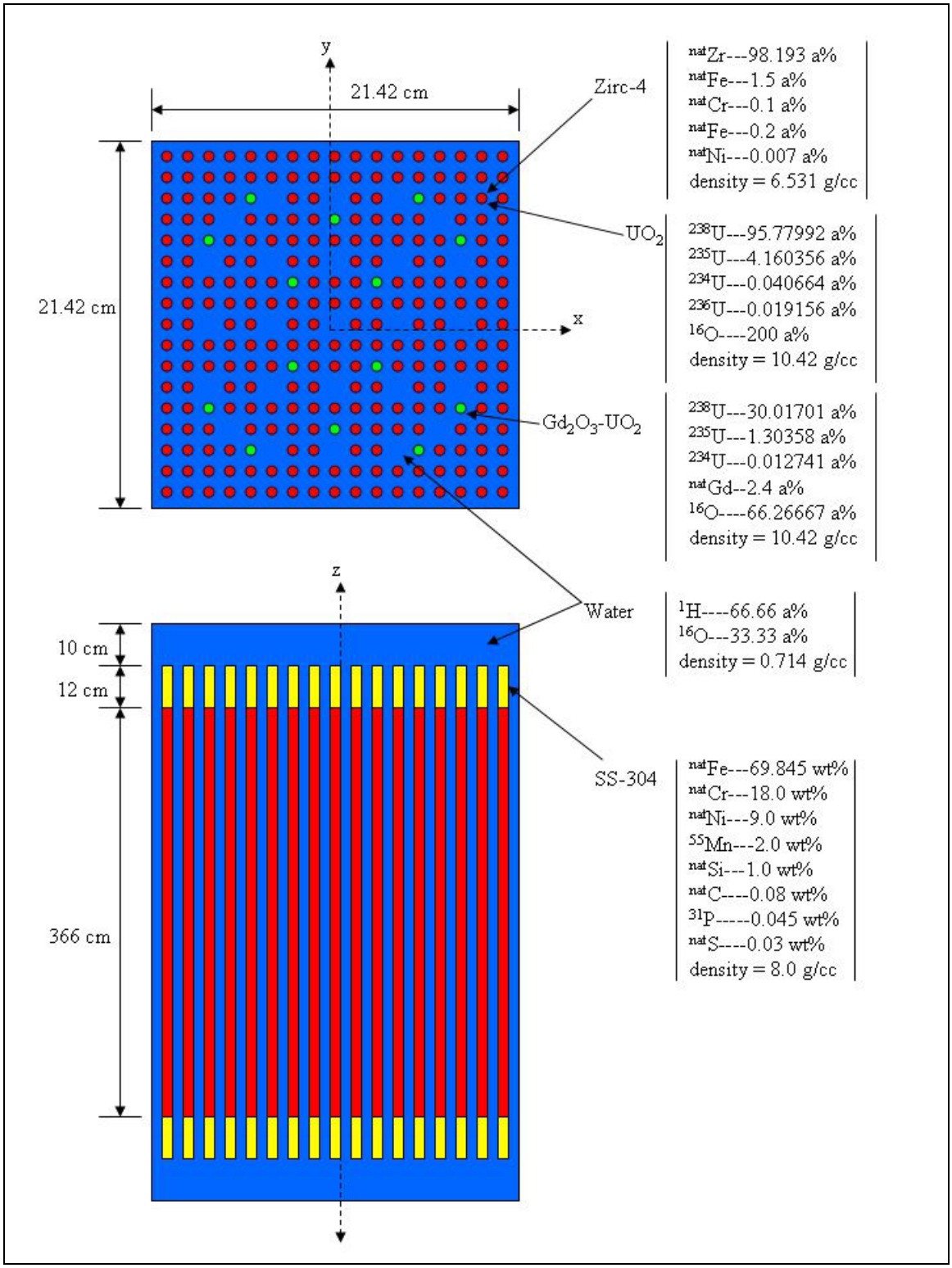

Fig. 14. Graphical representation of the 3D assembly model.

The results of both of the assembly models showed a decrease in accuracy compared to that of the advanced 2D pin cell. In particular, the concentration of ^{235}U was much lower. It was determined that the lack of boron in the system was again the problem with these models. Due to the number of particles required to run this model, the computational times for these models were significantly greater.

II.E. Comparison of Models

The results of all the different Takahama Unit #3 models can be seen in Table XIV. As can be seen, both the advanced 2D pin cell and the multi-region pin cell showed a greater level of accuracy for the isotopes being examined than did the other models. For most of the isotopes, both the advanced 2D pin cell and multi-region pin cell exhibited the same level of accuracy. The computational requirements of the multi-region pin cell were found to be seven times greater than that of the advanced 2D pin cell. As the multi-region pin cell did not have any significant advantages over the advanced 2D pin cell, it was decided that the advanced 2D pin cell would be used in further model development.

TABLE XIV

RMS Percent Error of Isotopes of Interest in Various Models

	Adv. 2D pin cell	Multi-region pin cell	Modified pin cell	2D assembly	3D assembly
^{235}U	1.56	1.49	5.03	2.22	2.26
^{238}U	0.04	0.05	0.13	0.08	0.07
^{238}Pu	8.25	10.76	19.59	12.79	12.63
^{239}Pu	4.41	4.63	11.63	6.32	6.26
^{240}Pu	2.58	2.34	1.96	1.81	1.85
^{241}Pu	6.81	6.70	13.47	7.71	7.69
^{237}Np	6.14	7.57	12.22	7.74	7.98
^{137}Cs	1.65	1.63	1.64	1.58	1.56
^{148}Nd	0.64	0.66	0.59	0.69	0.69
^{154}Eu	16.42	16.45	13.29	15.73	15.66

II.F. Additional Factors of Consideration

After analyzing the data, it was determined that other factors might need to be explored to ensure optimal accuracy of the models. The first of these factors was the value of Q-fission in the Monteburns input file. It is known that the fissioning of ^{235}U releases on average 196 MeV of energy per fission. However, throughout the irradiation process there is a buildup of other fissionable isotopes such as ^{239}Pu. As the concentration of these additional fissionable isotopes increases, the mean value of Q-fission will also change. While Monteburns does account for this change in the Q-fission

value, it is important to give it the correct starting point. The value used thus far for this term was 200 MeV per fission. This value was chosen because it is a more generic value for models such as this. Nonetheless, it was deemed necessary to re-run the best model (advanced 2D pin cell) with a value of 196 MeV per fission for Q-fission. As expected, the accuracy of the model utilizing 196 MeV per fission was lower than that of the 200 MeV per fission. Thus, 200 MeV per fission was retained as the value for Q-fission.

Of the isotopes being analyzed, only one of them showed a significant amount of error in its accuracy. This isotope was ^{154}Eu. Upon inspection of the cross sections and fission yields in the ORIGEN libraries, it was determined that there might be additional isotopes tallies necessary to add to the Monteburns input file. This determination was largely based on the fact that the most prominent path to ^{154}Eu was through the neutron absorption and decay of other isotopes through ^{153}Sm and ^{153}Eu. It was possible that Monteburns was not accurately calculating the neutron absorption cross sections of these two isotopes. As there were no cross section files available for ^{153}Sm, the model was re-run with only ^{153}Eu as an additional isotope tally.

The use of the ^{153}Eu isotope tally contributed to a decrease in the error of the accuracy by 50%. Even with this reduction in error, the accuracy was still not sufficient. It was thus decided to try adding the ^{153}Sm to the tally. As there were no cross section files for this isotope, one was created from the JEF 3.0 library using NJOY. Unfortunately, the use of the ^{153}Sm isotope tally did not show any real change in the isotopic composition of the model. For this reason, it was decided that ^{153}Sm would not be included in the isotope tallies. Table XV shows the RMS percent error of the isotopes of interest utilizing the additional correction factors on the advanced 2D pin cell.

TABLE XV

RMS Percent Error of Isotopes of Interest Utilizing Additional Correction Factors

	Adv. 2D pin cell	**^{153}Eu tally**	**196 MeV Q-fission**	**^{153}Sm tally**
^{235}U	1.56	1.56	2.95	1.56
^{238}U	0.04	0.04	0.03	0.04
^{238}Pu	8.25	8.25	8.32	8.25
^{239}Pu	4.41	4.41	4.45	4.41
^{240}Pu	2.58	2.58	3.11	2.58
^{241}Pu	6.81	6.81	5.83	6.81
^{237}Np	6.14	6.14	6.52	6.14
^{137}Cs	1.65	1.65	0.75	1.65
^{148}Nd	0.64	0.64	1.5	0.64
^{154}Eu	26.82	16.42	17.53	16.44

II.G. Best Estimate Model

The results of the Forward Model methodology showed conclusively that the advanced 2D pin cell provided the greatest level of accuracy while maintaining a minimum degree of computational time. It is also recommended that 200 MeV per fission be used as the value for Q-fission in the Monteburns input file. If the ^{154}Eu isotope is to be tallied, it will also be necessary to tally the ^{153}Eu isotope along with it. A complete list of measured versus calculated data can be found in Appendix B. Graphs of all of the isotopic data can be found in Appendix C.

CHAPTER III

FORWARD MODEL BENCHMARKING

III.A. Introduction

This chapter describes the Forward Model benchmarking process for the methodology developed in Chapter II. The first part of this chapter describes the various reactors and their respective data used to benchmark the methodology. The last sections describe the results of the benchmarking.

III.B. Calvert Cliffs Unit #1

Measured data has been collected extensively from the Calvert Cliffs Unit #1 reactor. This data has been used to determine the nuclide content of spent nuclear fuel as well as efforts to benchmark reactor codes [1]. Although not all of the isotopes of interest were included in the study [18], it was decided that it would be a good benchmarking tool for those isotopes that are included.

III.B.1. Reactor and Fuel Description

Calvert Cliffs is a Combustion Engineering designed 2-loop PWR operating at 883 MW electric. The core contains 82,854 kg UO_2 with a specific power of 30.9 W/g. There are 390 assemblies in a rectangular array, each containing a 14×14 square lattice of fuel rods and waterholes. There are a total of 172 fuel rods in the assembly. The enrichment of the fuel varies from 2.05 wt% to 2.99 wt% depending on the location in the core [18]. Table XVI shows the parameters for this reactor that were used in the benchmarking calculations. Although an assembly level model was not built for this

reactor, Fig. 15 shows a graphical representation of the fuel assembly. Figure 16 shows a graphical representation of the Calvert Cliffs Unit #1 pin cell.

TABLE XVI

Nominal Reactor Parameters for Calvert Cliffs Unit #1

Vendor	Combustion Engineering
Type	14×14 (square)
Pin-to-pin pitch	1.4754 cm
Fuel pellet diameter	0.964 cm
Clad outer diameter	1.117 cm
Fuel density	10.42 g/cm^3
Fuel enrichment	2.45 wt% ^{235}U
Active fuel length	347 cm
Clad material	Zircaloy-4
Clad density	6.53 g/cm^3
Coolant material	Light water
Coolant density	0.714 g/cm^3
Specific power	30.9 W/g

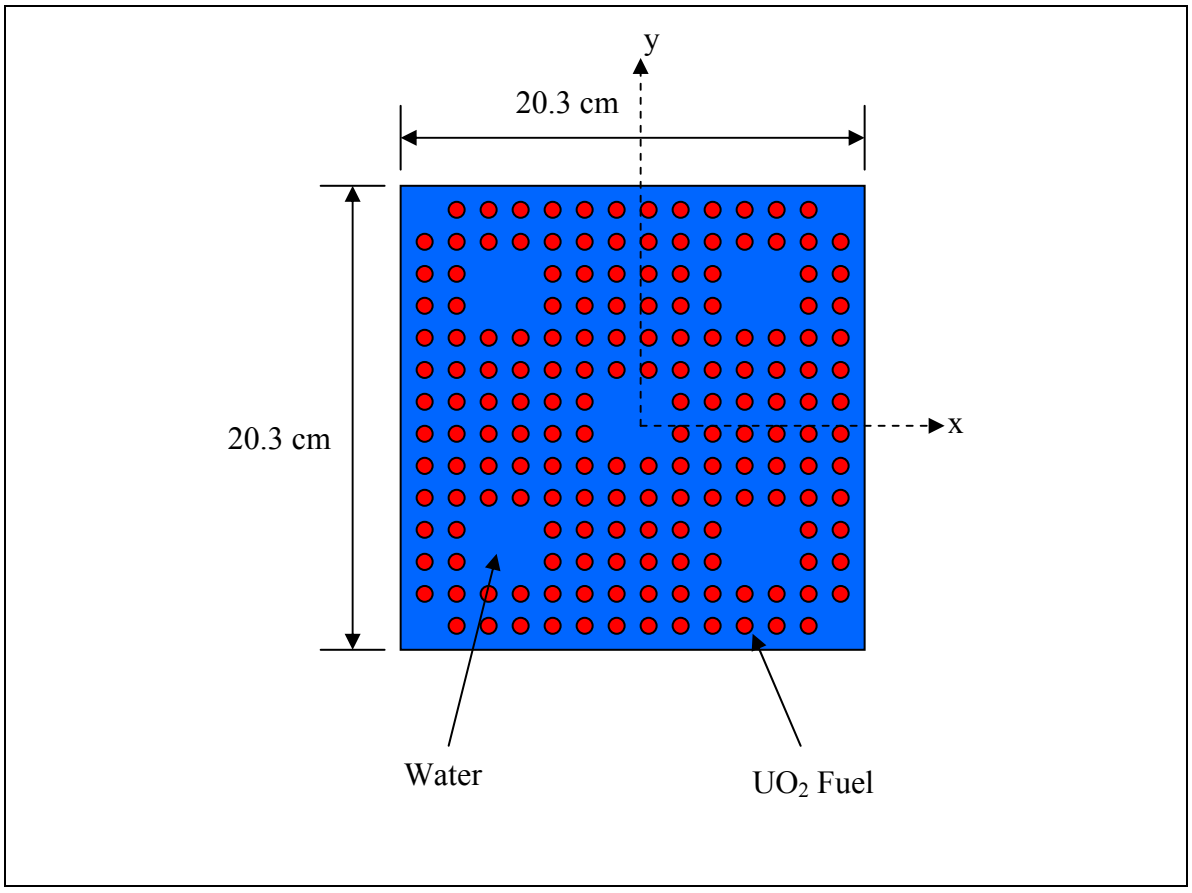

Fig. 15. Graphical representation of Calvert Cliffs Unit #1 fuel assembly.

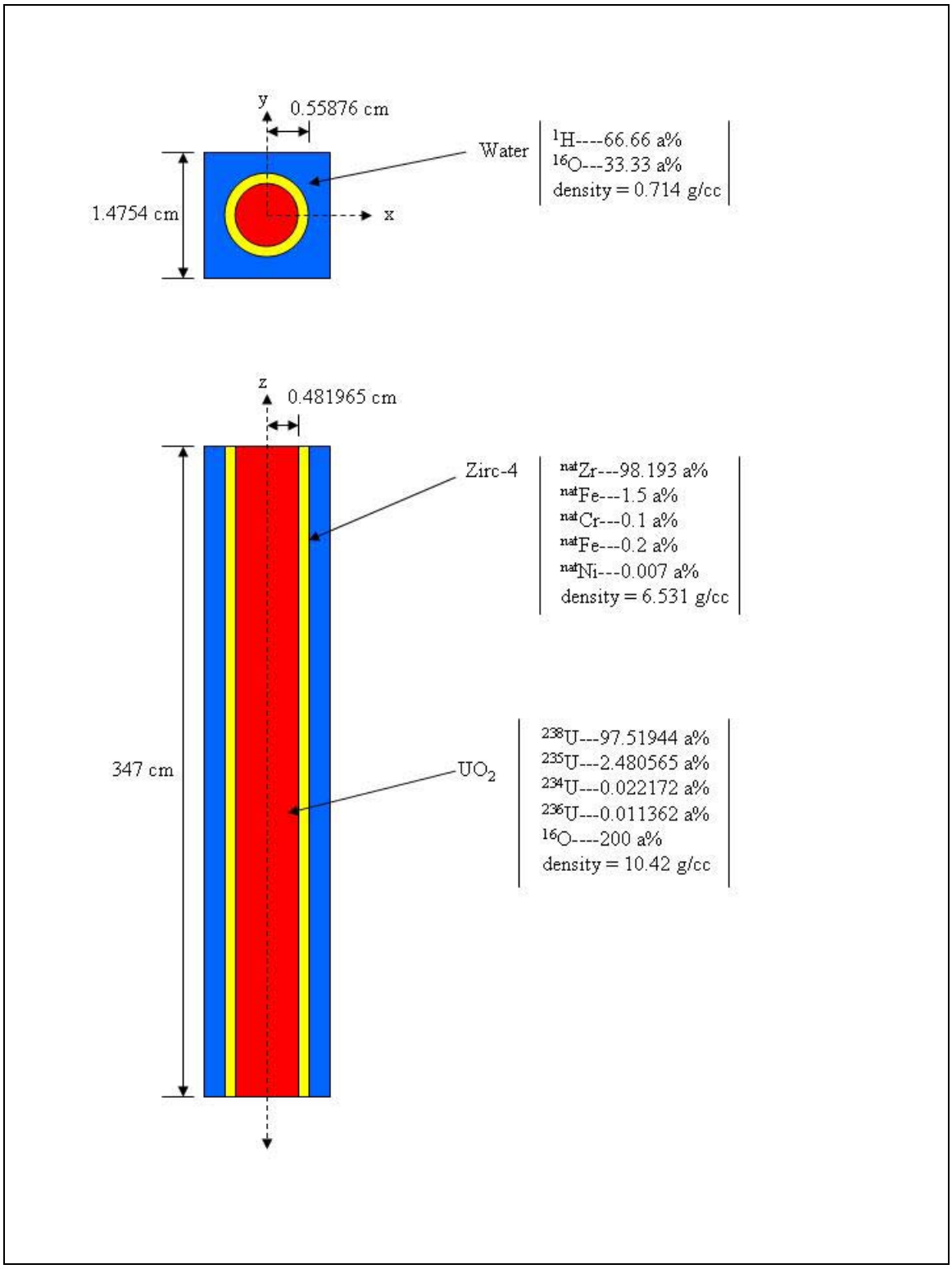

Fig. 16. Graphical representation of Calvert Cliffs Unit #1 pin cell.

III.B.2. Fuel Measurements

The specific fuel rod analyzed was AHS-023. This fuel rod came from the BT03 assembly which was irradiated for three cycles. Gamma scans were used to verify both the peak axial burnup region and that there was no pellet-pellet gaps in the fuel rod before making the sample selections. Five ½ inch long samples were selected over the axial region from 101.5 to 104 inches. The burnup of the samples was determined according to the ASTM method (^{148}Nd method) [23]. This process involves the chemical separation of neodymium from the irradiated fuel. The dissolved residue is then analyzed by isotopic dilution mass spectrometry. Destructive analyses were then performed using mass spectrometric analysis to determine the isotopic abundances in the fuel [24]. Table XVII shows the uncertainties of the measured isotopes for Calvert Cliffs Unit #1.

TABLE XVII

Uncertainties in Measured Isotopes for Calvert Cliffs Unit #1

Isotope	**1σ Standard Deviation (%)**
^{235}U	4.7
^{238}U	0.04
^{238}Pu	0.15
^{239}Pu	0.16
^{240}Pu	0.38
^{241}Pu	0.37
^{148}Nd	2.7

III.B.3. Forward Model Simulations

The model for this reactor was built using the methodology developed in Chapter II. According to this methodology, the model consisted of an advanced 2D pin cell with the following correction factors: appropriate fuel temperature cross section file, moderator density, S(α,β) tally, ^{234}U and ^{236}U initial fuel concentration, and 200 MeV per fission for Q-fission in the Monteburns input file. Since the measured data for this reactor did not include ^{154}Eu, the ^{153}Eu tally was not included.

Another differing aspect of the measured data was that it was not decay-corrected back to the time of discharge from the reactor. This posed an interesting problem as the Monteburns feed file does not allow for a secondary decay at each burnup step. Instead of a single feed file, 25 separate feed files were created as there were 25 burnup steps. Each feed file had one more burnup step than the last and was followed by a 570 day decay step. The outputs from the last step of each of these files were then combined as if it were a single output. This combined output could then be analyzed in the same manner as previous outputs. The use of 25 feed files implies that the model must be run 25 times. This correction, while lengthy to complete, turned out to be quite effective.

The data from the model was then compared to the measured data using the RMS method. Table XVIII shows the RMS percent error of the isotopes of interest for the Calvert Cliffs Unit #1 reactor model. Figure 17 shows the calculated linear fit of the ^{148}Nd data compared to the measured data. The measured data also shows 2.7% error bars as that was the measured error for that isotope. A complete list of measured versus calculated data can be found in Appendix B. Graphs of all of the isotopic data can be found in Appendix C.

TABLE XVIII

RMS Percent Error of Isotopes of Interest for Calvert Cliffs Unit #1

Isotope	1σ Standard Deviation (%)
^{235}U	3.55
^{238}U	0.02
^{238}Pu	2.68
^{239}Pu	1.67
^{240}Pu	3.92
^{241}Pu	1.21
^{148}Nd	1.75

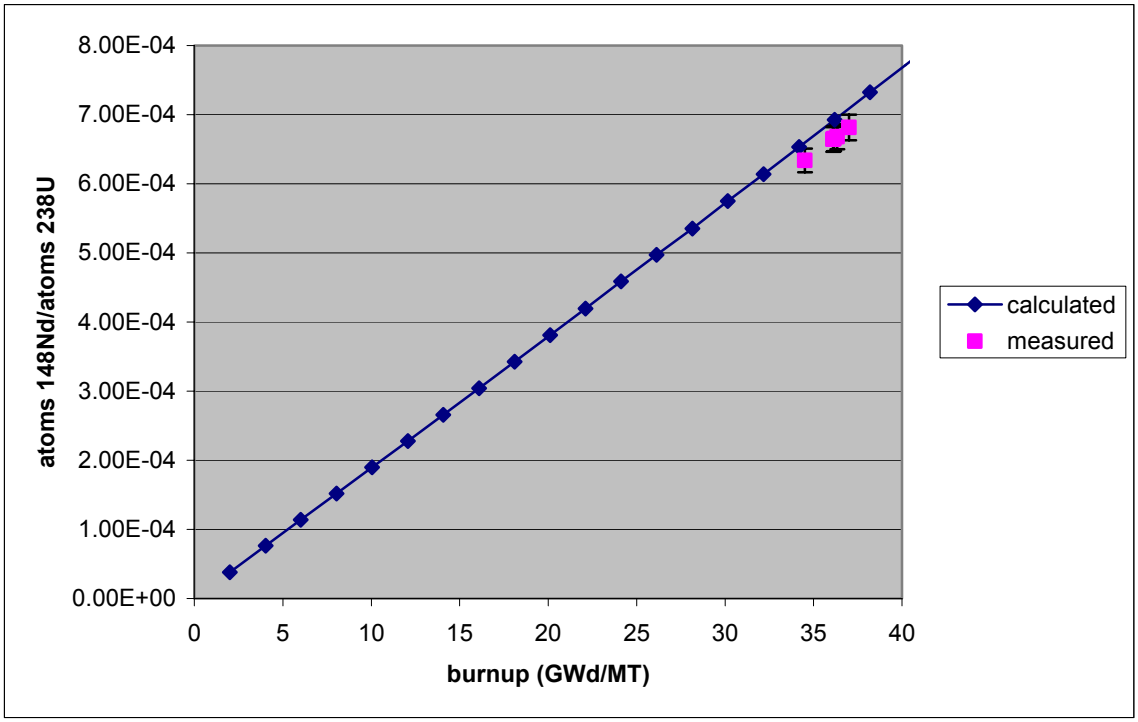

Fig. 17. Calculated and measured data of ^{148}Nd for Calvert Cliffs Unit #3.

III.C. Trino Vercelles Unit #2

The Trino Vercelles Unit #2 reactor is different from Takahama and Calvert Cliffs in that it does not contain uniform fuel assemblies. In this reactor, the control blades protrude into the fuel assemblies with varying amounts depending on the location of the assembly. This reactor was chosen to demonstrate the accuracy of the benchmarking methodology with non-standard fuel assemblies. The isotopic data [20] for this reactor also contained a good population of isotopes of interest, especially ^{154}Eu which was found to be an isotope of issue in the Takahama reactor.

III.C.1. Reactor and Fuel Description

Trino Vercelles is a Westinghouse designed PWR operating at 825 MW electric. The core contains 44,634 kg UO_2 and has fuel enrichment from 2.719 wt% to 3.897 wt% depending of the location in the core. The core also contains a 120 fuel assemblies divided into three radial zones. The fuel assemblies contain a 15×15 square lattice of 208 fuel rods. The remaining space in the assembly is taken by cruciform control blades [19, 20]. Table XIX shows the parameters for this reactor that were used in the benchmarking calculations. Although an assembly level model was not built for this reactor, Fig. 18 shows a graphical representation of the fuel assembly. Figure 19 shows a graphical representation of the Trino Vercelles Unit #2 pin cell.

TABLE XIX

Nominal Reactor Parameters for Trino Vercelles Unit #2

Vendor	Westinghouse
Type	15×15 (square)
Pin-to-pin pitch	1.303 cm
Fuel pellet diameter	0.902 cm
Clad outer diameter	0.978 cm
Fuel density	10.079 g/cm^3
Fuel enrichment	3.13 wt% ^{235}U
Active fuel length	264 cm
Clad material	SS-304
Clad density	8.0 g/cm^3
Coolant material	Light water
Coolant density	0.75 g/cm^3

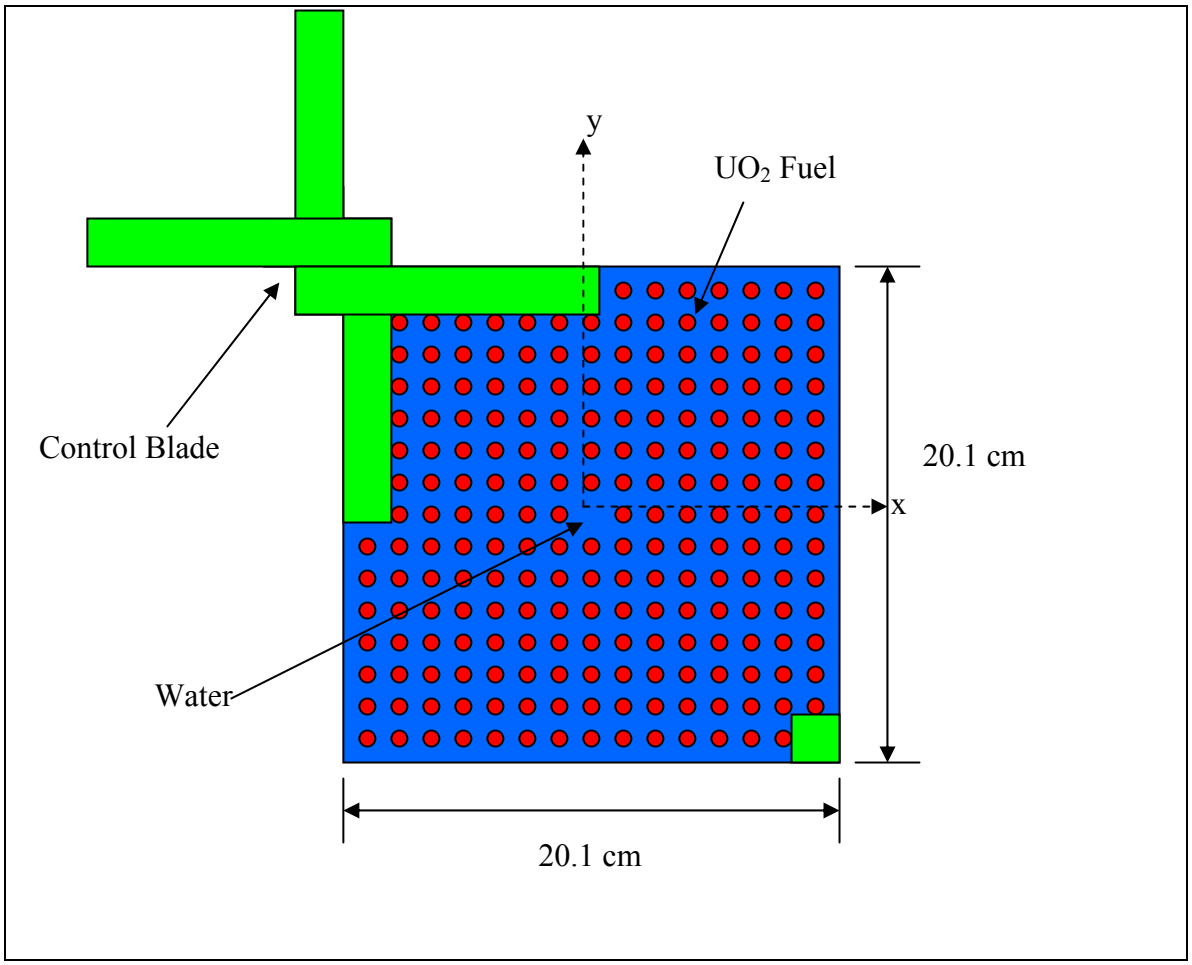

Fig. 18. Graphical representation of Trino Vercelles fuel assembly.

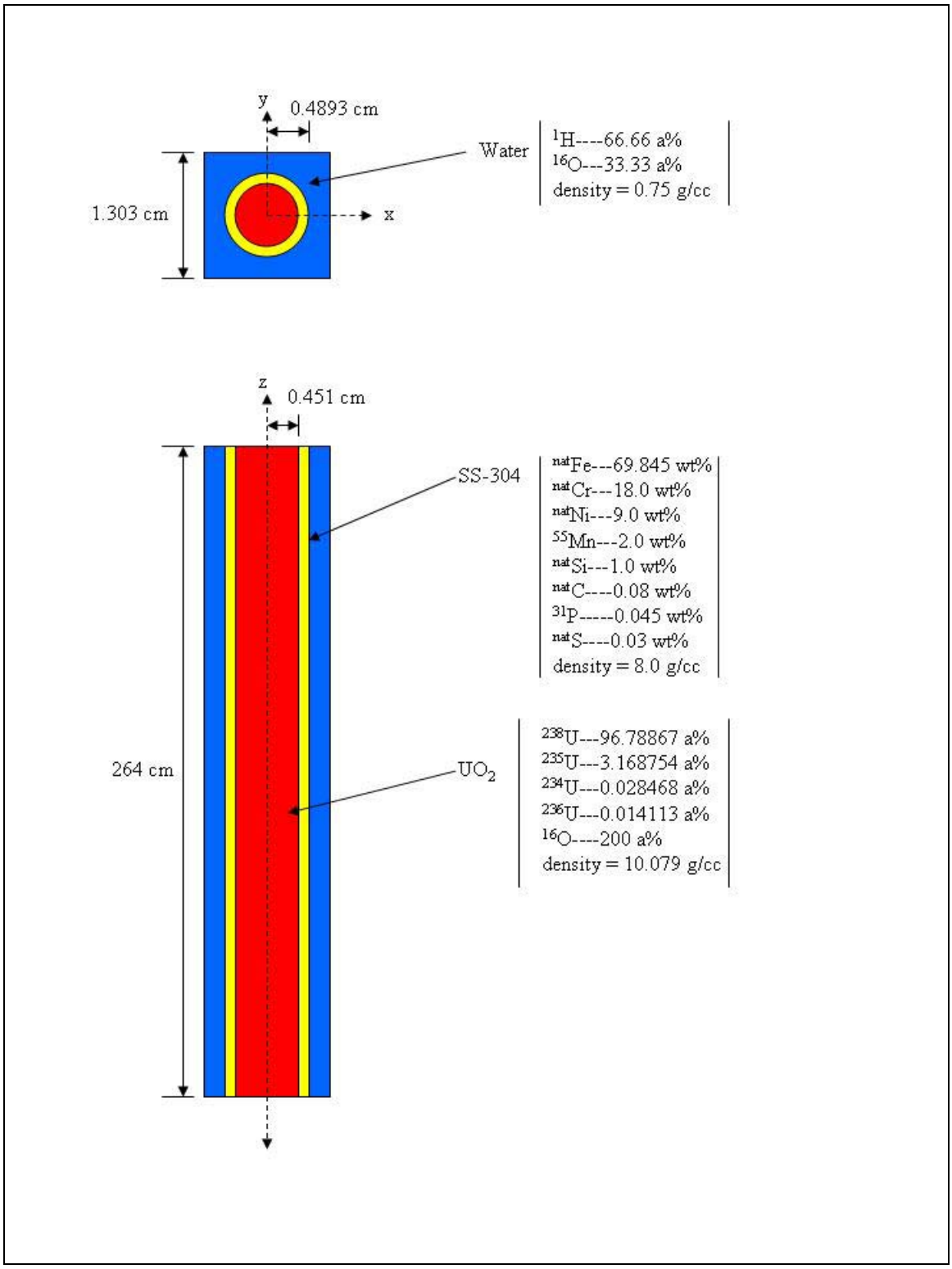

Fig. 19. Graphical representation of Trino Vercelles Unit #2 pin cell.

III.C.2. Fuel Measurements

The measured data was taken from the 509-069 fuel assembly of Unit #2 at the Trino Vercelles facility. From this assembly, 18 samples from various fuel rods and axial positions were analyzed. The analyses were performed at two separate facilities, Karlsruhe Laboratory and Ispra Laboratory, and their results compared. Each of the labs performed radiochemical analyses on the samples that included both alpha and gamma spectrometry. The methods by which they performed these tests can be found in [20]. After a comparison of the data between the two laboratories, the overall accuracy of the individual isotopes was calculated. Table XX shows the uncertainties of the measured isotopes for Trino Vercelles Unit #2.

TABLE XX

Uncertainties in Measured Isotopes for Trino Vercelles Unit #2

Isotope	**1σ Standard Deviation (%)**
^{235}U	1.03
^{238}U	2.05
^{239}Pu	0.88
^{240}Pu	0.99
^{241}Pu	1.15
^{154}Eu	5.0
^{148}Nd	1.43

III.C.3. Forward Model Simulations

The model for this reactor was also built using the methodology developed in Chapter II. As with the previous reactor model, this model consisted of an advanced 2D pin cell with the following correction factors: appropriate fuel temperature cross section file, moderator density, S(α,β) tally, ^{234}U and ^{236}U initial fuel concentration, and 200 MeV per fission for Q-fission in the Monteburns input file. The Trino Vercelles Unit #2 reactor model also contained the additional ^{153}Eu tally in the Monteburns input file as one of the isotopes of interest in the model was ^{154}Eu. The measured data for the reactor had already been decay corrected much like that of the Takahama Unit #3 measured data [17]. Because the measured data had already been decay corrected, the long process employed with the Calvert Cliffs Unit #1 reactor model could be avoided. Table XXI shows the RMS percent error of the isotopes of interest for the Trino Vercelles Unit #2 reactor model. A complete list of measured versus calculated data for each isotope can be found in Appendix B. Figure 20 shows the graph of the ^{235}U measured data compared to the calculated data. The measured data also shows 1.03% error bars as that was the measured error for that isotope. Graphs of all of the isotopes of interest can be found in Appendix C.

TABLE XXI

RMS Percent Error of Isotopes of Interest for Trino Vecelles Unit #2

Isotope	1σ Standard Deviation (%)
^{235}U	0.70
^{238}U	1.48
^{239}Pu	3.15
^{240}Pu	0.85
^{241}Pu	3.84
^{154}Eu	6.99
^{148}Nd	0.34

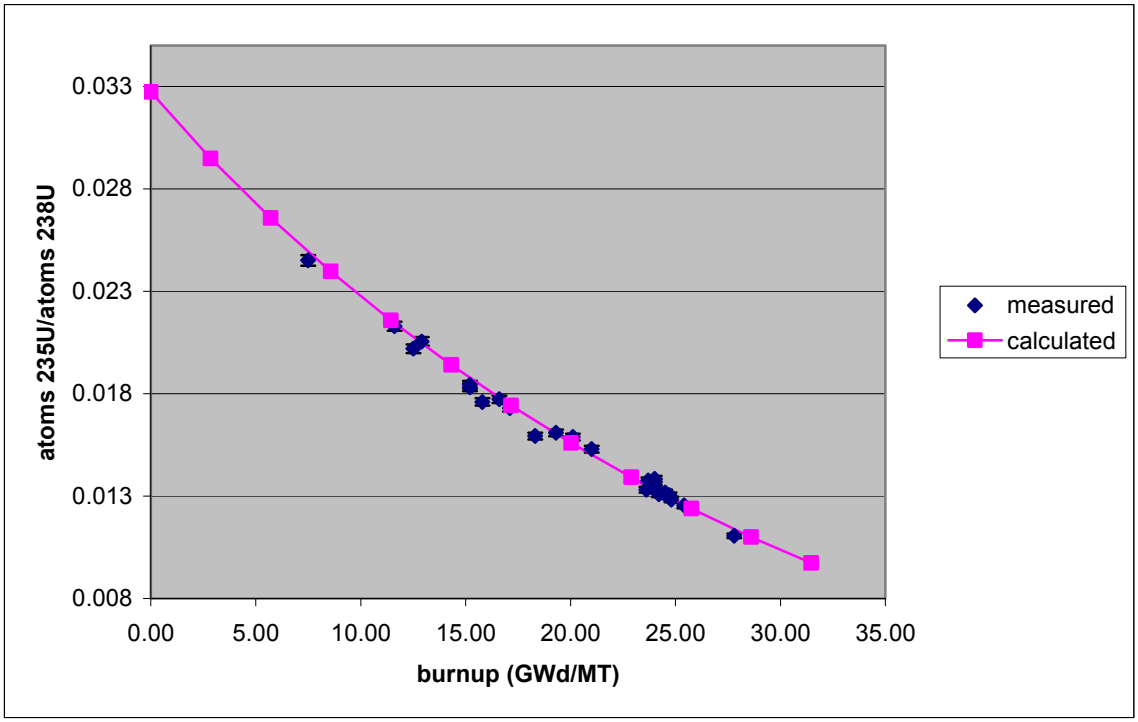

Fig. 20. Calculated and measured data of ^{235}U for Trino Vercelles Unit #2.

III.D. Discussion of Results

The benchmarking of the Forward Model methodology demonstrated good agreement of the isotopic concentrations being evaluated. The percent error in isotopic concentration for each reactor as well as the total of these values is shown in Table XXII. As can be seen, the total error associated with each isotope was less than 5% with the exception of ^{237}Np and ^{154}Eu. ^{237}Np, which can be used for enrichment verification, should probably be removed from the list of isotopes of interest. ^{154}Eu, which can be used as an age monitor and has considerable issues in accurately determining isotopic concentrations, should also be removed from the list of isotopes of interest as ^{241}Pu and ^{137}Cs can be calculated much more accurately. Two isotopes, ^{238}U and ^{148}Nd, had total errors of less than 1%, which is exceptional. This is very important as ^{148}Nd is the primary isotope for determining the burnup of the fuel. If the burnup of the fuel is wrong, that error will propagate throughout the entire system.

TABLE XXII

RMS Percent Error for Benchmarked Isotopics

	Takahama	**Calvert Cliffs**	**Trino**	**Total**
^{235}U	1.56	3.55	0.70	1.31
^{238}U	0.04	0.02	1.48	0.49
^{237}Np	6.14			6.14
^{238}Pu	8.25	2.68		4.34
^{239}Pu	4.41	1.67	3.15	1.89
^{240}Pu	2.58	3.92	0.85	1.59
^{241}Pu	6.81	1.21	3.84	2.64
^{137}Cs	1.65			1.65
^{148}Nd	0.64	1.75	0.34	0.63
^{154}Eu	16.42		6.99	8.92

CHAPTER IV

CONCLUSIONS

A Forward Model methodology for determining the specific reactor facility of origin for spent nuclear fuel used in an RDD was developed using the LANL code Monteburns. Models of the Takahama Unit #3 reactor were established utilizing optimization techniques to determine the required level of fidelity necessary to achieve statistical accuracies for the isotopes of interest. Along with model fidelity, a variety of correction factors were also examined to determine their effectiveness in improving the accuracy of isotopic concentrations. Using this Forward Model methodology, the Forensics project will be able to generate one-group cross sections and verify isotopic compositions with a level of accuracy that is necessary to yield unique reactor facilities in the event of an RDD event.

Once the Forward Model methodology had been developed, it was verified by a benchmarking technique. The Calvert Cliffs Unit #1 and Trino Vercelles Unit #2 reactors were modeled using the Forward Model methodology. The isotopic concentrations from all three reactor models were then compared to determine the level of agreement between them.

The results from the Forward Model methodology showed that the advanced pin cell with seven radial regions and several correction factors gave the greatest degree of accuracy. However, the computational time required for this model was seven times greater than that of the single-region advanced pin cell and the difference in accuracy was only 0.7% for ^{235}U. For this reason, the single radial region advanced pin cell with the

above mentioned correction factors was established as the Forward Model methodology. The correction factors employed were as follows: appropriate fuel temperature cross section file, moderator density, S(α,β) tally, ^{234}U and ^{236}U initial fuel concentration, and ^{153}Eu tally if the ^{154}Eu isotope is being examined.

With the exception of ^{154}Eu and ^{237}Np, the total error associated with each isotope was less than 5%. Two isotopes, ^{238}U and ^{148}Nd, had total errors of less than 1% which is exceptional. ^{154}Eu, which can be used as an age monitor, was unfortunately shown to not be as accurate as needed for this research. The total percent error for each isotope, as shown in Table XXII, will be used in the reactor verification portion of the forensics problem as the standard deviations associated with each isotope.

Future research into this type of model analysis should focus itself on determining better isotopic correction methods to be employed in the input files. A prime example of this is ^{154}Eu. While the cross sections for this isotope were found to be very accurate, there is some debate as to the accuracy of the fission yield values of ^{154}Eu as well as other isotopes that through neutron absorption and decay would form ^{154}Eu. It was found that the majority of ^{154}Eu does not actually come as a direct fission product but through the neutron absorption and decay of other isotopes. This also raises the question as to the legitimacy of the neutron absorption cross sections of these isotopes. Solving this problem can be a very daunting task as the number of variables involved can be quite large.

REFERENCES

1. W.S. Charlton, R.T. Perry, B.L. Fearey, and T.A. Parish, "Calculated Actinide and Fission Product Concentration Ratios for Gaseous Effluent Monitoring Using Monteburns 3.01," *Nuclear Technology*, **131**, 1-18 (2000).
2. W.S. Charlton, W.D. Stanbro, and R.T. Perry, "Comparisons of HELIOS, ORIGEN2, and Monteburns Calculated ^{241}Am and ^{243}Am Concentrations to Measured Values for PWR, BWR, and VVER Spent Fuel," *J. Nuclear Science and Technology*, **37(7)**, 615-623 (2000).
3. J.L. Ford, "Radiological Dispersal Devices: Assessing the Transnational Threat," Institute for National Strategic Studies, National Defense University, Strategic Forum Number 136 (1998).
4. "Fact Sheet on Dirty Bombs", www.nrc.gov, Nuclear Regulatory Commission (2005).
5. J.F. Briesmeister, "MCNP – A General Monte Carlo N-Particle Transport Code Version 4B," LA-12625-M, Los Alamos National Laboratory (1997).
6. M. Edenius, K. Ekberg, and B.H. Forssén, "CASMO-4 - A Fuel Assembly Burnup Program - User's Manual," Studsvik Report SOA-95/1, Studsvik of America (1995).
7. M. Edenius, B.H. Forssen, and C. Gragg, "The Physics Model of CASMO-4," *Proc. International Topical Meeting on Advances in Mathematics, Computations, and Reactor Physics*, April 28-May 2, Pittsburgh, Pa (1991).
8. E.A. Villarino, R.J.J. Stamm'ler, and A.A. Ferri, "HELIOS: Angularly Dependent Collision Probabilities," *Nuclear Science and Engineering*, **112**, 16-31 (1992).

9. "SCALE: A Modular Code System for Performing Standardized Computer Analyses for Licensing Evaluation," NUREG/CR-0200, Rev. 6 (ORNL/NUREG/CSD-2/R6), Vols. I, II, and III, Nuclear Regulatory Commission (2000).

10. M.D. Dehart and O.W. Hermann, "An Extension of the Validation of SCALE (SAS2H) Isotopic Predictions for PWR Spent Fuel," ORNL/TM-13317, Oak Ridge National Laboratory (1996).

11. A.G. Croff, "A User's Manual for the ORIGEN2 Computer Code," ORNL/TM-7175, Oak Ridge National Laboratory (1980).

12. M.J. Bell, "ORIGEN: The ORNL Isotope Generation and Depletion Code," ORNL-4628, Oak Ridge National Laboratory (1973).

13. R.J. Guenther, "Characterization of Spent Fuel Approved Testing Material-ATM-106," PNL-5109-106, Pacific Northwest National Laboratory (1988).

14. J.R. Askew, "A Characteristic Formulation of the Neutron Transport Equation in Complicated Geometries," AEEW-M-1108, U.K. Atomic Energy Authority (1972).

15. D.L. Poston, and H.R. Trellue, "User's Manual, Version 2.0 for MONTEBURNS Version 1.0," LA-UR-99-4999, Los Alamos National Laboratory (1999).

16. "Illicit Nuclear Trafficking Statistics," www.iaea.org, International Atomic Energy Agency (2005).

17. Y. Nakahara, "Nuclide Composition Benchmark Data Set for Verifying Burnup Codes on Spent Light Water Reactor Fuels," *Nuclear Technology*, **137**, 111-125 (2002).

18. S.R. Pati and P.A. VanSaun, "Isotopics and Transuranic Nuclide Content of Three- and Four-Cycle Calvert Cliffs-1 Fuel," Research Project 1755-1, Combustion Engineering (1982).

19. "Isotopic and Criticality Validation for PWR Actinide-Only Burnup Credit," DOE/RW-0497, U.S. Department of Energy (1997).

20. S. Guardini and G. Guzzi, "Benchmark Reference Data on Post Irraditaion Analysis of Light Water Reactor Fuel Samples," EUR-7879-EN, Nuclear Science and Technology, Commission of the European Communities (1983).

21. "Atom Percent Fission of Uranium and Plutonium (Nd-148 Method)," *Annual Book of ASTM Standards*, **45**; ASTM-E--321-96, American Society for Testing and Materials (1984).

22. M.J. Moran and H.N. Shapiro, *Fundamentals of Engineering Thermodynamics*, Fourth Edition, John Wiley & Sons, Inc., New York (2000).

23. "Standard Test Method for Atom Percent Fission in Uranium and Plutonium Fuel (Neodynium-148 Method)," *Annual Book ASTM Standards*, **45**; ASTM-E--321-75, American Society for Testing and Materials (1979).

24. "Standard Test Method for Uranium and Plutonium Concentrations and isotopic Abundances," *Annual Book ASTM Standards*, **45**; ASTM-E--267-70, American Society for Testing and Materials (1979).

APPENDIX A

EXAMPLE MCNP AND MONTEBURNS INPUT DECKS

```
MCNP input file
Takahama Unit #3
pin cell 4.11 wt% enriched
1   1   -10.42   -2 3 -4          imp:n=1
2   2   -6.531  -1 2 3 -4         imp:n=1
3   3   -0.714  -5 6 -7 8 1 3 -4 imp:n=1
4   0   #1 #2 #3                  imp:n=0

1    cz    0.475 $Clad OD
2    cz    0.4025 $fuel OD
*3   pz    0.0  $bottom
*4   pz    366.0 $top
*5   px    0.63
*6   px   -0.63
*7   py    0.63
*8   py   -0.63

kcode 1000 1.0 10 325
ksrc  0.0 0.0 195.0
      0.0 0.0 97.5
      0.0 0.0 292.5
m1    92234.60c      0.040664
      92235.15c      4.160356
      92238.15c     95.77992
      92236.60c      0.019056
       8016.60c    200.0
m2    40000.60c     98.193
      24000.50c      0.10
      26000.50c      0.20
      28000.50c      0.007
      50000.40c      1.500
m3     1001.60c      2
       8016.60c      1
mt3    lwtr.62t
```

```
Monteburns input file
Takahama Unit #3
PC
1                     !Number of MCNP Materials to Burn
1                     !MCNP Material "m" Numbers
186.2785              !Volume of Cells Containing the Materials
0.063983              !Power in MWt
-200.0                !Q-value for Fission
0.0                   !Total Number of Days Burned
25                    !Number of Outer Burn Steps
10                    !Number of Inner Burn Steps
1                     !Number of Predictor Steps
0                     !Step to Restart After
pwru                  !ORIGEN2 Library
/packages/origen/origen22/libs  !Location of ORIGEN2 Library
0.005                 !Fractional Importance Limit
1                     !Flag for Intermediate keff Calculations
29                    !Number of Automatic Tally Isotopes
92233.60c
92234.60c
92235.15c
92236.60c
92237.50c
92238.15c
92239.35c
93237.60c
93238.42c
93239.60c
94238.60c
94239.15c
94240.60c
94241.60c
94242.60c
95241.60c
95242.50c
95243.60c
43099.60c
44101.50c
47109.60c
55137.60c
60148.50c
61147.50c
62147.50c
63153.60c
63154.50c
64156.60c
64157.60c
```

```
Monteburns feed file
Takahama Unit #3
   1   55.00   1.0000  1   0      0.0      0.0    0  0.000 0 0.00 0 0.00
   2   55.00   1.0000  1   0      0.0      0.0    0  0.000 0 0.00 0 0.00
   3   55.00   1.0000  1   0      0.0      0.0    0  0.000 0 0.00 0 0.00
   4   55.00   1.0000  1   0      0.0      0.0    0  0.000 0 0.00 0 0.00
   5   55.00   1.0000  1   0      0.0      0.0    0  0.000 0 0.00 0 0.00
   6   55.00   1.0000  1   0      0.0      0.0    0  0.000 0 0.00 0 0.00
   7   55.00   1.0000  1   0      0.0      0.0    0  0.000 0 0.00 0 0.00
   8   55.00   1.0000  1   0      0.0      0.0    0  0.000 0 0.00 0 0.00
   9   55.00   1.0000  1   0      0.0      0.0    0  0.000 0 0.00 0 0.00
   10  55.00   1.0000  1   0      0.0      0.0    0  0.000 0 0.00 0 0.00
   11  55.00   1.0000  1   0      0.0      0.0    0  0.000 0 0.00 0 0.00
   12  55.00   1.0000  1   0      0.0      0.0    0  0.000 0 0.00 0 0.00
   13  55.00   1.0000  1   0      0.0      0.0    0  0.000 0 0.00 0 0.00
   14  55.00   1.0000  1   0      0.0      0.0    0  0.000 0 0.00 0 0.00
   15  55.00   1.0000  1   0      0.0      0.0    0  0.000 0 0.00 0 0.00
   16  55.00   1.0000  1   0      0.0      0.0    0  0.000 0 0.00 0 0.00
   17  55.00   1.0000  1   0      0.0      0.0    0  0.000 0 0.00 0 0.00
   18  55.00   1.0000  1   0      0.0      0.0    0  0.000 0 0.00 0 0.00
   19  55.00   1.0000  1   0      0.0      0.0    0  0.000 0 0.00 0 0.00
   20  55.00   1.0000  1   0      0.0      0.0    0  0.000 0 0.00 0 0.00
   21  55.00   1.0000  1   0      0.0      0.0    0  0.000 0 0.00 0 0.00
   22  55.00   1.0000  1   0      0.0      0.0    0  0.000 0 0.00 0 0.00
   23  55.00   1.0000  1   0      0.0      0.0    0  0.000 0 0.00 0 0.00
   24  55.00   1.0000  1   0      0.0      0.0    0  0.000 0 0.00 0 0.00
   25  55.00   1.0000  1   0      0.0      0.0    0  0.000 0 0.00 0 0.00
  0                              ! # of feed specs
  0                              ! # of removal
```

```
MCNP input file
Takahama Unit #3
3D Assembly 4.11% enriched
1   1   -10.42  -2 6 -7      u=1 imp:n=1
2   2   -6.531  -1 2 6 -7    u=1 imp:n=1
3   3   -0.714   1 5 -8      u=1 imp:n=1
4   3   -0.714   8 -4        u=1 imp:n=1
5   3   -0.714  -5 3         u=1 imp:n=1
6   3   -0.714  -17          u=3 imp:n=1
7   4   -10.42  -2 6 -7      u=4 imp:n=1
8   2   -6.531  -1 2 6 -7    u=4 imp:n=1
9   3   -0.714   1 5 -8      u=4 imp:n=1
10  3   -0.714   8 -4        u=4 imp:n=1
11  3   -0.714  -5 3         u=4 imp:n=1
12  5   -8.0    -1 7 -8      u=1 imp:n=1
13  5   -8.0    -1 -6 5      u=1 imp:n=1
14  5   -8.0    -1 7 -8      u=4 imp:n=1
15  5   -8.0    -1 -6 5      u=4 imp:n=1
21  0   -9 10 -11 12 lat=1 u=2 imp:n=1 fill=-8:8 -8:8 0:0
     1 1 1 1 1 1 1 1 1 1 1 1 1 1 1 1 1
     1 1 1 1 1 1 1 1 1 1 1 1 1 1 1 1 1
     1 1 1 1 4 3 1 1 3 1 1 3 4 1 1 1 1
     1 1 1 3 1 1 1 1 4 1 1 1 1 3 1 1 1
     1 1 4 1 1 1 1 1 1 1 1 1 1 1 4 1 1
     1 1 3 1 1 3 1 1 3 1 1 3 1 1 3 1 1
     1 1 1 1 1 1 4 1 1 1 4 1 1 1 1 1 1
     1 1 1 1 1 1 1 1 1 1 1 1 1 1 1 1 1
     1 1 3 1 1 3 1 1 3 1 1 3 1 1 3 1 1
     1 1 1 1 1 1 1 1 1 1 1 1 1 1 1 1 1
     1 1 1 1 1 1 4 1 1 1 4 1 1 1 1 1 1
     1 1 3 1 1 3 1 1 3 1 1 3 1 1 3 1 1
     1 1 4 1 1 1 1 1 1 1 1 1 1 1 4 1 1
     1 1 1 3 1 1 1 1 4 1 1 1 1 3 1 1 1
     1 1 1 1 4 3 1 1 3 1 1 3 4 1 1 1 1
     1 1 1 1 1 1 1 1 1 1 1 1 1 1 1 1 1
     1 1 1 1 1 1 1 1 1 1 1 1 1 1 1 1 1
22  0  -13 14 -15 16 3 -4 fill=2 imp:n=1
31  0  -3             imp:n=0
32  0   4             imp:n=0
33  0   13 3 -4        imp:n=0
34  0  -14 3 -4       imp:n=0
35  0   15 -13 14 3 -4 imp:n=0
36  0  -16 -13 14 3 -4 imp:n=0

1    cz    0.475 $Clad OD
2    cz    0.4025 $fuel OD
3    pz    0.0  $bottom
4    pz    410.0 $top
5    pz    10.0  $rod bottom
6    pz    22.0  $fuel bottom
7    pz    388.0 $fuel top
8    pz    400.0 $rod top
```

```
9    px    0.63
10   px   -0.63
11   py    0.63
12   py   -0.63
*13  px    10.71
*14  px   -10.71
*15  py    10.71
*16  py   -10.71
17   cz    1.00

kcode 1000 1.0 20 325
ksrc  5.0 5.0 175.0
      5.0 -5.0 175.0
      -5.0 5.0 175.0
      -5.0 -5.0 175.0
      0.0  0.0  175.0
      5.0 5.0 250.0
      5.0 -5.0 250.0
      -5.0 5.0 250.0
      -5.0 -5.0 250.0
      0.0  0.0  250.0
      5.0 5.0 100.0
      5.0 -5.0 100.0
      -5.0 5.0 100.0
      -5.0 -5.0 100.0
      0.0  0.0  100.0
prdmp 200 5 0 5 0
m1    92235.15c      4.160362
      92238.15c     95.79897
      92234.60c      0.040664
      8016.60c     200.0
m2    40000.60c     98.193
      24000.50c      0.10
      26000.50c      0.20
      28000.50c      0.007
      50000.40c      1.500
m3    1001.60c     2
      8016.60c     1
m4    92235.15c    1.30358
      92238.15c    30.01701
      92234.60c    0.012741
      8016.60c     66.26667
      64000.35c    2.4
m5    6000.60c      -0.08
      24000.50c    -18
      26000.50c    -69.845
      25055.60c     -2
      28000.50c     -9
      15031.60c     -0.045
      16000.60c     -0.03
      14000.60c     -1
mt3   lwtr.62t
```

```
Monteburns input file
Takahama Unit #3 3D Assembly
PC
1                    !Number of MCNP Materials to Burn
1                    !MCNP Material "m" Numbers
46569.62             !Volume of Cells Containing the Materials
16.891               !Power in MWt (change to .0485 if used
again)
-200.0               !Q-value for Fission
0.0                  !Total Number of Days Burned
25                   !Number of Outer Burn Steps
10                   !Number of Inner Burn Steps
1                    !Number of Predictor Steps
0                    !Step to Restart After
pwru                 !ORIGEN2 Library
/packages/origen/origen22/libs  !Location of ORIGEN2 Library
0.005                !Fractional Importance Limit
1                    !Flag for Intermediate keff Calculations
29                   !Number of Automatic Tally Isotopes
92233.60c
92234.60c
92235.15c
92236.60c
92237.50c
92238.15c
92239.35c
93237.60c
93238.42c
93239.60c
94238.60c
94239.15c
94240.60c
94241.60c
94242.60c
95241.60c
95242.50c
95243.60c
43099.60c
44101.50c
47109.60c
55137.60c
60148.50c
61147.50c
62147.50c
63153.60c
63154.50c
64156.60c
64157.60c
```

```
Monteburns feed file
Takahama Unit #3 3D Assembly
   1   55.00   1.0000  1   0     0.0     0.0   0  0.000 0 0.00 0 0.00
   2   55.00   1.0000  1   0     0.0     0.0   0  0.000 0 0.00 0 0.00
   3   55.00   1.0000  1   0     0.0     0.0   0  0.000 0 0.00 0 0.00
   4   55.00   1.0000  1   0     0.0     0.0   0  0.000 0 0.00 0 0.00
   5   55.00   1.0000  1   0     0.0     0.0   0  0.000 0 0.00 0 0.00
   6   55.00   1.0000  1   0     0.0     0.0   0  0.000 0 0.00 0 0.00
   7   55.00   1.0000  1   0     0.0     0.0   0  0.000 0 0.00 0 0.00
   8   55.00   1.0000  1   0     0.0     0.0   0  0.000 0 0.00 0 0.00
   9   55.00   1.0000  1   0     0.0     0.0   0  0.000 0 0.00 0 0.00
   10  55.00   1.0000  1   0     0.0     0.0   0  0.000 0 0.00 0 0.00
   11  55.00   1.0000  1   0     0.0     0.0   0  0.000 0 0.00 0 0.00
   12  55.00   1.0000  1   0     0.0     0.0   0  0.000 0 0.00 0 0.00
   13  55.00   1.0000  1   0     0.0     0.0   0  0.000 0 0.00 0 0.00
   14  55.00   1.0000  1   0     0.0     0.0   0  0.000 0 0.00 0 0.00
   15  55.00   1.0000  1   0     0.0     0.0   0  0.000 0 0.00 0 0.00
   16  55.00   1.0000  1   0     0.0     0.0   0  0.000 0 0.00 0 0.00
   17  55.00   1.0000  1   0     0.0     0.0   0  0.000 0 0.00 0 0.00
   18  55.00   1.0000  1   0     0.0     0.0   0  0.000 0 0.00 0 0.00
   19  55.00   1.0000  1   0     0.0     0.0   0  0.000 0 0.00 0 0.00
   20  55.00   1.0000  1   0     0.0     0.0   0  0.000 0 0.00 0 0.00
   21  55.00   1.0000  1   0     0.0     0.0   0  0.000 0 0.00 0 0.00
   22  55.00   1.0000  1   0     0.0     0.0   0  0.000 0 0.00 0 0.00
   23  55.00   1.0000  1   0     0.0     0.0   0  0.000 0 0.00 0 0.00
   24  55.00   1.0000  1   0     0.0     0.0   0  0.000 0 0.00 0 0.00
   25  55.00   1.0000  1   0     0.0     0.0   0  0.000 0 0.00 0 0.00
  0                            ! # of feed specs
  0                            ! # of removal
```

```
MCNP input file
Calvert Cliffs Unit #2
Pin Cell 2.45 wt% enriched
1 1 -10.4215  -1 7 -8            imp:n=1
2 2 -6.531    -2 1 7 -8          imp:n=1
3 3 -0.714     2 -3 4 -5 6 7 -8  imp:n=1
4 0            #1 #2 #3          imp:n=0

1        cz       0.481965
2        cz       0.55876
*3       px       0.7377
*4       px      -0.7377
*5       py       0.7377
*6       py      -0.7377
*7       pz       0.0
*8       pz       347.0

kcode 900 1.0 10 325
ksrc  0.000000 0.000000 73.5
      0.000000 0.000000 175.0
      0.000000 0.000000 270.0
m1    92235.15c          2.480565 $fuel
      92238.15c         97.51944
      92234.60c          0.022172
      92236.60c          0.011362
      8016.60c         200.00
m2    50000.42c          1.5  $cladding
      26000.50c          0.2
      24000.50c          0.1
      28000.50c          0.007
      40000.60c         98.193
m3    1001.60c           2.0  $coolant
      8016.60c           1.0
mt3   lwtr.62t
```

```
Monteburns input file
Calvert Cliffs Unit #1
PC
1                    !Number of MCNP Materials to Burn
1                    !MCNP Material "m" Numbers
253.2272             !Volume of Cells Containing the Materials
0.071881             !Power in MWt
-200.0               !Q-value for Fission
0.0                  !Total Number of Days Burned
26                   !Number of Outer Burn Steps
10                   !Number of Inner Burn Steps
1                    !Number of Predictor Steps
0                    !Step to Restart After
pwru                 !ORIGEN2 Library
/packages/origen/origen22/libs  !Location of ORIGEN2 Library
0.005                !Fractional Importance Limit
1                    !Flag for Intermediate keff Calculations
19                   !Number of Automatic Tally Isotopes
92233.60c
92234.60c
92235.15c
92236.60c
92237.50c
92238.15c
92239.35c
93237.60c
93238.42c
93239.60c
94238.60c
94239.15c
94240.60c
94241.60c
94242.60c
95241.60c
95242.50c
95243.60c
60148.50c
```

```
Monteburns feed file
Calvert Cliffs Unit #1
   1   65.00   1.0000  1   0      0.0      0.0    0  0.000 0 0.00 0 0.00
   2   65.00   1.0000  1   0      0.0      0.0    0  0.000 0 0.00 0 0.00
   3   65.00   1.0000  1   0      0.0      0.0    0  0.000 0 0.00 0 0.00
   4   65.00   1.0000  1   0      0.0      0.0    0  0.000 0 0.00 0 0.00
   5   65.00   1.0000  1   0      0.0      0.0    0  0.000 0 0.00 0 0.00
   6   65.00   1.0000  1   0      0.0      0.0    0  0.000 0 0.00 0 0.00
   7   65.00   1.0000  1   0      0.0      0.0    0  0.000 0 0.00 0 0.00
   8   65.00   1.0000  1   0      0.0      0.0    0  0.000 0 0.00 0 0.00
   9   65.00   1.0000  1   0      0.0      0.0    0  0.000 0 0.00 0 0.00
   10  65.00   1.0000  1   0      0.0      0.0    0  0.000 0 0.00 0 0.00
   11  65.00   1.0000  1   0      0.0      0.0    0  0.000 0 0.00 0 0.00
   12  65.00   1.0000  1   0      0.0      0.0    0  0.000 0 0.00 0 0.00
   13  65.00   1.0000  1   0      0.0      0.0    0  0.000 0 0.00 0 0.00
   14  65.00   1.0000  1   0      0.0      0.0    0  0.000 0 0.00 0 0.00
   15  65.00   1.0000  1   0      0.0      0.0    0  0.000 0 0.00 0 0.00
   16  65.00   1.0000  1   0      0.0      0.0    0  0.000 0 0.00 0 0.00
   17  65.00   1.0000  1   0      0.0      0.0    0  0.000 0 0.00 0 0.00
   18  65.00   1.0000  1   0      0.0      0.0    0  0.000 0 0.00 0 0.00
   19  65.00   1.0000  1   0      0.0      0.0    0  0.000 0 0.00 0 0.00
   20  65.00   1.0000  1   0      0.0      0.0    0  0.000 0 0.00 0 0.00
   21  65.00   1.0000  1   0      0.0      0.0    0  0.000 0 0.00 0 0.00
   22  65.00   1.0000  1   0      0.0      0.0    0  0.000 0 0.00 0 0.00
   23  65.00   1.0000  1   0      0.0      0.0    0  0.000 0 0.00 0 0.00
   24  65.00   1.0000  1   0      0.0      0.0    0  0.000 0 0.00 0 0.00
   25  65.00   1.0000  1   0      0.0      0.0    0  0.000 0 0.00 0 0.00
   26  570.00  0.0000  1   0      0.0      0.0    0  0.000 0 0.00 0 0.00
  0                              ! # of feed specs
  0                              ! # of removal groups
```

```
MCNP input file
Trino Vercelles Unit #2
pin cell 3.13 wt% enriched
1   1   -10.079   -2 3 -4          imp:n=1
2   2   -8.0     -1 2 3 -4         imp:n=1
3   3   -0.75    -5 6 -7 8 1 3 -4  imp:n=1
4   0   #1 #2 #3                   imp:n=0

1    cz    0.4893 $Clad OD
2    cz    0.451 $fuel OD
*3    pz    0.0  $bottom
*4    pz    264.0 $top
*5   px    0.6515
*6   px   -0.6515
*7   py    0.6515
*8   py   -0.6515

kcode 1000 1.0 10 325
ksrc  0.0 0.0 63.0
      0.0 0.0 126.5
      0.0 0.0 189.5
m1    92234.60c      0.028468
      92235.15c      3.168754
      92238.15c     96.78867
      92236.60c      0.014113
       8016.60c    200.0
m2    6000.60c      -0.08
      24000.50c    -18
      26000.50c    -69.845
      25055.60c     -2
      28000.50c     -9
      15031.60c     -0.045
      16000.60c     -0.03
      14000.60c     -1
m3     1001.60c      2
       8016.60c      1
mt3    lwtr.62t
```

```
Monteburns input file
Trino Vercelles Unit #2
PC
1                     !Number of MCNP Materials to Burn
1                     !MCNP Material "m" Numbers
168.6968151           !Volume of Cells Containing the Materials
0.035706              !Power in MWt
-200.0                !Q-value for Fission
0.0                   !Total Number of Days Burned
11                    !Number of Outer Burn Steps
10                    !Number of Inner Burn Steps
1                     !Number of Predictor Steps
0                     !Step to Restart After
pwru                  !ORIGEN2 Library
/packages/origen/origen22/libs  !Location of ORIGEN2 Library
0.005                 !Fractional Importance Limit
1                     !Flag for Intermediate keff Calculations
29                    !Number of Automatic Tally Isotopes
92233.60c
92234.60c
92235.15c
92236.60c
92237.50c
92238.15c
92239.35c
93237.60c
93238.42c
93239.60c
94238.60c
94239.15c
94240.60c
94241.60c
94242.60c
95241.60c
95242.50c
95243.60c
43099.60c
44101.50c
47109.60c
55137.60c
60148.50c
61147.50c
62147.50c
63153.60c
63154.50c
64156.60c
64157.60c
```

```
Monteburns feed file
Trino Vercelles Unit #2
   1   120.00   1.0000  1   0     0.0     0.0   0  0.000 0 0.00 0 0.00
   2   120.00   1.0000  1   0     0.0     0.0   0  0.000 0 0.00 0 0.00
   3   120.00   1.0000  1   0     0.0     0.0   0  0.000 0 0.00 0 0.00
   4   120.00   1.0000  1   0     0.0     0.0   0  0.000 0 0.00 0 0.00
   5   120.00   1.0000  1   0     0.0     0.0   0  0.000 0 0.00 0 0.00
   6   120.00   1.0000  1   0     0.0     0.0   0  0.000 0 0.00 0 0.00
   7   120.00   1.0000  1   0     0.0     0.0   0  0.000 0 0.00 0 0.00
   8   120.00   1.0000  1   0     0.0     0.0   0  0.000 0 0.00 0 0.00
   9   120.00   1.0000  1   0     0.0     0.0   0  0.000 0 0.00 0 0.00
   10  120.00   1.0000  1   0     0.0     0.0   0  0.000 0 0.00 0 0.00
   11  120.00   1.0000  1   0     0.0     0.0   0  0.000 0 0.00 0 0.00
  0                           ! # of feed specs
  0                           ! # of removal groups
```

APPENDIX B

MEASURED VERSUS CALCULATED ISOTOPIC DATA

Takahama Unit #3

^{235}U

Rod	Burnup	Measured	Calculated	% Difference
SF95-1	14.30	26740.00	26805.98	0.25
SF95-2	24.35	19270.00	19205.42	-0.34
SF95-3	35.42	13260.00	12729.52	-4.17
SF95-4	36.69	12300.00	12097.69	-1.67
SF95-5	30.40	15440.00	15442.17	0.01
SF97-2	30.73	15710.00	15252.88	-3.00
SF97-3	42.16	10300.00	9607.82	-7.20
SF97-4	47.03	8179.00	7680.60	-6.49
SF97-5	47.25	7932.00	7599.44	-4.38
SF97-6	40.79	10160.00	10197.53	0.37

^{238}U

Rod	Burnup	Measured	Calculated	% Difference
SF95-1	14.30	949900.00	949757.88	-0.01
SF95-2	24.35	942400.00	943088.98	0.07
SF95-3	35.42	933800.00	935086.59	0.14
SF95-4	36.69	933500.00	934124.50	0.07
SF95-5	30.40	938800.00	938800.80	0.00
SF97-2	30.73	937700.00	938560.98	0.09
SF97-3	42.16	928200.00	929877.17	0.18
SF97-4	47.03	924600.00	925954.29	0.15
SF97-5	47.25	924700.00	925773.93	0.12
SF97-6	40.79	931000.00	930956.72	0.00

^{238}Pu

Rod	Burnup	Measured	Calculated	% Difference
SF95-1	14.30	17.18	14.73	-16.65
SF95-2	24.35	71.02	57.76	-22.96
SF95-3	35.42	153.90	138.01	-11.52
SF95-4	36.69	158.80	149.41	-6.28
SF95-5	30.40	102.00	97.35	-4.78
SF97-2	30.73	125.00	99.80	-25.25
SF97-3	42.16	258.10	203.73	-26.69
SF97-4	47.03	319.90	259.16	-23.44
SF97-5	47.25	318.80	261.83	-21.76
SF97-6	40.79	217.50	189.34	-14.87

^{239}Pu

Rod	Burnup	Measured	Calculated	% Difference
SF95-1	14.30	4227.00	4093.76	-3.25
SF95-2	24.35	5655.00	5190.12	-8.96
SF95-3	35.42	6194.00	5458.45	-13.48
SF95-4	36.69	6005.00	5455.05	-10.08
SF95-5	30.40	5635.00	5418.67	-3.99
SF97-2	30.73	5928.00	5424.65	-9.28
SF97-3	42.16	6217.00	5413.90	-14.83
SF97-4	47.03	6037.00	5388.97	-12.03
SF97-5	47.25	5976.00	5389.07	-10.89
SF97-6	40.79	5677.00	5425.77	-4.63

^{240}Pu

Rod	Burnup	Measured	Calculated	% Difference
SF95-1	14.30	780.20	763.68	-2.16
SF95-2	24.35	1539.00	1490.16	-3.28
SF95-3	35.42	2186.00	2262.70	3.39
SF95-4	36.69	2207.00	2342.25	5.77
SF95-5	30.40	1821.00	1926.04	5.45
SF97-2	30.73	1871.00	1949.07	4.01
SF97-3	42.16	2471.00	2649.96	6.75
SF97-4	47.03	2668.00	2864.23	6.85
SF97-5	47.25	2648.00	2872.33	7.81
SF97-6	40.79	2326.00	2578.83	9.80

^{241}Pu

Rod	Burnup	Measured	Calculated	% Difference
SF95-1	14.30	369.00	346.22	-6.58
SF95-2	24.35	957.80	772.76	-23.94
SF95-3	35.42	1486.00	1236.20	-20.21
SF95-4	36.69	1466.00	1282.24	-14.33
SF95-5	30.40	1153.00	1036.21	-11.27
SF97-2	30.73	1235.00	1050.06	-17.61
SF97-3	42.16	1689.00	1451.21	-16.39
SF97-4	47.03	1770.00	1550.44	-14.16
SF97-5	47.25	1754.00	1553.56	-12.90
SF97-6	40.79	1494.00	1413.93	-5.66

^{237}Np

Rod	Burnup	Measured	Calculated	% Difference
SF97-2	30.73	403.40	355.17	-13.58
SF97-3	42.16	584.50	516.71	-13.12
SF97-4	47.03	660.40	577.46	-14.36
SF97-5	47.25	670.10	580.02	-15.53
SF97-6	40.79	557.00	498.46	-11.74

^{137}Cs

Rod	Burnup	Measured	Calculated	% Difference
SF95-1	14.30	540.50	528.23	-2.32
SF95-2	24.35	933.60	892.91	-4.56
SF95-3	35.42	1347.00	1288.33	-4.55
SF95-4	36.69	1400.00	1333.27	-5.01
SF95-5	30.40	1148.00	1109.83	-3.44
SF97-2	30.73	1151.00	1121.61	-2.62
SF97-3	42.16	1582.00	1525.84	-3.68
SF97-4	47.03	1749.00	1695.94	-3.13
SF97-5	47.25	1761.00	1703.60	-3.37
SF97-6	40.79	1531.00	1477.76	-3.60

^{148}Nd

Rod	Burnup	Measured	Calculated	% Difference
SF95-1	14.30	159.20	162.33	1.93
SF95-2	24.35	273.60	275.53	0.70
SF95-3	35.42	397.90	399.45	0.39
SF95-4	36.69	412.60	413.61	0.24
SF95-5	30.40	340.10	343.35	0.95
SF97-2	30.73	338.90	347.05	2.35
SF97-3	42.16	466.20	474.50	1.75
SF97-4	47.03	520.40	528.54	1.54
SF97-5	47.25	522.60	530.98	1.58
SF97-6	40.79	450.40	459.27	1.93

^{154}Eu

Rod	Burnup	Measured	Calculated	% Difference
SF95-1	14.30	4.09	5.48	25.34
SF95-2	24.35	13.06	18.37	28.92
SF95-3	35.42	25.25	38.98	35.22
SF95-4	36.69	26.57	41.66	36.22
SF95-5	30.40	18.17	28.96	37.26
SF97-2	30.73	19.73	29.59	33.32
SF97-3	42.16	32.93	53.75	38.73
SF97-4	47.03	37.39	65.05	42.52
SF97-5	47.25	37.07	65.57	43.46
SF97-6	40.79	28.59	50.65	43.55

Calvert Cliffs Unit #1

^{235}U

Sample	Burnup	Measured	Calculated	% Difference
023-1	37	0.39	0.37	-5.17
023-2	36.33	0.35	0.38	9.27
023-3	36.1	0.39	0.39	0.18
023-4	34.51	0.37	0.43	14.22
023-5	36.15	0.39	0.39	0.14

^{238}U

Sample	Burnup	Measured	Calculated	% Difference
023-1	37	99.24	99.27	0.03
023-2	36.33	99.32	99.26	-0.06
023-3	36.1	99.24	99.26	0.02
023-4	34.51	99.29	99.22	-0.07
023-5	36.15	99.24	99.26	0.02

^{238}Pu

Sample	Burnup	Measured	Calculated	% Difference
023-1	37	2.27	2.28	0.36
023-2	36.33	2.27	2.21	-2.53
023-3	36.1	2.28	2.19	-3.98
023-4	34.51	2.28	2.03	-12.05
023-5	36.15	2.27	2.19	-3.51

^{239}Pu

Sample	Burnup	Measured	Calculated	% Difference
023-1	37	4.72E-03	4.88E-03	3.33
023-2	36.33	4.74E-03	4.89E-03	3.14
023-3	36.1	4.74E-03	4.90E-03	3.30
023-4	34.51	4.74E-03	4.92E-03	3.55
023-5	36.15	4.65E-03	4.90E-03	5.04

^{240}Pu

Sample	Burnup	Measured	Calculated	% Difference
023-1	37	28.46	31.27	8.99
023-2	36.33	28.34	31.09	8.86
023-3	36.1	28.22	31.03	9.08
023-4	34.51	28.20	30.59	7.79
023-5	36.15	28.23	31.05	9.06

^{241}Pu

Sample	Burnup	Measured	Calculated	% Difference
023-1	37	1.23E-03	1.28E-03	3.31
023-2	36.33	1.24E-03	1.26E-03	2.19
023-3	36.1	1.22E-03	1.26E-03	2.71
023-4	34.51	1.24E-03	1.23E-03	-1.06
023-5	36.15	1.22E-03	1.26E-03	3.54

^{148}Nd

Sample	Burnup	Measured	Calculated	% Difference
023-1	37	6.82E-04	7.09E-04	3.81
023-2	36.33	6.68E-04	6.96E-04	3.93
023-3	36.1	6.64E-04	6.91E-04	3.90
023-4	34.51	6.34E-04	6.60E-04	4.06
023-5	36.15	6.65E-04	6.92E-04	3.89

Trino Vercelles Unit #2

^{235}U

Rod	Burnup	Measured	Calculated	% Difference
509-032	7.50	2.45E-02	2.51E-02	2.24
509-032	15.20	1.83E-02	1.88E-02	2.42
509-032	15.80	1.76E-02	1.83E-02	3.98
509-032	11.60	2.13E-02	2.15E-02	1.18
509-032	16.60	1.77E-02	1.78E-02	0.19
509-032	17.10	1.73E-02	1.74E-02	0.67
509-032	12.50	2.02E-02	2.08E-02	2.98
509-032	18.30	1.59E-02	1.66E-02	4.09
509-032	23.70	1.38E-02	1.34E-02	-2.82
509-032	24.70	1.30E-02	1.29E-02	-1.41
509-032	19.30	1.61E-02	1.60E-02	-0.81
509-032	24.00	1.38E-02	1.32E-02	-4.67
509-032	24.30	1.32E-02	1.31E-02	-0.80
509-032	12.90	2.06E-02	2.05E-02	-0.22
509-032	21.00	1.53E-02	1.49E-02	-2.54
509-032	23.60	1.33E-02	1.34E-02	0.94
509-032	24.20	1.31E-02	1.31E-02	0.21
509-032	24.50	1.32E-02	1.30E-02	-1.61
509-032	23.80	1.35E-02	1.33E-02	-0.91
509-032	20.10	1.59E-02	1.55E-02	-2.79
509-032	24.00	1.37E-02	1.32E-02	-3.53
509-032	24.50	1.31E-02	1.30E-02	-0.91
509-032	15.20	1.84E-02	1.88E-02	1.72
509-032	27.80	1.11E-02	1.14E-02	2.82
509-032	24.80	1.28E-02	1.28E-02	-0.17
509-032	25.40	1.25E-02	1.25E-02	-0.27

^{238}U

Rod	Burnup	Measured	Calculated	% Difference
509-069	12.86	9.61	9.30	-3.30
509-069	20.60	16.50	15.37	-7.32
509-069	23.72	18.94	17.91	-5.75
509-069	24.30	19.12	18.39	-3.95
509-069	23.87	19.13	18.03	-6.09
509-069	24.55	19.96	18.60	-7.31
509-069	23.93	19.80	18.08	-9.49
509-069	24.36	20.10	18.44	-8.99
509-069	24.33	19.60	18.42	-6.43
509-069	24.31	21.09	18.40	-14.61
509-069	23.70	19.13	17.89	-6.90
509-069	24.70	19.96	18.72	-6.61
509-069	19.30	15.11	14.32	-5.48
509-069	24.00	19.64	18.14	-8.25
509-069	24.30	21.09	18.39	-14.68
509-069	12.90	9.61	9.33	-2.96
509-069	21.00	16.49	15.69	-5.09
509-069	23.60	18.94	17.81	-6.33
509-069	24.20	19.58	18.31	-6.95
509-069	24.50	19.12	18.56	-3.04
509-069	23.80	18.55	17.98	-3.19
509-069	20.10	14.50	14.97	3.11
509-069	24.00	18.90	18.14	-4.18
509-069	24.50	20.10	18.56	-8.32
509-069	15.20	11.88	11.10	-7.03
509-069	27.80	20.16	21.32	5.46
509-069	24.80	20.36	18.81	-8.27
509-069	25.40	19.85	19.30	-2.83
509-032	7.50	5.28	5.31	0.55
509-032	15.20	11.84	11.10	-6.67
509-032	15.80	11.62	11.57	-0.47
509-032	11.60	8.93	8.35	-6.95
509-032	16.60	12.82	12.19	-5.17
509-032	17.10	13.38	12.58	-6.34
509-032	12.50	8.78	9.03	2.77
509-032	18.30	12.56	13.53	7.16

^{239}Pu

Rod	Burnup	Measured	Calculated	% Difference
509-032	7.50	3.62E-03	3.15E-03	-15.13
509-032	15.20	5.52E-03	4.82E-03	-14.39
509-032	15.80	5.48E-03	4.91E-03	-11.78
509-032	11.60	4.61E-03	4.19E-03	-10.00
509-032	16.60	5.42E-03	5.01E-03	-8.26
509-032	17.10	5.49E-03	5.07E-03	-8.26
509-032	12.50	4.61E-03	4.37E-03	-5.42
509-032	18.30	5.21E-03	5.20E-03	-0.25
509-069	23.70	6.30E-03	5.61E-03	-12.17
509-069	24.70	6.41E-03	5.67E-03	-13.11
509-069	19.30	5.54E-03	5.30E-03	-4.68
509-069	24.00	6.40E-03	5.63E-03	-13.67
509-069	24.30	6.32E-03	5.65E-03	-11.83
509-069	12.90	4.79E-03	4.45E-03	-7.71
509-069	21.00	6.14E-03	5.44E-03	-12.84
509-069	23.60	6.31E-03	5.61E-03	-12.55
509-069	24.20	6.34E-03	5.64E-03	-12.37
509-069	24.50	6.50E-03	5.66E-03	-14.90
509-069	23.80	6.38E-03	5.62E-03	-13.58
509-069	20.10	6.05E-03	5.37E-03	-12.75
509-069	24.00	6.30E-03	5.63E-03	-11.93
509-069	24.50	6.42E-03	5.66E-03	-13.40
509-069	15.20	4.89E-03	4.82E-03	-1.45
509-069	27.80	6.09E-03	5.83E-03	-4.42
509-069	24.80	6.15E-03	5.68E-03	-8.42
509-069	25.40	6.33E-03	5.71E-03	-10.98

^{240}Pu

Rod	Burnup	Measured	Calculated	% Difference
509-032	7.50	4.58E-04	4.79E-04	4.29
509-032	15.20	1.17E-03	1.11E-03	-4.67
509-032	15.80	1.19E-03	1.16E-03	-1.93
509-032	11.60	8.05E-04	8.17E-04	1.42
509-032	16.60	1.26E-03	1.23E-03	-2.81
509-032	17.10	1.30E-03	1.27E-03	-2.38
509-032	12.50	8.61E-04	8.91E-04	3.45
509-032	18.30	1.36E-03	1.37E-03	1.08
509-069	23.70	1.86E-03	1.82E-03	-2.19
509-069	24.70	1.91E-03	1.90E-03	-0.59
509-069	19.30	1.39E-03	1.45E-03	4.08
509-069	24.00	1.87E-03	1.84E-03	-1.41
509-069	24.30	1.89E-03	1.86E-03	-1.30
509-069	12.90	8.79E-04	9.24E-04	4.90
509-069	21.00	1.62E-03	1.59E-03	-1.48
509-069	23.60	1.87E-03	1.81E-03	-3.27
509-069	24.20	1.88E-03	1.86E-03	-1.48
509-069	24.50	1.93E-03	1.88E-03	-2.80
509-069	23.80	1.86E-03	1.82E-03	-1.78
509-069	20.10	1.51E-03	1.52E-03	0.48
509-069	24.00	1.91E-03	1.84E-03	-3.64
509-069	24.50	1.93E-03	1.88E-03	-2.54
509-069	15.20	1.07E-03	1.11E-03	4.04
509-069	27.80	2.06E-03	2.15E-03	4.20
509-069	24.80	1.92E-03	1.91E-03	-0.58
509-069	25.40	1.99E-03	1.96E-03	-1.92

^{241}Pu

Rod	Burnup	Measured	Calculated	% Difference
509-032	7.50	1.76E-04	1.51E-04	-16.48
509-032	15.20	6.34E-04	5.16E-04	-22.71
509-032	15.80	6.37E-04	5.50E-04	-15.99
509-032	11.60	3.81E-04	3.29E-04	-15.87
509-032	16.60	6.92E-04	5.94E-04	-16.44
509-032	17.10	7.11E-04	6.22E-04	-14.22
509-032	12.50	4.18E-04	3.74E-04	-11.67
509-032	18.30	7.19E-04	6.90E-04	-4.24
509-069	23.70	1.11E-03	9.92E-04	-12.34
509-069	24.70	1.13E-03	1.04E-03	-8.59
509-069	19.30	7.76E-04	7.47E-04	-3.90
509-069	24.00	1.15E-03	1.01E-03	-14.23
509-069	24.30	1.12E-03	1.02E-03	-9.53
509-069	12.90	4.24E-04	3.94E-04	-7.55
509-069	21.00	9.44E-04	8.43E-04	-11.97
509-069	23.60	1.10E-03	9.86E-04	-11.23
509-069	24.20	1.10E-03	1.02E-03	-7.84
509-069	24.50	1.13E-03	1.03E-03	-9.68
509-069	23.80	1.11E-03	9.97E-04	-11.24
509-069	20.10	8.40E-04	7.92E-04	-6.03
509-069	24.00	1.13E-03	1.01E-03	-11.95
509-069	24.50	1.13E-03	1.03E-03	-9.58
509-069	15.20	5.40E-04	5.16E-04	-4.55
509-069	27.80	1.24E-03	1.20E-03	-3.90
509-069	24.80	1.13E-03	1.05E-03	-8.05
509-069	25.40	1.17E-03	1.08E-03	-8.22

^{148}Nd

Rod	Burnup	Measured	Calculated	% Difference
509-069	20.60	3.90E-04	3.93E-04	0.88
509-069	23.72	4.50E-04	4.54E-04	0.80
509-069	24.30	4.61E-04	4.65E-04	0.85
509-069	23.87	4.52E-04	4.57E-04	0.99
509-069	24.55	4.65E-04	4.70E-04	1.00
509-069	23.93	4.54E-04	4.58E-04	0.80
509-069	24.36	4.62E-04	4.66E-04	0.88
509-069	24.33	4.59E-04	4.65E-04	1.39

^{154}Eu

Rod	Burnup	Measured	Calculated	% Difference
509-069	12.86	5.17E+07	5.92E+07	12.62
509-069	20.60	1.40E+08	1.65E+08	15.22
509-069	23.72	1.78E+08	2.21E+08	19.67
509-069	24.30	1.65E+08	2.33E+08	29.17
509-069	23.87	1.77E+08	2.24E+08	21.33
509-069	24.55	1.92E+08	2.38E+08	19.31
509-069	24.36	1.72E+08	2.34E+08	26.62
509-069	24.33	1.77E+08	2.33E+08	24.27
509-069	24.31	1.85E+08	2.33E+08	20.69
509-069	23.70	1.77E+08	2.21E+08	20.17
509-069	24.70	1.92E+08	2.41E+08	20.34
509-069	19.30	1.15E+08	1.44E+08	19.99
509-069	24.00	1.77E+08	2.27E+08	22.10
509-069	24.30	1.85E+08	2.33E+08	20.60
509-069	12.90	5.17E+07	5.96E+07	13.24
509-069	21.00	1.40E+08	1.72E+08	18.57
509-069	23.60	1.78E+08	2.19E+08	18.83
509-069	24.20	1.57E+08	2.31E+08	32.09
509-069	24.50	1.65E+08	2.37E+08	30.34
509-069	24.50	1.72E+08	2.37E+08	27.47
509-069	15.20	5.68E+07	8.58E+07	33.77
509-069	24.80	1.69E+08	2.43E+08	30.59

APPENDIX C

ISOTOPIC GRAPHS

Takahama Unit #3
(5% error bar)

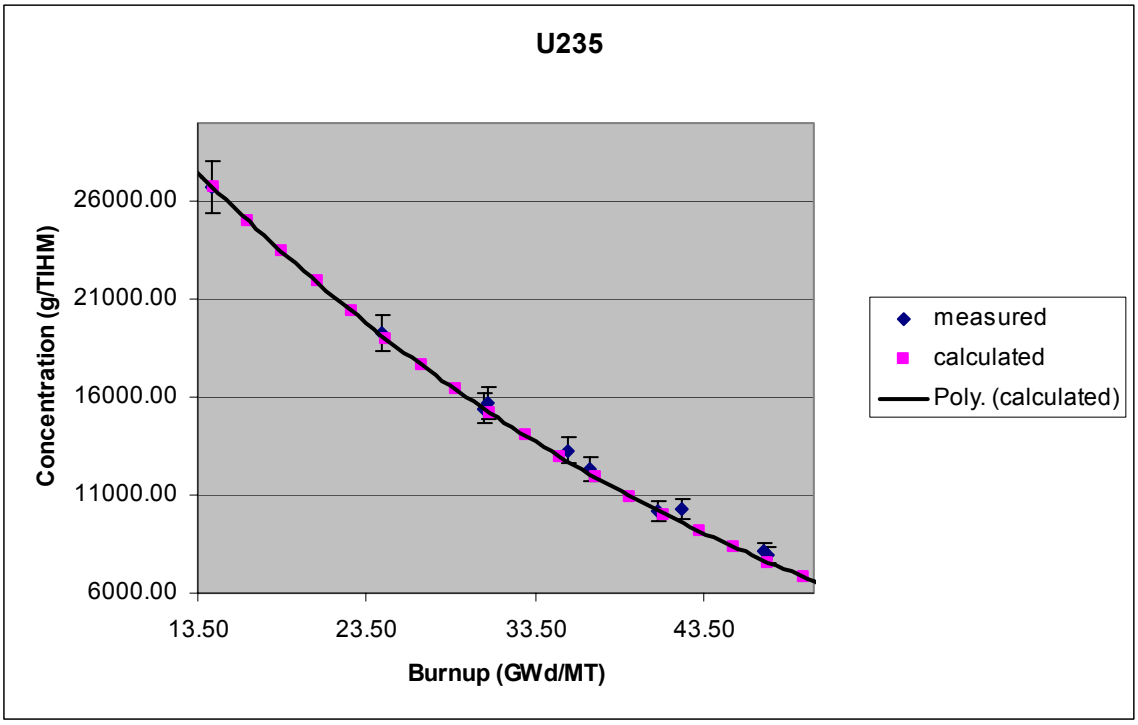

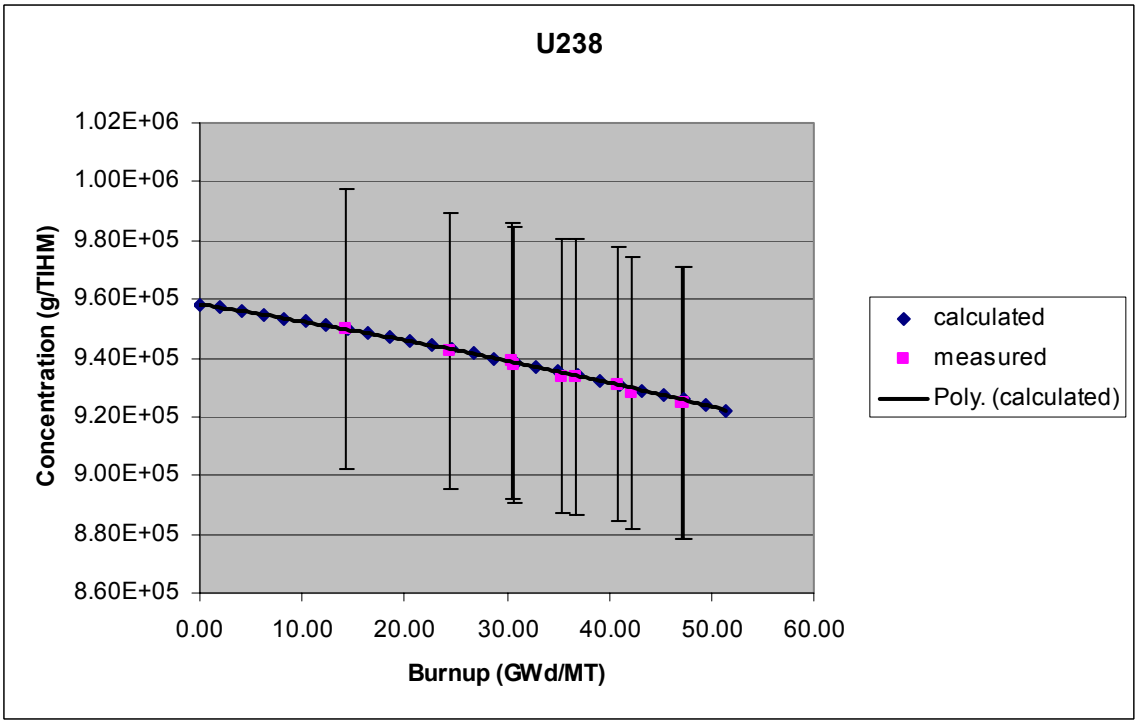

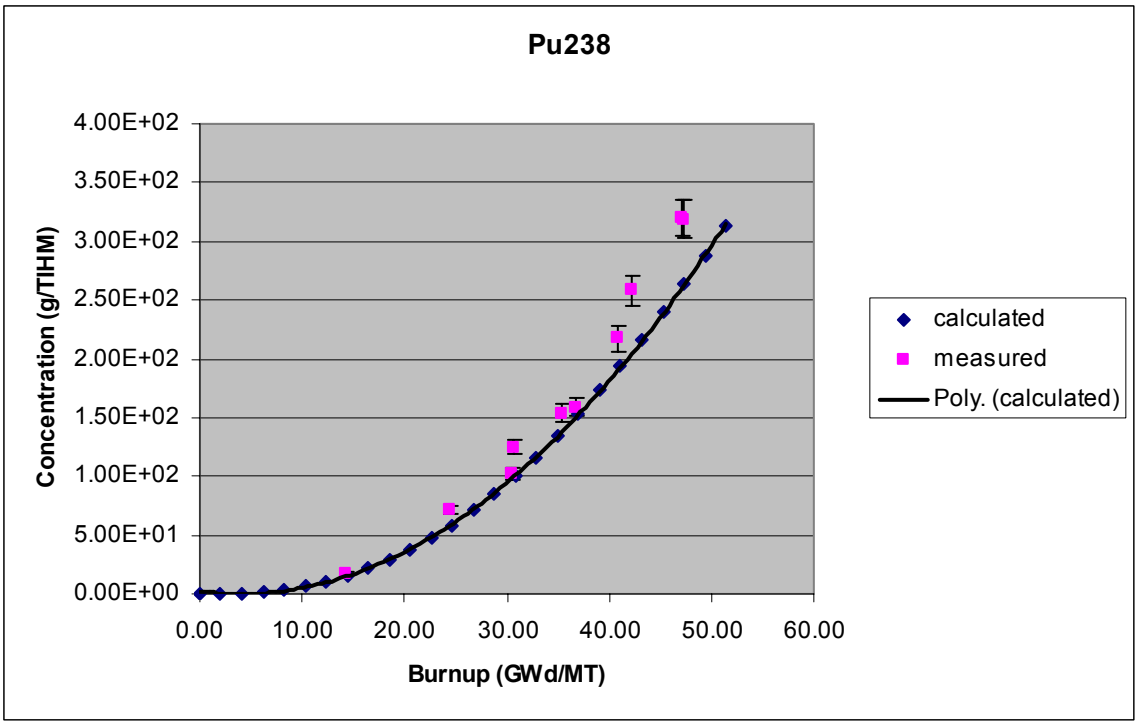
Pu238
4.00E+02
3.50E+02
3.00E+02
2.50E+02
2.00E+02
1.50E+02
1.00E+02
5.00E+01
0.00E+00
Concentration (g/TIHM)
0.00
10.00
20.00
30.00
40.00
50.00
60.00
Burnup (GWd/MT)
calculated
measured
Poly. (calculated)

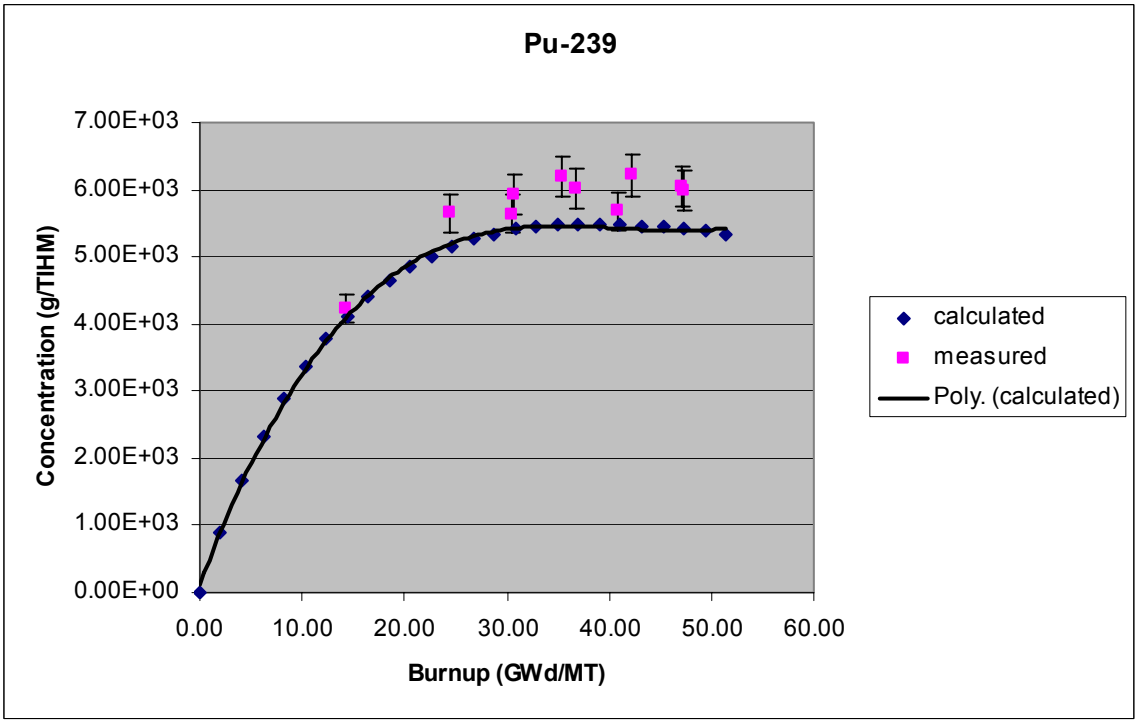
Pu-239
7.00E+03
6.00E+03
5.00E+03
4.00E+03
3.00E+03
2.00E+03
1.00E+03
0.00E+00
Concentration (g/TIHM)
0.00
10.00
20.00
30.00
40.00
50.00
60.00
Burnup (GWd/MT)
calculated
measured
Poly. (calculated)

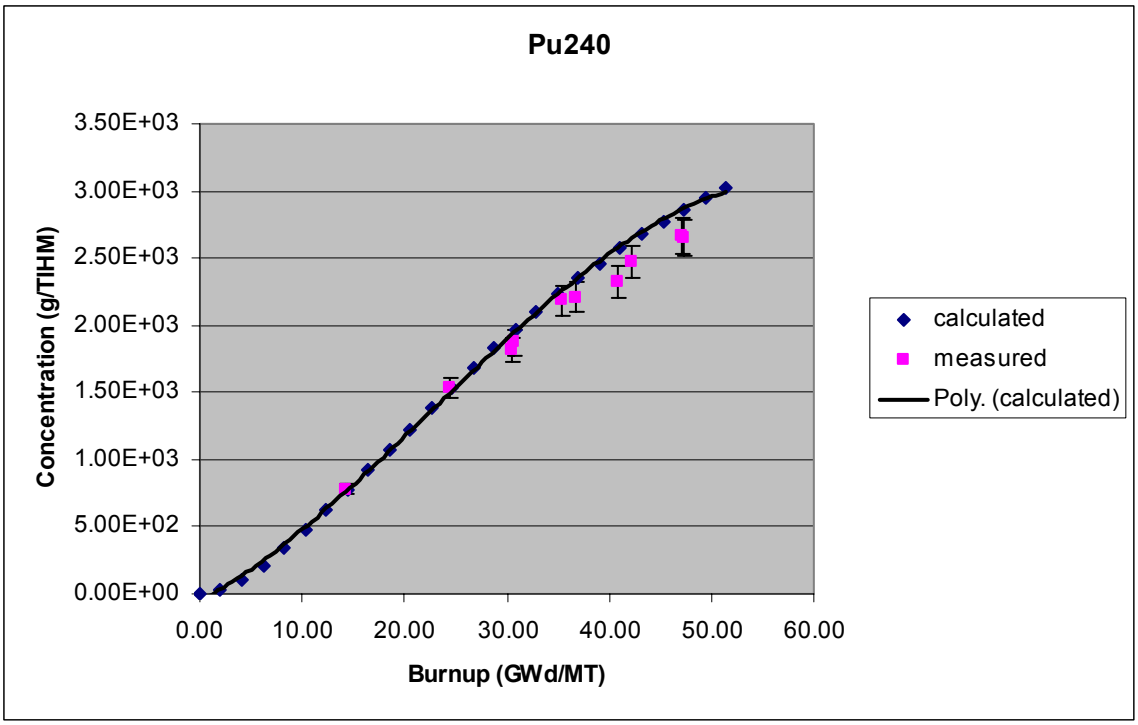
Pu240
Concentration (g/TIHM)
3.50E+03
3.00E+03
2.50E+03
2.00E+03
1.50E+03
1.00E+03
5.00E+02
0.00E+00
0.00
10.00
20.00
30.00
40.00
50.00
60.00
Burnup (GWd/MT)
calculated
measured
Poly. (calculated)

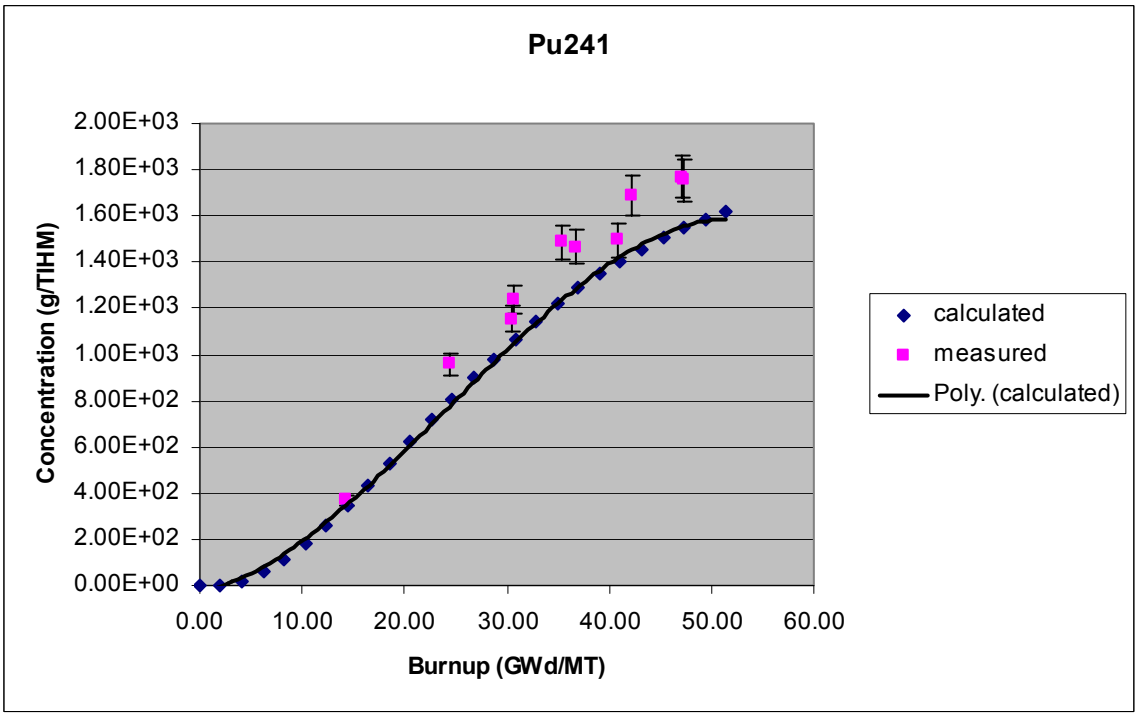
Pu241
Concentration (g/TIHM)
2.00E+03
1.80E+03
1.60E+03
1.40E+03
1.20E+03
1.00E+03
8.00E+02
6.00E+02
4.00E+02
2.00E+02
0.00E+00
0.00
10.00
20.00
30.00
40.00
50.00
60.00
Burnup (GWd/MT)
calculated
measured
Poly. (calculated)

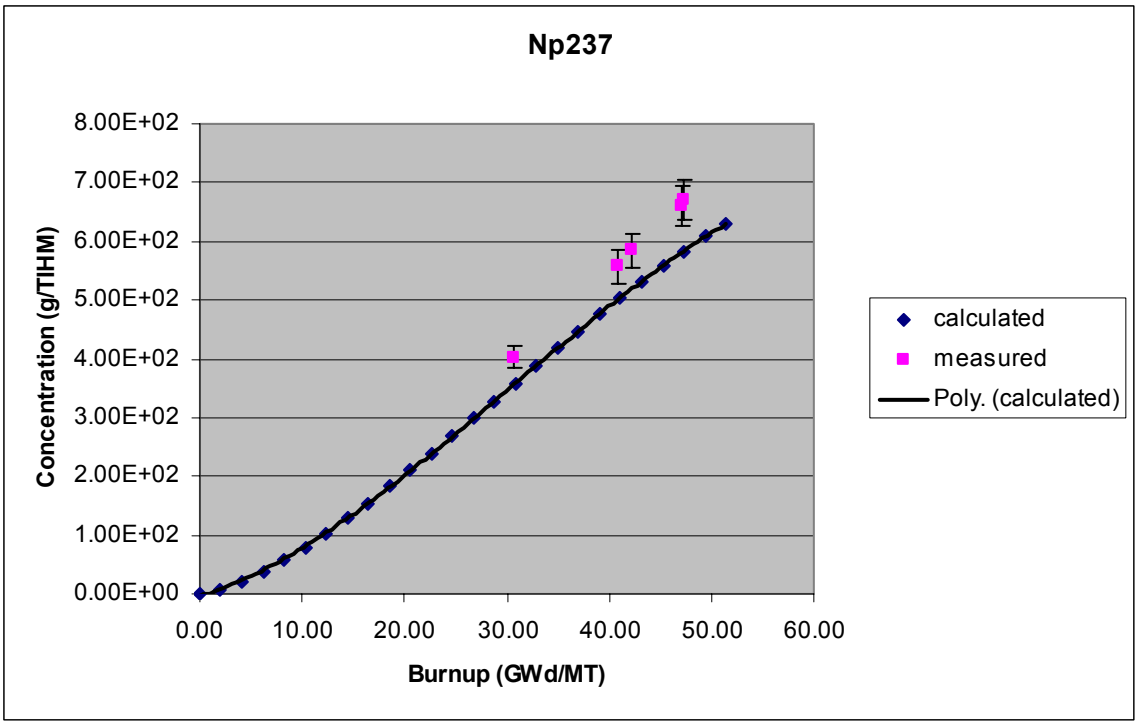
Np237
8.00E+02
7.00E+02
6.00E+02
5.00E+02
4.00E+02
3.00E+02
2.00E+02
1.00E+02
0.00E+00
Concentration (g/TIHM)
0.00
10.00
20.00
30.00
40.00
50.00
60.00
Burnup (GWd/MT)
calculated
measured
Poly. (calculated)

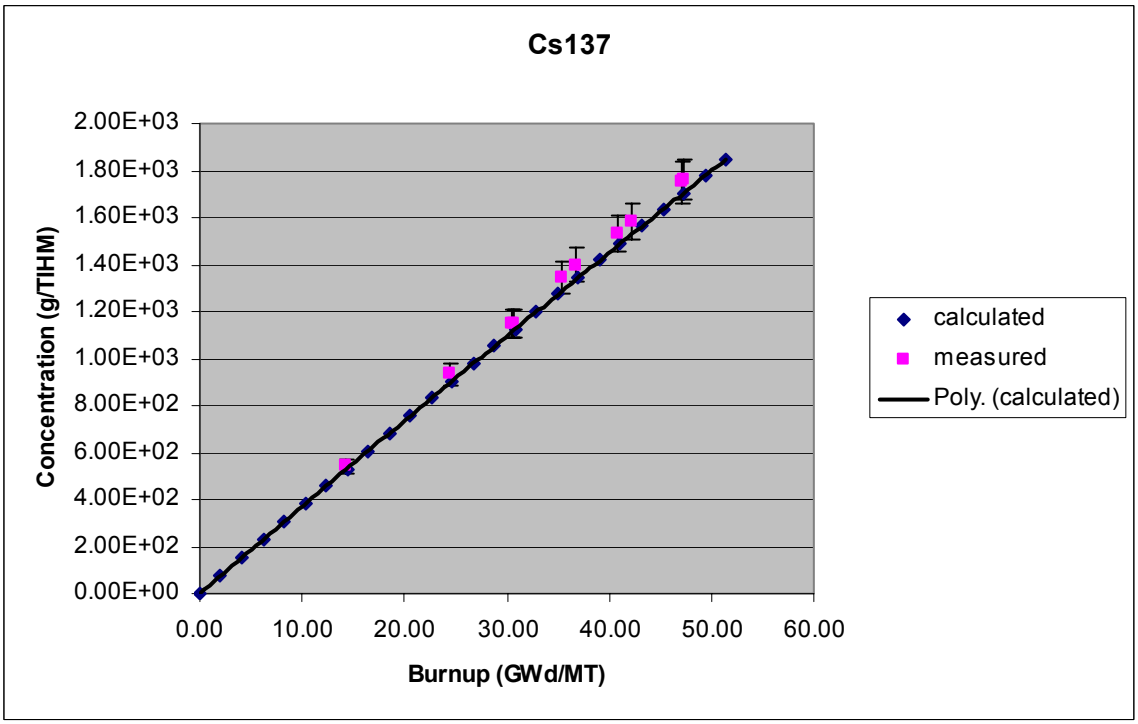
Cs137
2.00E+03
1.80E+03
1.60E+03
1.40E+03
1.20E+03
1.00E+03
8.00E+02
6.00E+02
4.00E+02
2.00E+02
0.00E+00
Concentration (g/TIHM)
0.00
10.00
20.00
30.00
40.00
50.00
60.00
Burnup (GWd/MT)
calculated
measured
Poly. (calculated)

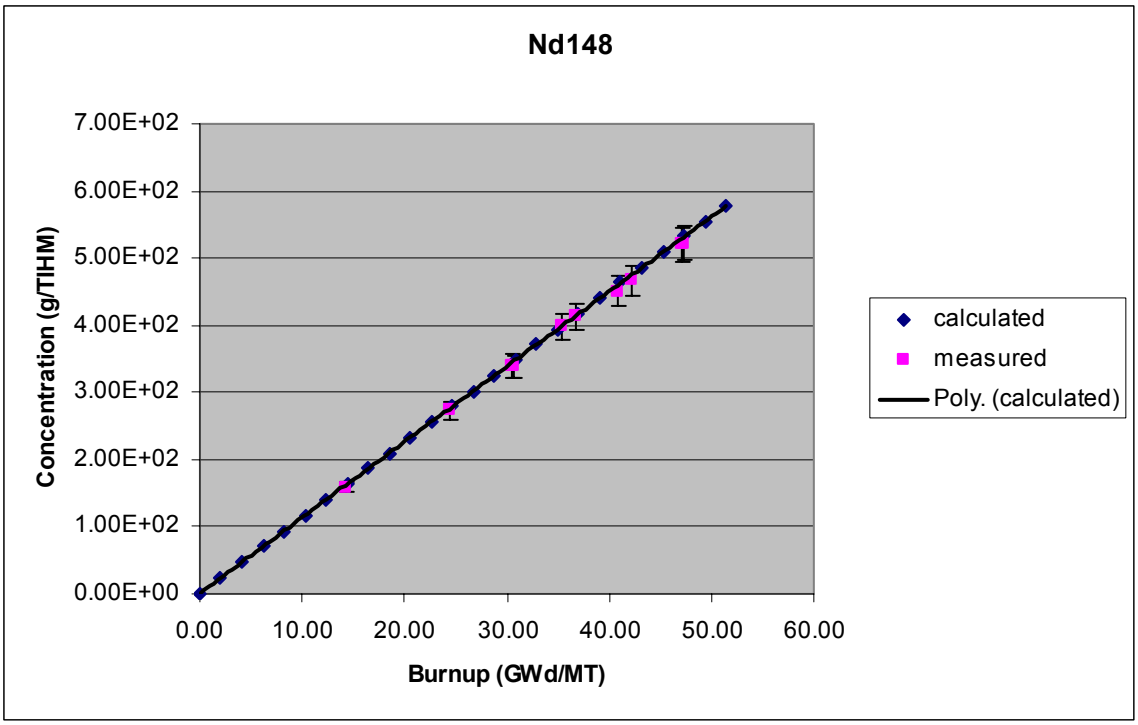
Nd148
7.00E+02
6.00E+02
5.00E+02
4.00E+02
3.00E+02
2.00E+02
1.00E+02
0.00E+00
Concentration (g/TIHM)
0.00
10.00
20.00
30.00
40.00
50.00
60.00
Burnup (GWd/MT)
calculated
measured
Poly. (calculated)

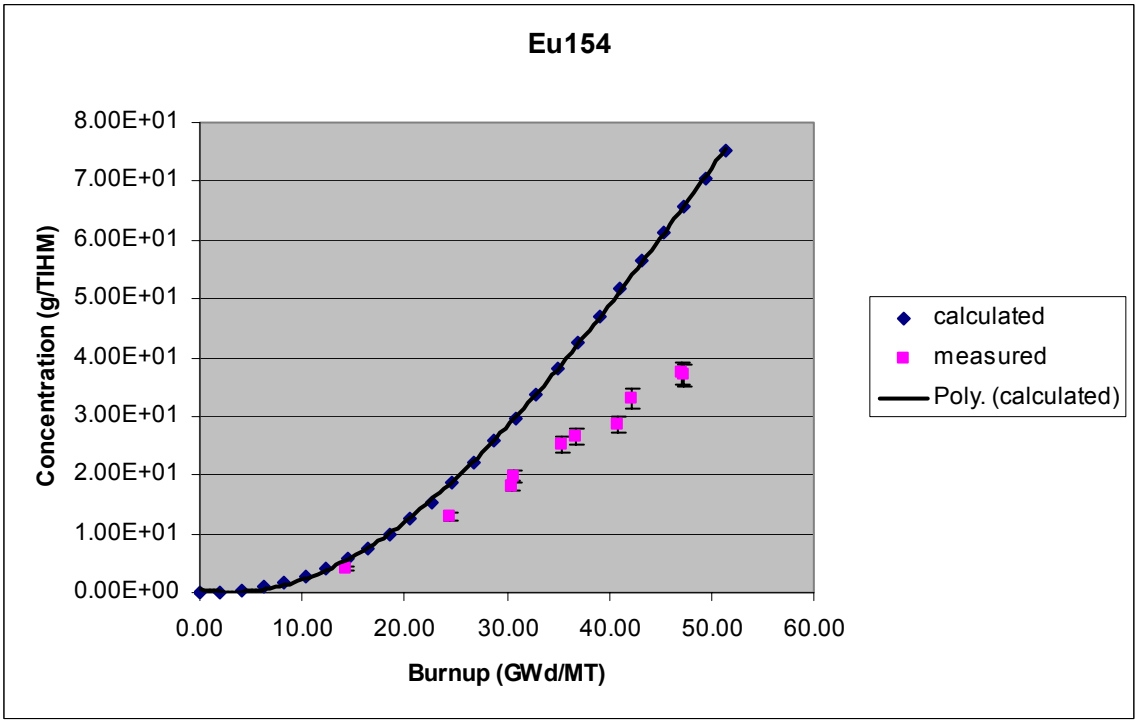
Eu154
8.00E+01
7.00E+01
6.00E+01
5.00E+01
4.00E+01
3.00E+01
2.00E+01
1.00E+01
0.00E+00
Concentration (g/TIHM)
0.00
10.00
20.00
30.00
40.00
50.00
60.00
Burnup (GWd/MT)
calculated
measured
Poly. (calculated)

Calvert Cliffs Unit #1
(5% error bar)

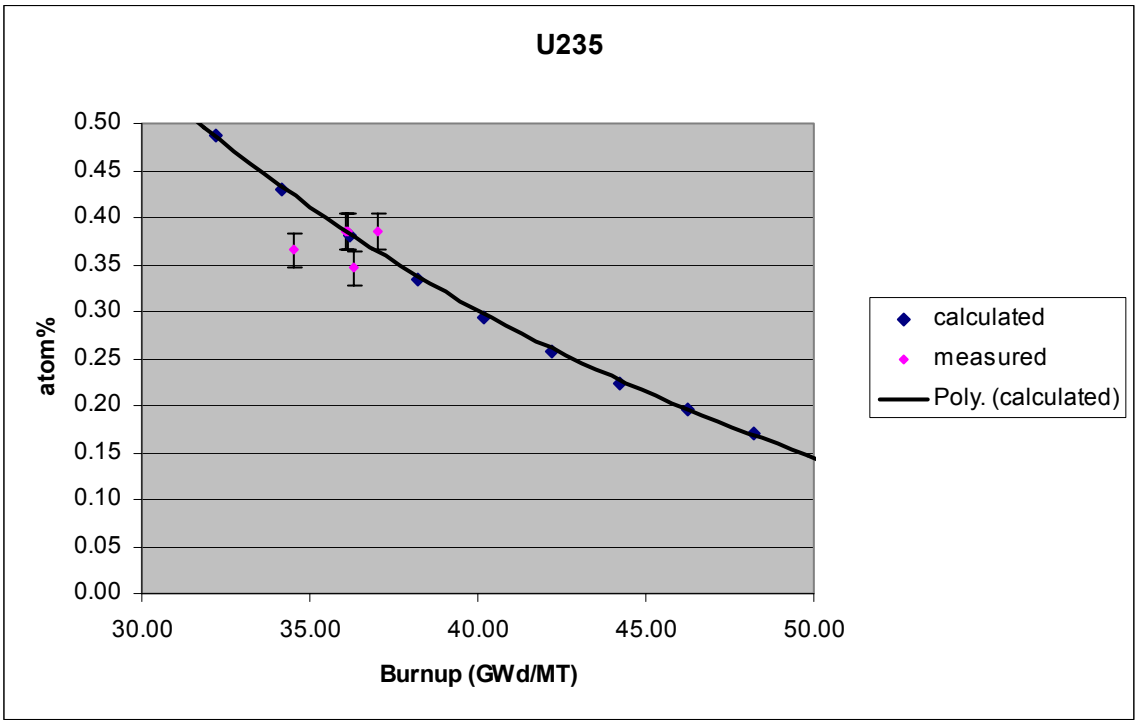

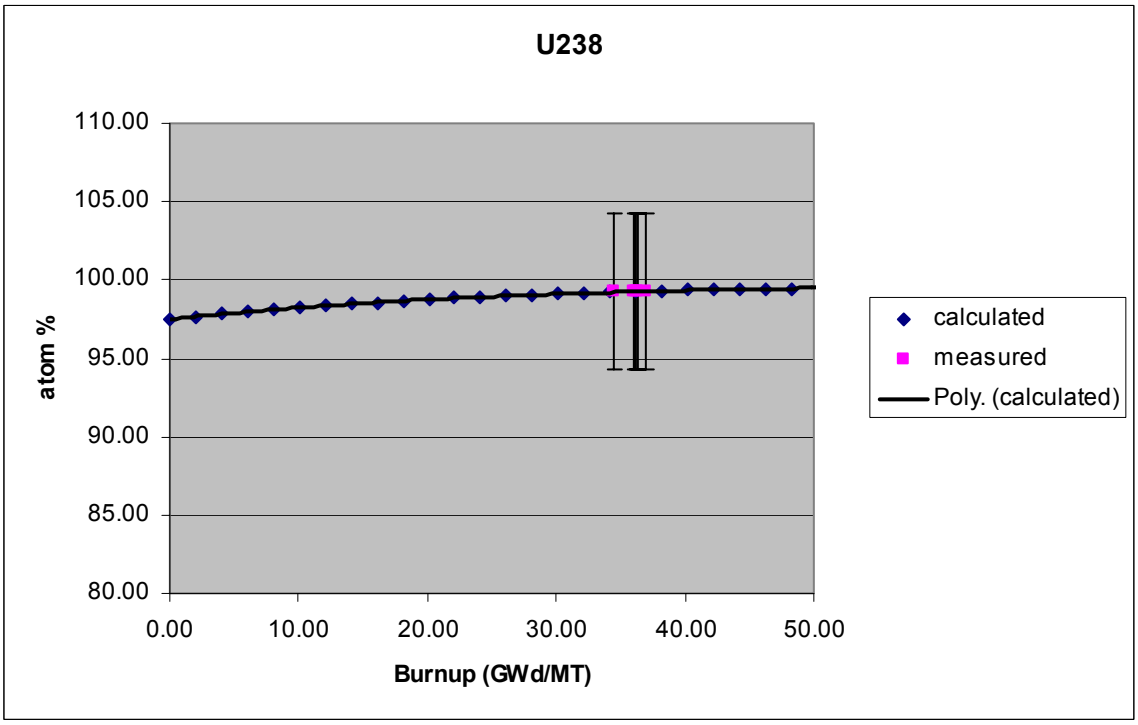

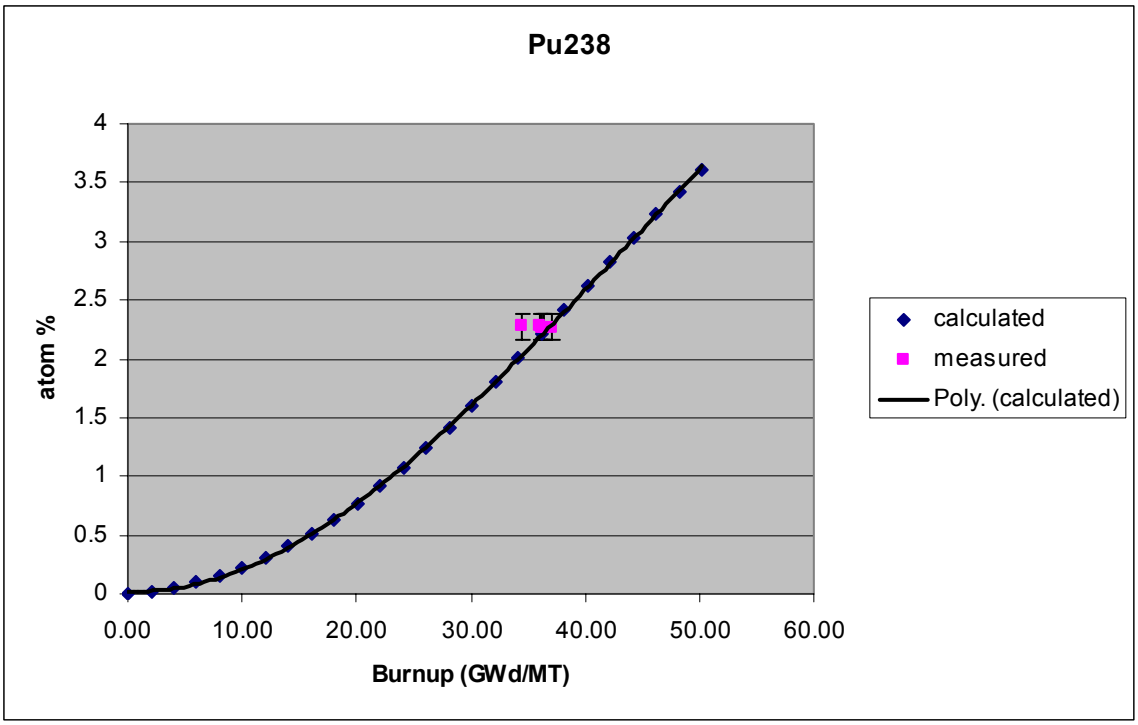
Pu238
atom %
4
3.5
3
2.5
2
1.5
1
0.5
0
0.00
10.00
20.00
30.00
40.00
50.00
60.00
Burnup (GWd/MT)
calculated
measured
Poly. (calculated)

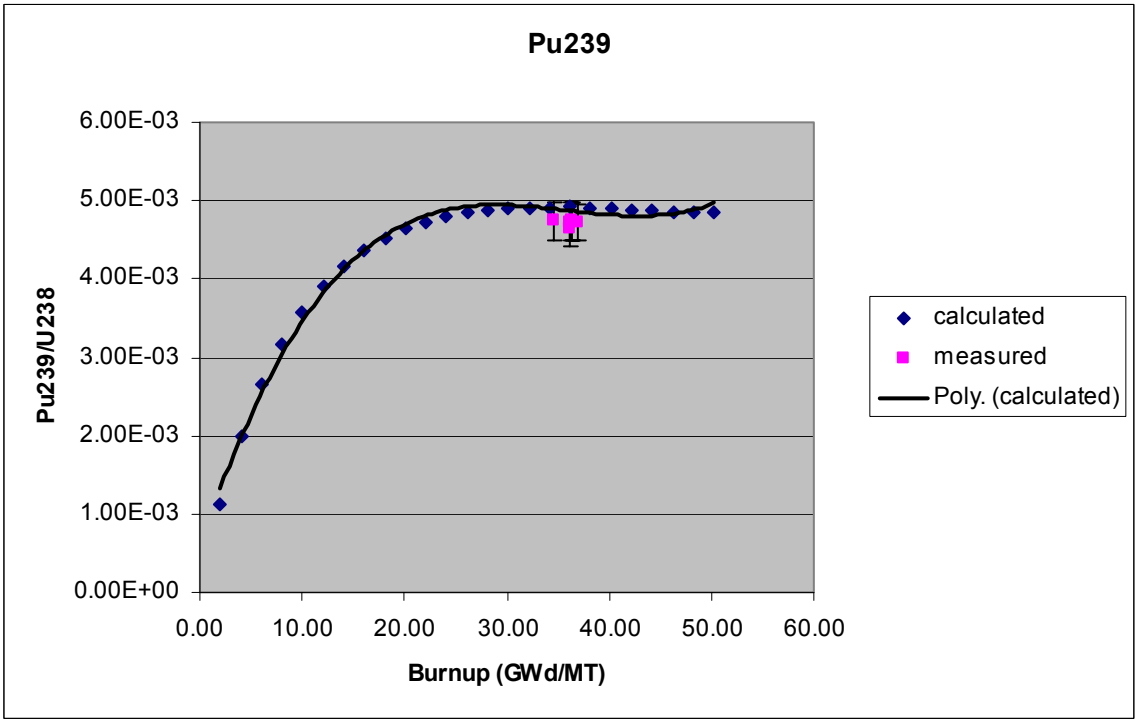
Pu239
Pu239/U238
6.00E-03
5.00E-03
4.00E-03
3.00E-03
2.00E-03
1.00E-03
0.00E+00
0.00
10.00
20.00
30.00
40.00
50.00
60.00
Burnup (GWd/MT)
calculated
measured
Poly. (calculated)

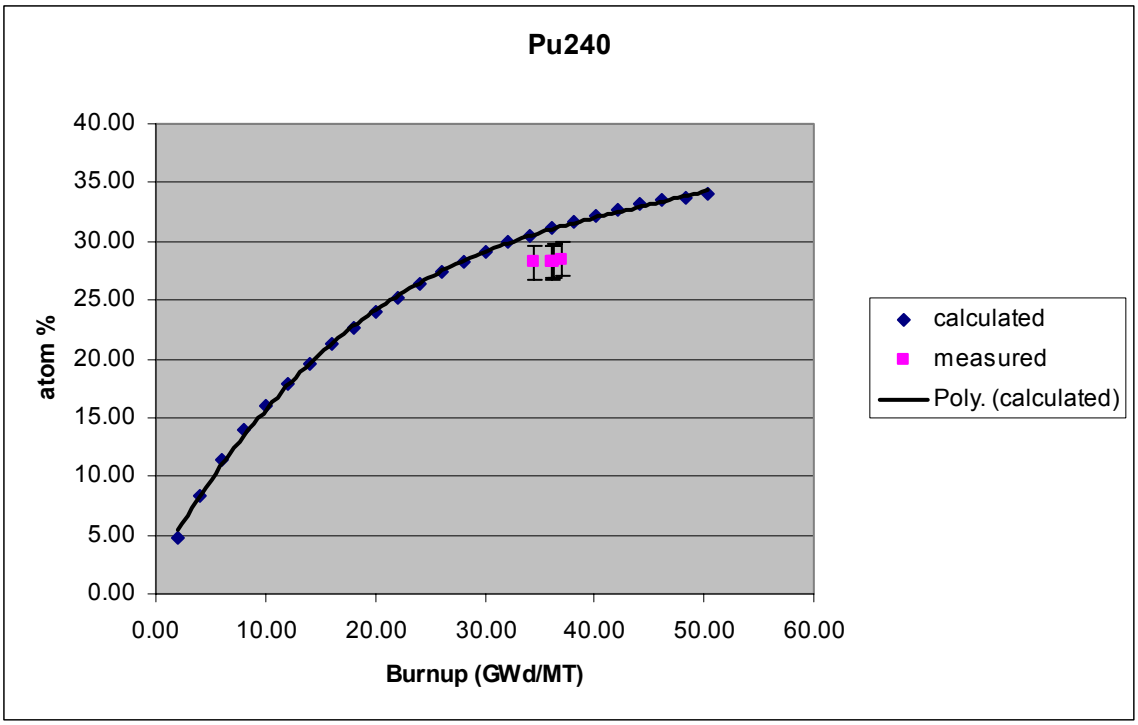
Pu240
40.00
35.00
30.00
25.00
20.00
15.00
10.00
5.00
0.00
atom %
0.00
10.00
20.00
30.00
40.00
50.00
60.00
Burnup (GWd/MT)
calculated
measured
Poly. (calculated)

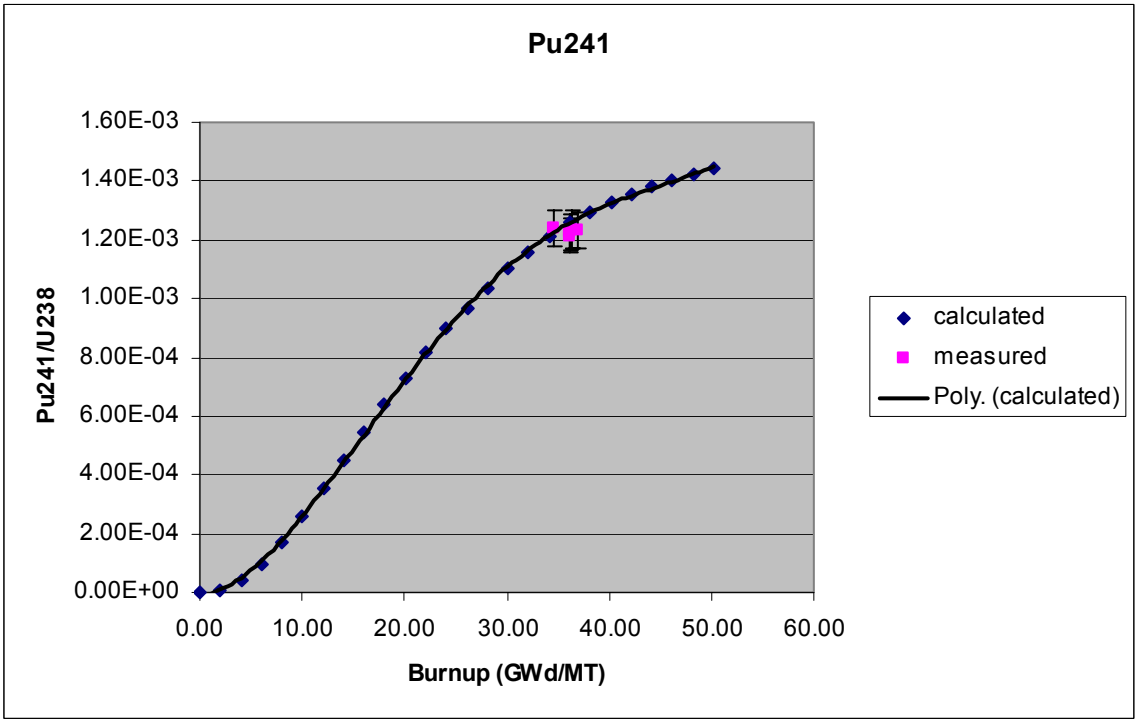
Pu241
1.60E-03
1.40E-03
1.20E-03
1.00E-03
8.00E-04
6.00E-04
4.00E-04
2.00E-04
0.00E+00
Pu241/U238
0.00
10.00
20.00
30.00
40.00
50.00
60.00
Burnup (GWd/MT)
calculated
measured
Poly. (calculated)

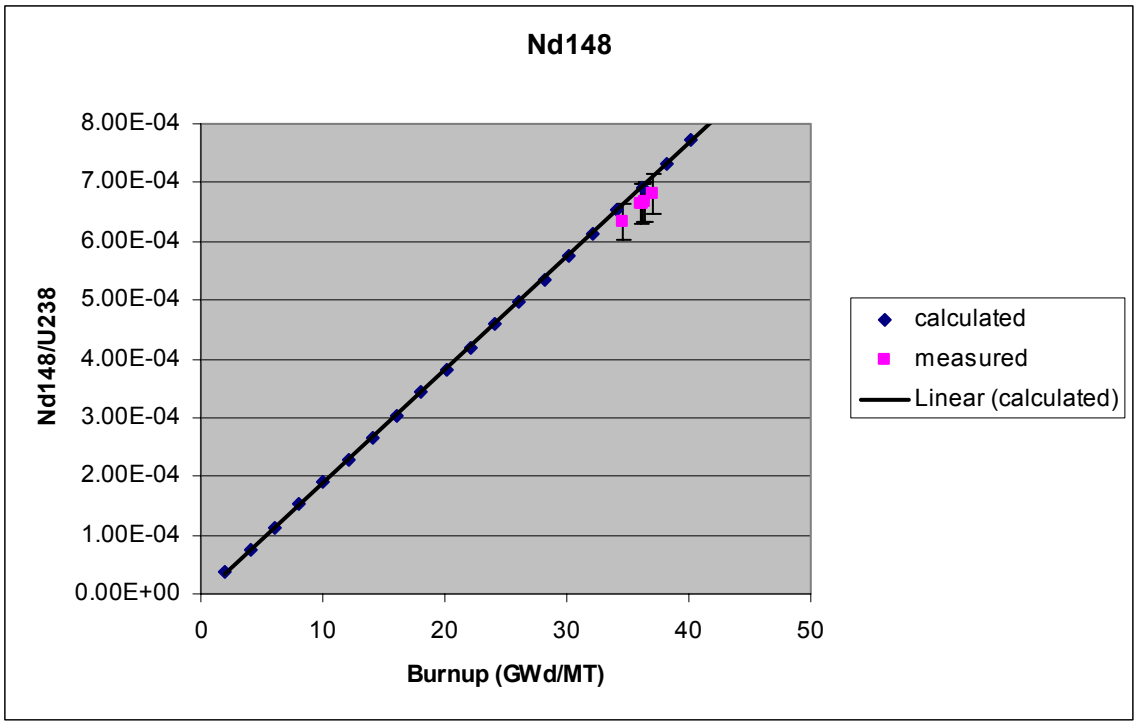
Nd148
8.00E-04
7.00E-04
6.00E-04
5.00E-04
4.00E-04
3.00E-04
2.00E-04
1.00E-04
0.00E+00
Nd148/U238
0
10
20
30
40
50
Burnup (GWd/MT)
calculated
measured
Linear (calculated)

Trino Vercelles Unit #2
(5% error bar)

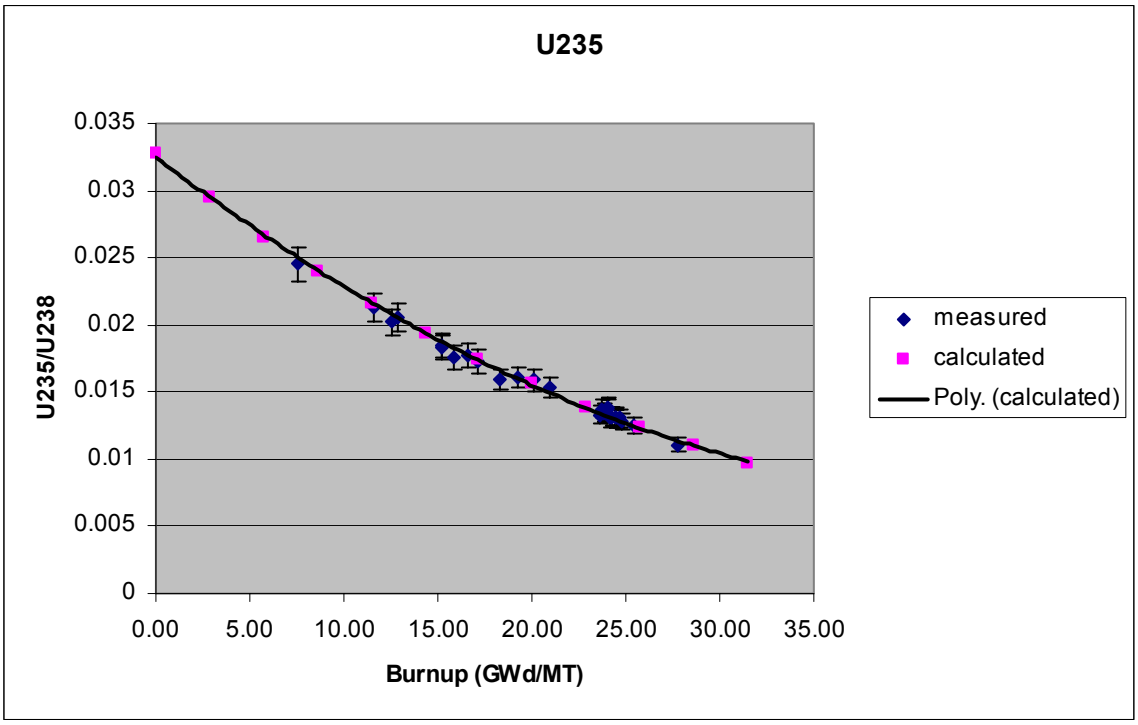

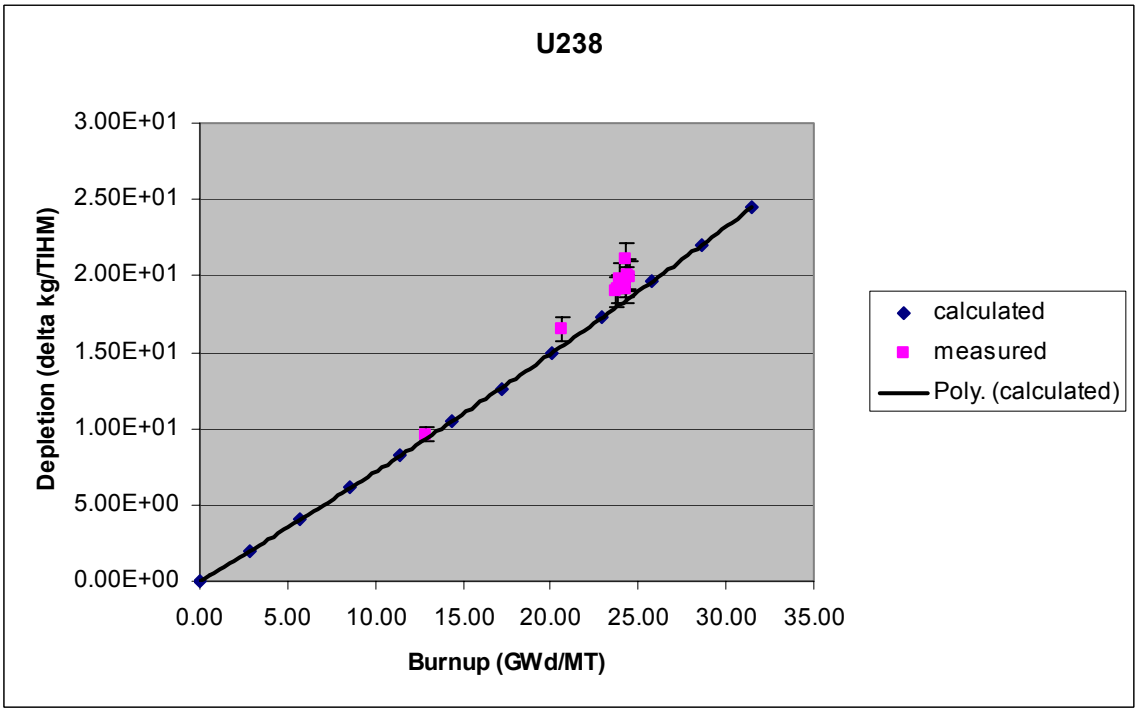

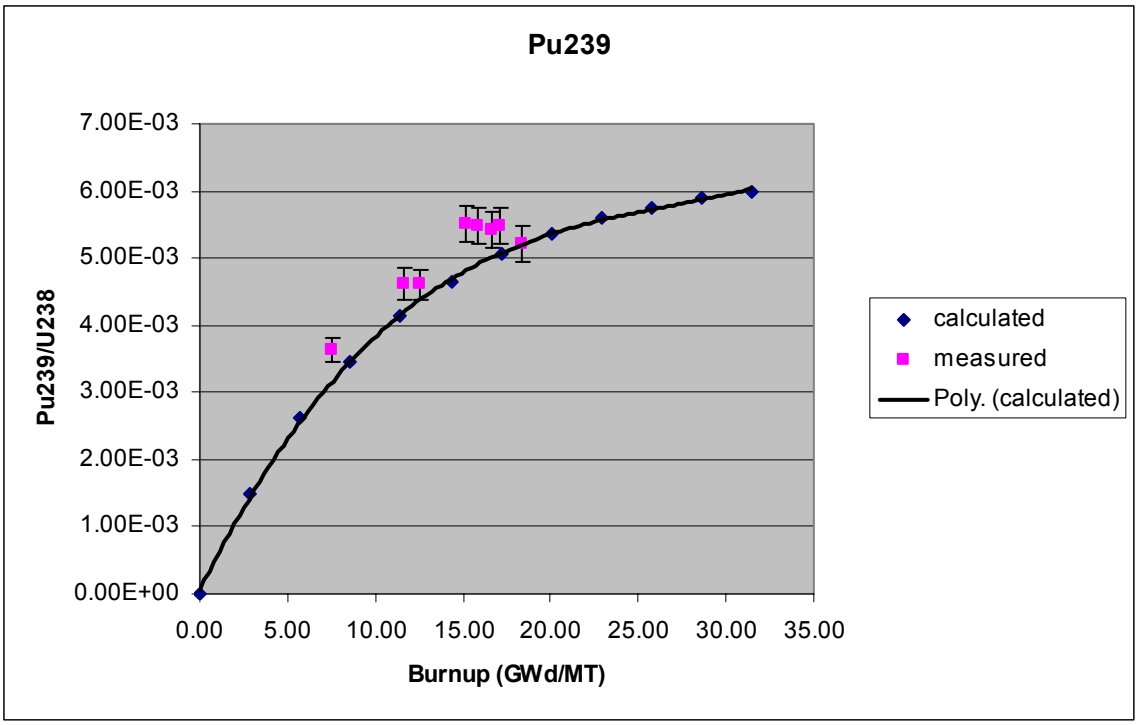
Pu239
7.00E-03
6.00E-03
5.00E-03
4.00E-03
3.00E-03
2.00E-03
1.00E-03
0.00E+00
Pu239/U238
0.00
5.00
10.00
15.00
20.00
25.00
30.00
35.00
Burnup (GWd/MT)
calculated
measured
Poly. (calculated)

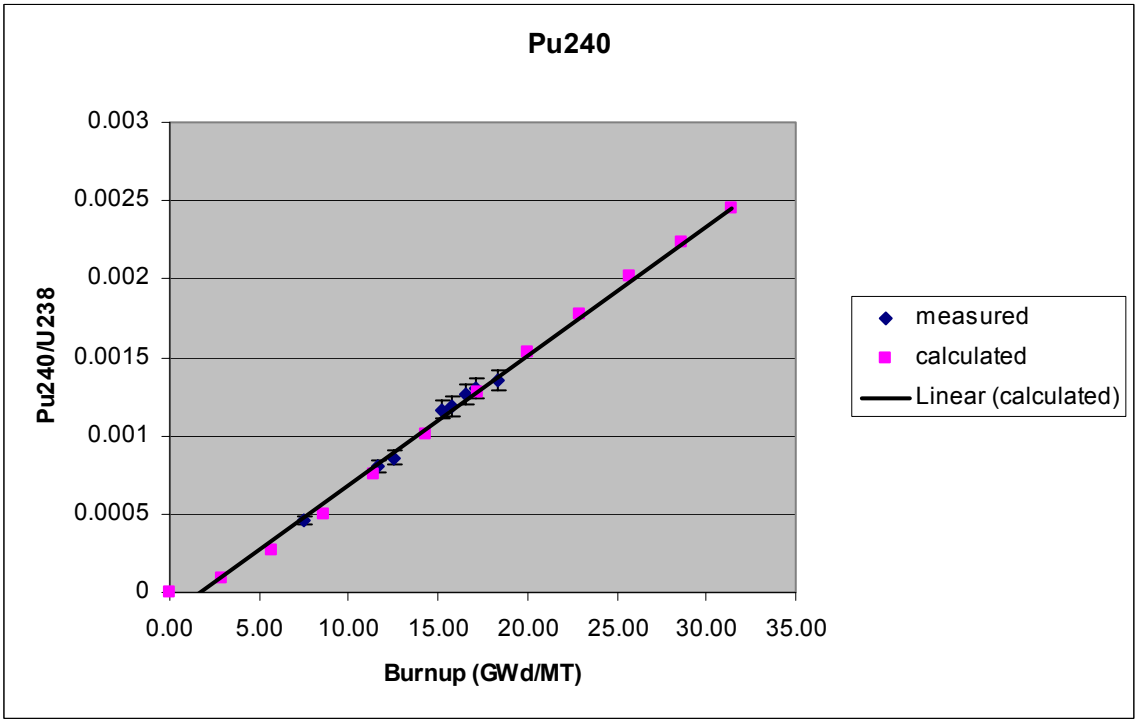
Pu240
0.003
0.0025
0.002
0.0015
0.001
0.0005
0
Pu240/U238
0.00
5.00
10.00
15.00
20.00
25.00
30.00
35.00
Burnup (GWd/MT)
measured
calculated
Linear (calculated)

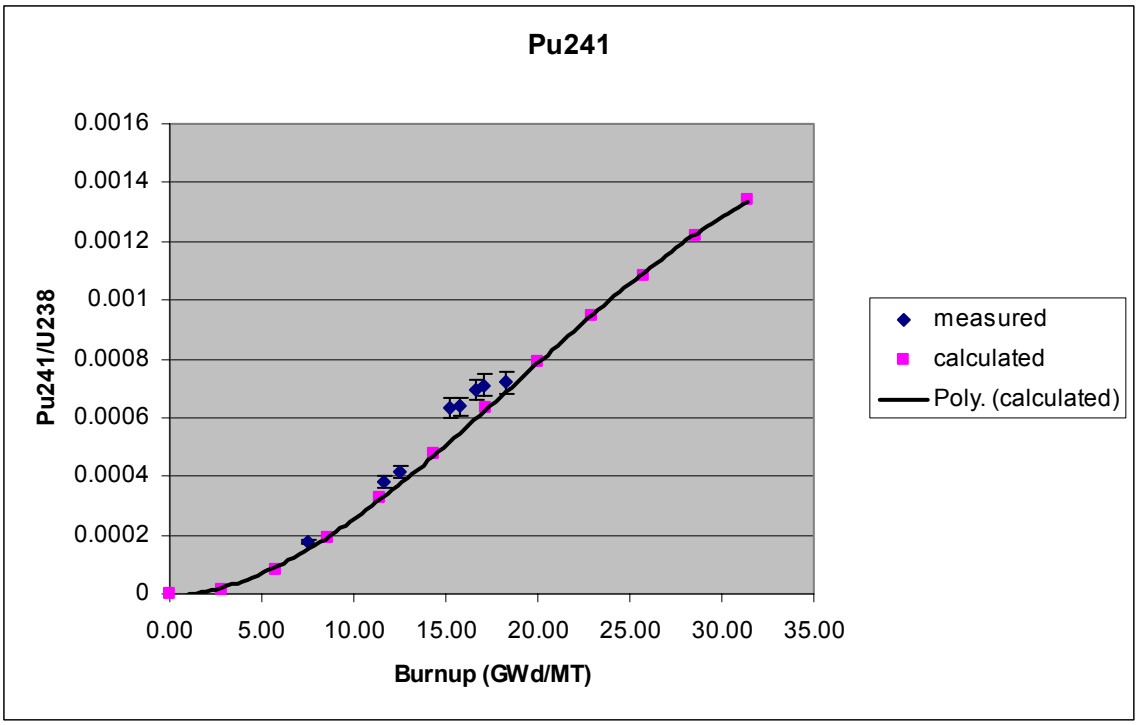
Pu241
0.0016
0.0014
0.0012
0.001
0.0008
0.0006
0.0004
0.0002
0
Pu241/U238
0.00
5.00
10.00
15.00
20.00
25.00
30.00
35.00
Burnup (GWd/MT)
measured
calculated
Poly. (calculated)

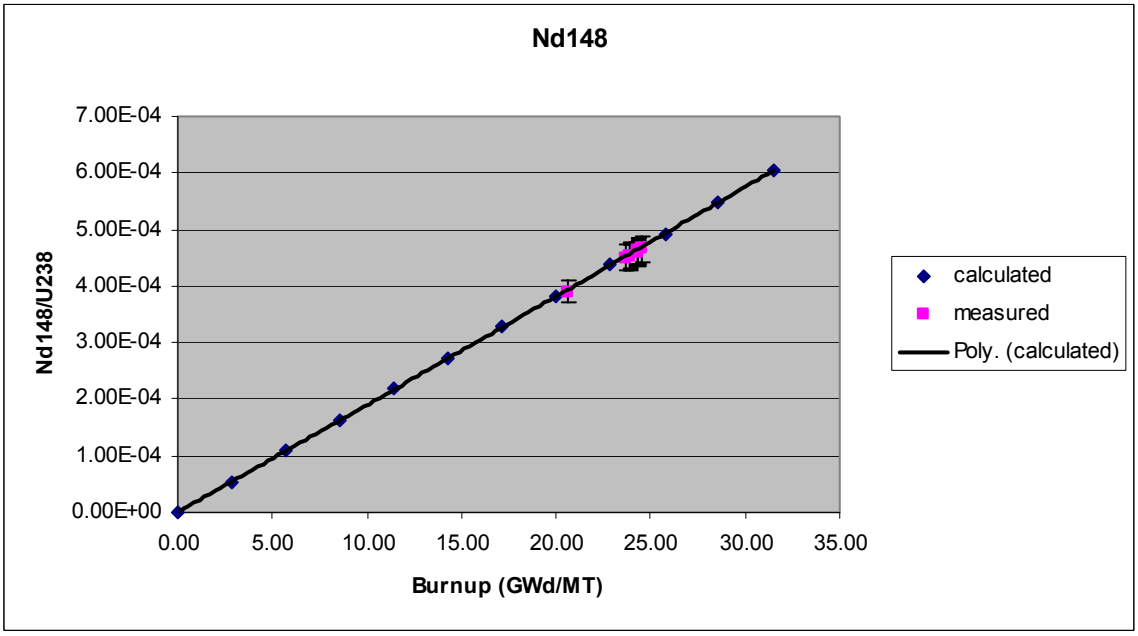
Nd148
7.00E-04
6.00E-04
5.00E-04
4.00E-04
3.00E-04
2.00E-04
1.00E-04
0.00E+00
Nd148/U238
0.00
5.00
10.00
15.00
20.00
25.00
30.00
35.00
Burnup (GWd/MT)
calculated
measured
Poly. (calculated)

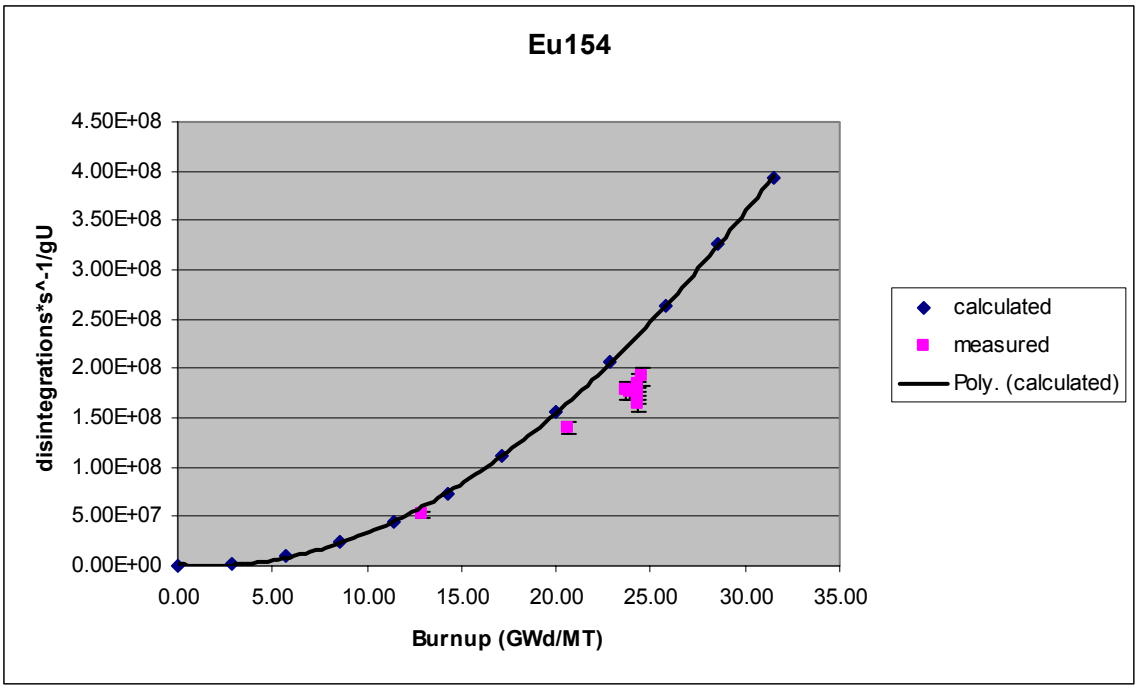
Eu154
4.50E+08
4.00E+08
3.50E+08
3.00E+08
2.50E+08
2.00E+08
1.50E+08
1.00E+08
5.00E+07
0.00E+00
disintegrations*s^-1/gU
0.00
5.00
10.00
15.00
20.00
25.00
30.00
35.00
Burnup (GWd/MT)
calculated
measured
Poly. (calculated)

VITA

David Edward Burk was born on the 30th of September 1978 to Edward and Marie Burk of Magnolia, Arkansas. He graduated from the Arkansas School for Mathematics and Sciences in May 1997. He received an Associate of Science in Nuclear Technology and a Bachelor of Science in Mechanical Engineering from Arkansas Tech University at Russellville, Arkansas in December 2002. His mail can be forwarded through the Department of Nuclear Engineering, c/o Dr. William Charlton, Texas A&M University, College Station, TX 77843-3133.